PHYSICAL REVIEW B **91**, 235111 (2015)

Anderson localization and the topology of classifying spaces

Takahiro Morimoto,[1] Akira Furusaki,[1,2] and Christopher Mudry[3]
[1]*Condensed Matter Theory Laboratory, RIKEN, Wako, Saitama, 351-0198, Japan*
[2]*RIKEN Center for Emergent Matter Science (CEMS), Wako, Saitama, 351-0198, Japan*
[3]*Condensed Matter Theory Group, Paul Scherrer Institute, CH-5232 Villigen PSI, Switzerland*
(Received 18 March 2015; revised manuscript received 18 May 2015; published 8 June 2015)

We construct the generic phase diagrams encoding the topologically distinct localized and delocalized phases of noninteracting fermionic quasiparticles for any symmetry class from the tenfold way in one, two, and three dimensions. To this end, we start from a massive Dirac Hamiltonian perturbed by a generic disorder for any dimension of space and for any one of the ten symmetry classes from the tenfold way. The physics of Anderson localization is then encoded by a two-dimensional phase diagram that we deduce from the topology of the space of normalized Dirac masses. This approach agrees with previously known results and gives an alternative explanation for the even-odd effect in the one-dimensional chiral symmetry classes. We also give a qualitative explanation for the Gade singularity and Griffiths effects in the density of states using the first homotopy group of the normalized Dirac masses in two dimensions. Finally, this approach is used to analyze the stability of massless Dirac fermions on the surface of three-dimensional topological crystalline insulators.

DOI: 10.1103/PhysRevB.91.235111 PACS number(s): 72.10.−d, 73.20.−r, 73.43.Cd

I. INTRODUCTION

Anderson localization is the nonperturbative phenomenon by which the plane-wave solutions to a linear differential equation become exponentially localized upon the breaking of translation symmetry by a local random potential [1,2]. Anderson localization always prevails for metals in one-dimensional (1D) space and for metals without spin-orbit coupling in two-dimensional (2D) space, however small the disorder [3,4]. It requires the disorder to be large enough, of the order of the Fermi energy, otherwise [3,4]. Until the experimental discovery of the integer quantum Hall effect (IQHE) in 1980 [5], the most important challenge brought about by Anderson localization had been to understand the metal-insulator transition.

The IQHE is defined by the quantized value of the Hall conductivity at fixed filling fraction and by a sharp (quantum) transition between two consecutive quantized values of the Hall conductivity, the plateau transition in short, when the filling fraction is tuned. It is explained by the topological character of the Hall conductivity when the chemical potential is in between two consecutive Landau levels of a two-dimensional electron gas subjected to a uniform magnetic field and by the fact that this topological character is retained in the regime of Anderson localization [6–10]. The IQHE teaches two important lessons. First, there can be topologically distinct insulating phases of electronic matter. Second, direct continuous (quantum) transitions between these phases are possible. Several approaches have been used to study the plateau transition from an analytical and a computational point of view. Effective models such as nonlinear sigma models (NLSMs) [11–13], quantum network models [14], and Dirac fermions [15] were proposed. In parallel, the two-parameter scaling theory of Khmelnitskii and Levine *et al.* was verified through numerous large-scale numerical simulations [16]. In this paper, we will generalize the approach pioneered by Ludwig *et al.* in Ref. [15] by which they showed that the minimal continuum model that captures the IQHE in both the clean and disordered limits is a Dirac Hamiltonian with random mass and gauge fields.

Integer quantum Hall states are examples of topological insulators and superconductors defined as follows. Topological insulators and superconductors are states of matter such that fermionic quasiparticles are gapped in the bulk but gapless on the boundary [17,18]. There are many materials that realize topological insulators, say Bi_2Se_3 [17,18]. Topological crystalline insulators differ from topological insulators in that it is a spatial symmetry as opposed to a "generic" symmetry such as time-reversal symmetry that endows the boundary states with a topological protection. SnTe materials are examples of topological crystalline insulators supporting an even number of massless Dirac cones on their mirror-symmetric boundaries [19–22]. Weyl and Dirac semimetals are yet another family of noninteracting fermionic Hamiltonians displaying gap-closing points, although in the Brillouin zone now, that are topologically stable [23–26].

A defining property of (strong) topological insulators and superconductors in d-dimensional space is that their boundary states are immune to Anderson localization provided the disorder strength is smaller than the bulk gap [27]. This defining property was used by Schnyder *et al.* to establish a classification of topological insulators and superconductors as follows [28–30]. For a local disorder that is not too strong, its effect on extended boundary states dispersing through the gap of the bulk states can be treated as a problem of Anderson localization in $(d-1)$ dimensions. Following the classification by Altland and Zirnbauer of metallic or superconducting quantum dots (zero-dimensional space) in terms of ten universality classes [31–33], Schnyder *et al.* examined the possibility of adding either a Wess-Zumino-Witten (WZW) term or a $\mathbb{Z}_2$ topological term to the NLSM describing $(d-1)$-dimensional transport along a boundary under the assumption that the presence of such topological terms prevents Anderson localization of the boundary states. There follows a table with the ten Altland-Zirnbauer (AZ) symmetry classes as rows and the dimensionality d of space as columns (see Table I). The entries of this table, the tenfold way of topological insulators and superconductors, are identified as either a trivial insulator/superconductor when

TABLE I. The ten Altland-Zirnbauer (AZ) symmetry classes and their topological classification in terms of the zeroth homotopy groups of their classifying spaces. Two complex and eight real symmetry classes are characterized by the presence or the absence of time-reversal symmetry (T), particle-hole symmetry (C), and chiral symmetry (Γ). Their presence is complemented by the sign multiplying the identity in $T^2 = \pm 1$ or $C^2 = \pm 1$, and by 1 for Γ. Their absence is indicated by 0. For each symmetry class and for the dimension d of space, the relevant extension problem with its solution in terms of the classifying space $V_d \equiv \lim_{N\to\infty} V_{d,r_{\min} N}$ are given in the fifth and sixth columns, respectively. The zeroth homotopy groups of the classifying spaces for $d = 0, \ldots, 7$ are given in the last eight columns. Each entry with a nontrivial zeroth homotopy group of the classifying space defines a noninteracting topological (superconductor) insulator.

Class	T	C	Γ	Extension	V_d	$\pi_0(V_{d=0})$	$\pi_0(V_{d=1})$	$\pi_0(V_{d=2})$	$\pi_0(V_{d=3})$	$\pi_0(V_{d=4})$	$\pi_0(V_{d=5})$	$\pi_0(V_{d=6})$	$\pi_0(V_{d=7})$
A	0	0	0	$Cl_d \to Cl_{d+1}$	C_{0+d}	$\mathbb{Z}$	0	$\mathbb{Z}$	0	$\mathbb{Z}$	0	$\mathbb{Z}$	0
AIII	0	0	1	$Cl_{d+1} \to Cl_{d+2}$	C_{1+d}	0	$\mathbb{Z}$	0	$\mathbb{Z}$	0	$\mathbb{Z}$	0	$\mathbb{Z}$
AI	+1	0	0	$Cl_{0,d+2} \to Cl_{1,d+2}$	R_{0-d}	$\mathbb{Z}$	0	0	0	$\mathbb{Z}$	0	$\mathbb{Z}_2$	$\mathbb{Z}_2$
BDI	+1	+1	1	$Cl_{d+1,2} \to Cl_{d+1,3}$	R_{1-d}	$\mathbb{Z}_2$	$\mathbb{Z}$	0	0	0	$\mathbb{Z}$	0	$\mathbb{Z}_2$
D	0	+1	0	$Cl_{d,2} \to Cl_{d,3}$	R_{2-d}	$\mathbb{Z}_2$	$\mathbb{Z}_2$	$\mathbb{Z}$	0	0	0	$\mathbb{Z}$	0
DIII	−1	+1	1	$Cl_{d,3} \to Cl_{d,4}$	R_{3-d}	0	$\mathbb{Z}_2$	$\mathbb{Z}_2$	$\mathbb{Z}$	0	0	0	$\mathbb{Z}$
AII	−1	0	0	$Cl_{2,d} \to Cl_{3,d}$	R_{4-d}	$\mathbb{Z}$	0	$\mathbb{Z}_2$	$\mathbb{Z}_2$	$\mathbb{Z}$	0	0	0
CII	−1	−1	1	$Cl_{d+3,0} \to Cl_{d+3,1}$	R_{5-d}	0	$\mathbb{Z}$	0	$\mathbb{Z}_2$	$\mathbb{Z}_2$	$\mathbb{Z}$	0	0
C	0	−1	0	$Cl_{d+2,0} \to Cl_{d+2,1}$	R_{6-d}	0	0	$\mathbb{Z}$	0	$\mathbb{Z}_2$	$\mathbb{Z}_2$	$\mathbb{Z}$	0
CI	+1	−1	1	$Cl_{d+2,1} \to Cl_{d+2,2}$	R_{7-d}	0	0	0	$\mathbb{Z}$	0	$\mathbb{Z}_2$	$\mathbb{Z}_2$	$\mathbb{Z}$

no WZW and no $\mathbb{Z}_2$ topological term are allowed, a $\mathbb{Z}$ topological insulator/superconductor when a WZW term is allowed, or a $\mathbb{Z}_2$ topological insulator/superconductor when a $\mathbb{Z}_2$ topological term is allowed [28–30].

An alternative derivation of this table was proposed independently by Kitaev using K theory [34]. K theory enables a systematic study of a homotopical structure of gapped Hamiltonians in the bulk (upon the imposition of periodic boundary conditions, say) in the clean limit. Appropriately normalized gapped Hamiltonians define "a classifying space" for each AZ symmetry class. The tenfold way of topological insulators follows from the homotopy groups of the classifying spaces, with the additional insight that it obeys a periodicity that originates from the Bott periodicity in K theory. Since the periodic table is also obtained by using a representation theory of massive Dirac Hamiltonians [30], the approach relying on K theory also delivers a systematic classification of Dirac masses entering Dirac Hamiltonians satisfying the AZ symmetry constraints [35].

The goal of this paper is to reverse the logic of Schnyder *et al.* Instead of classifying topological insulators as an exercise in evading Anderson localization on the boundary, we seek to understand how topology determines Anderson localization in the bulk of a disordered insulator. To this end, we marry the approach pioneered by Ludwig *et al.* for the IQHE with that of Kitaev. In any dimension d and for any AZ symmetry class, we study all random Dirac Hamiltonians that support a Dirac mass. In particular, we show that the homotopy groups of the classifying spaces, regarded as the space of normalized Dirac masses in each AZ symmetry class, are essential to establish the phase diagram encoding Anderson localization for these random Dirac Hamiltonians.

Our approach gives a qualitative understanding of a generic global phase diagram of Anderson localization for any AZ symmetry class in one, two, three, etc. dimensions. Our phase diagram is consistent with previously known results and gives a simple and alternative explanation for the even-odd effect in the one-dimensional chiral classes [36–39]. We can also give a qualitative explanation for the Gade singularity [40–43] and Griffiths effects [44] in two dimensions for five out of the ten AZ symmetry classes in terms of the first homotopy group of the classifying spaces.

Our approach can also be adapted to analyze the stability of massless Dirac fermions on the surface of 3D topological crystalline insulators. We establish the conditions for the stability of the boundary states of statistical topological crystalline insulators (STCIs) that are protected by a crystalline (here a reflection) symmetry on average for the ten AZ symmetry classes. In this way, we show that the alloy $Sn_{1-x}Pb_xTe$ has surface states that are protected by the local symmetry class AII and the average reflection symmetry.

This paper is organized as follows. In Sec. II, we review the classification of topological insulators and superconductors using the K theory and present classifying spaces of normalized Dirac masses in Dirac Hamiltonians. In Sec. III, we relate the topology of classifying spaces to Anderson localization. In Secs. IV–VI, we apply our method to 1D, 2D, and 3D systems, respectively, to infer global phase diagrams. In Sec. VII, we briefly explain how one may use the classifying spaces to study the stability of boundary states of topological insulators. In Sec. VIII, we study the stability of the boundary states in a STCI. We present a summary in Sec. IX. In Appendix A, we present explicit constructions of 1D massive Dirac Hamiltonians and discuss some topological properties of the space of normalized Dirac masses. Finally, we discuss one-loop renormalization-group flows of random masses and potentials for 2D Dirac Hamiltonians in Appendix B.

II. CLASSIFYING SPACES OF NORMALIZED DIRAC MASSES

The key object of this paper is the set of allowed normalized Dirac masses for each dimension d of space, rank of the Dirac matrices, and AZ symmetry classes. This set can be attached a topology, i.e., it becomes a topological space. As a topological space, it is given by a classifying space associated with the extension problem of a Clifford algebra, which we

review in this section. Classifying spaces are characterized by homotopy groups that obey Bott periodicity, a property that carries over to the allowed normalized Dirac masses. The homotopy groups characterizing the allowed normalized Dirac masses are used to characterize the physics of Anderson localization in Secs. III–V.

This section is devoted to the systematic construction of the classifying spaces V_d that are given in the sixth column of Table I. To this end, we shall proceed in the following steps. First, we review the algebraic definition of Clifford algebras. Second, we review the relation between Clifford algebras and Dirac Hamiltonians. Third, we review the tenfold way for Clifford algebras. Fourth, we review the tenfold way for classifying spaces.

A. Definitions of Clifford algebras and their classifying spaces

The complex Clifford algebra

$$Cl_q \equiv \{e_1,\ldots,e_q\} \tag{2.1a}$$

is a complex vector space $\mathbb{C}^{2^q}$ of dimension 2^q that is spanned by the basis with the basis elements

$$e_{n_1\ldots n_q} \equiv \prod_{\iota=1}^{q}(e_\iota)^{n_\iota}, \quad n_1,\ldots,n_q = 0,1, \tag{2.1b}$$

whereby the multiplication rule

$$\{e_\iota,e_{\iota'}\} = 2\,\delta_{\iota,\iota'} \tag{2.1c}$$

applies $\iota,\iota' = 1,\ldots,q$. The vector space Cl_q is closed under multiplication of any two of its elements owing to Eq. (2.1c). Hence Cl_q is also an associative algebra.

The real Clifford algebra

$$Cl_{p,q} \equiv \{e_1,\ldots,e_p;e_{p+1},\ldots,e_{p+q}\} \tag{2.2a}$$

is a real vector space $\mathbb{R}^{2^{p+q}}$ of dimension 2^{p+q} that is spanned by the basis with the basis elements

$$e_{n_1\ldots n_{p+q}} \equiv \prod_{\iota=1}^{p+q}(e_\iota)^{n_\iota}, \quad n_1,\ldots,n_{p+q} = 0,1, \tag{2.2b}$$

whereby the multiplication rule

$$\{e_\iota,e_{\iota'}\} = 2\,\eta_{\iota,\iota'},$$
$$\eta_{\iota,\iota'} = \mathrm{diag}(\overbrace{-1,\ldots,-1}^{p\text{ times}},\overbrace{+1,\ldots,+1}^{q\text{ times}}), \tag{2.2c}$$

applies for $\iota,\iota' = 1,\ldots,p+q$. The vector space $Cl_{p,q}$ is closed under multiplication of any two of its elements owing to Eq. (2.2c). Hence $Cl_{p,q}$ is also an associative algebra.

Given a representation of the complex Clifford algebra Cl_q, "the extension problem" denoted

$$Cl_q \to Cl_{q+1} \tag{2.3}$$

consists in identifying "the classifying space" C_q that parameterizes the representation of the generator e_{q+1} present in Cl_{q+1} but absent in Cl_q. Similarly, given a representation of the real Clifford algebra $Cl_{p,q}$, there are two possible extension problems. There is the extension problem

$$Cl_{p,q} \to Cl_{p,q+1} \tag{2.4}$$

that consists in identifying the classifying space R_{q-p} that parameterizes the representation of the generator e_{p+q+1} present in $Cl_{p,q+1}$ and thus satisfying $e^2_{p+q+1} = +1$, but absent in $Cl_{p,q}$. There is the extension problem

$$Cl_{p,q} \to Cl_{p+1,q} \tag{2.5}$$

that consists in identifying the classifying space R_{p-q+2} that parameterizes the representation of the generator e_{p+1} present in $Cl_{p+1,q}$ and thus satisfying $e^2_{p+1} = -1$, but absent in $Cl_{p,q}$. The latter extension problem can be related to the former one through the homeomorphism

$$Cl_{p,q} \otimes Cl_{0,2} \simeq Cl_{q,p+2}, \tag{2.6}$$

where $Cl_{0,2}$ is a linear algebra of real two-dimensional matrices and does not affect the extension problem. Classifying spaces depend on the difference $q-p$ only because of the homeomorphism

$$Cl_{p+1,q+1} \simeq Cl_{p,q} \otimes Cl_{1,1} \simeq Cl_{p,q} \otimes Cl_{0,2}, \tag{2.7}$$

where dropping $Cl_{0,2}$ does not affect the extension problem.

Now, K theory makes the remarkable prediction that there are two families of complex classifying spaces C_0 and C_1, while there are eight families of real classifying spaces $R_0,\ldots,R_7$. In other words, the dependence on q enters modulo two for the complex classifying spaces,

$$C_{q+2} \simeq C_q, \tag{2.8a}$$

while it enters modulo eight for the real classifying spaces,

$$R_{q+8} \simeq R_q, \tag{2.8b}$$

according to Bott's periodicity [45]. All families of classifying spaces V in Table II are labeled by the integer number N entering the rank

$$r = r_{\min}N \tag{2.9}$$

assumed for the representation of the Clifford algebras.

B. Definition of minimal massive Dirac Hamiltonians

We assume that space is d-dimensional. The kinetic part of a translation-invariant Dirac Hamiltonian is

$$\mathcal{H}_{\mathrm{kin}}(\boldsymbol{k}) = \sum_{i=1}^{d} k_i\,\alpha_i, \tag{2.10a}$$

where $\boldsymbol{k} \equiv (k_1,\ldots,k_d) \in \mathbb{R}^d$ is the momentum and $\boldsymbol{\alpha} \equiv (\alpha_1,\ldots,\alpha_d)$ are the (Hermitian) Dirac matrices that obey the algebra

$$\{\alpha_i,\alpha_j\} = 2\delta_{i,j}, \quad i,j = 1,\ldots,d. \tag{2.10b}$$

On the one hand, we assume that the dimensionality of the representation of the matrices $\boldsymbol{\alpha}$ is sufficiently large so that there exists at least one Hermitian matrix β such that it anticommutes with all the components of $\boldsymbol{\alpha}$ and it squares to the identity matrix,

$$\{\beta,\mathcal{H}_{\mathrm{kin}}(\boldsymbol{k})\} = 0, \quad \beta^2 = 1. \tag{2.10c}$$

TABLE II. Complex and real classifying spaces are a list of ten topological spaces that are built out of the compact Lie groups U(N), O(N), and Sp(N)—the unitary, orthogonal, and symplectic matrix groups, respectively—and their quotients as is given in the column "Classifying space." The symbols denoting them are given in the column "Label." The number N is related to the rank $r = r_{\min} N$ of the Dirac matrices that form the Clifford algebras, i.e., $N = 1,2,\ldots$ is the number of copies of the minimal massive Dirac Hamiltonian of rank $r_{\min}$. Let $p = 0,1,\ldots$ index the pth homotopy group. The complex classifying spaces obey the periodicity condition $\pi_p(C_q) = \pi_{p+2}(C_q)$ for $q = 0,1$. The real classifying spaces obey the periodicity condition $\pi_p(R_q) = \pi_{p+8}(R_q)$ for $q = 0,\ldots,7$. Hence, an exhaustive list of the homotopy groups of the classifying spaces is shown in the columns "$\pi_0(V)$", "$\pi_1(V)$",...,"$\pi_7(V)$". In each homotopy column, the three entries $\mathbb{Z}$ hold for N larger than an integer (infinity included) that depends on the order of the homotopy group and the classifying space, the two entries $\mathbb{Z}_2$ hold for N larger than an integer that also depends on the order of the homotopy group and the classifying space. The entry 0 is a short hand for the group {0} made of the single element 0.

Label	Classifying space V	$\pi_0(V)$	$\pi_1(V)$	$\pi_2(V)$	$\pi_3(V)$	$\pi_4(V)$	$\pi_5(V)$	$\pi_6(V)$	$\pi_7(V)$
C_0	$\cup_{n=0}^{N}\{\mathrm{U}(N)/[\mathrm{U}(n)\times\mathrm{U}(N-n)]\}$	$\mathbb{Z}$	0	$\mathbb{Z}$	0	$\mathbb{Z}$	0	$\mathbb{Z}$	0
C_1	$\mathrm{U}(N)$	0	$\mathbb{Z}$	0	$\mathbb{Z}$	0	$\mathbb{Z}$	0	$\mathbb{Z}$
R_0	$\cup_{n=0}^{N}\{\mathrm{O}(N)/[\mathrm{O}(n)\times\mathrm{O}(N-n)]\}$	$\mathbb{Z}$	$\mathbb{Z}_2$	$\mathbb{Z}_2$	0	$\mathbb{Z}$	0	0	0
R_1	$\mathrm{O}(N)$	$\mathbb{Z}_2$	$\mathbb{Z}_2$	0	$\mathbb{Z}$	0	0	0	$\mathbb{Z}$
R_2	$\mathrm{O}(2N)/\mathrm{U}(N)$	$\mathbb{Z}_2$	0	$\mathbb{Z}$	0	0	0	$\mathbb{Z}$	$\mathbb{Z}_2$
R_3	$\mathrm{U}(2N)/\mathrm{Sp}(N)$	0	$\mathbb{Z}$	0	0	0	$\mathbb{Z}$	$\mathbb{Z}_2$	$\mathbb{Z}_2$
R_4	$\cup_{n=0}^{N}\{\mathrm{Sp}(N)/[\mathrm{Sp}(n)\times\mathrm{Sp}(N-n)]\}$	$\mathbb{Z}$	0	0	0	$\mathbb{Z}$	$\mathbb{Z}_2$	$\mathbb{Z}_2$	0
R_5	$\mathrm{Sp}(N)$	0	0	0	$\mathbb{Z}$	$\mathbb{Z}_2$	$\mathbb{Z}_2$	0	$\mathbb{Z}$
R_6	$\mathrm{Sp}(N)/\mathrm{U}(N)$	0	0	$\mathbb{Z}$	$\mathbb{Z}_2$	$\mathbb{Z}_2$	0	$\mathbb{Z}$	0
R_7	$\mathrm{U}(N)/\mathrm{O}(N)$	0	$\mathbb{Z}$	$\mathbb{Z}_2$	$\mathbb{Z}_2$	0	$\mathbb{Z}$	0	0

It is then possible to write the translation-invariant massive Dirac Hamiltonian

$$\mathcal{H}(\boldsymbol{k}) = \sum_{i=1}^{d} k_i\,\alpha_i + m\,\beta, \tag{2.10d}$$

where $m \in \mathbb{R}$ is a mass. However, the matrix β with its mass m (i.e., mass matrix in short) may not be unique. For example, if the Dirac matrices are chosen to be of rank two, then there are two linearly independent mass matrices anticommuting with each other in $d = 1$, one possible mass matrix in $d = 2$, and none in $d = 3$. On the other hand, the translation-invariant massive Dirac Hamiltonian (2.10d) becomes reducible for sufficiently large rank of the Dirac matrices. In any of the AZ symmetry classes, we may start from a sufficiently large matrix representation of the translation-invariant massive Dirac Hamiltonian (2.10d), which we then reduce until we reach the rank of the Dirac matrices below which we would lose all mass matrices. In this way, one obtains for each AZ symmetry class and dimension d an irreducible translation-invariant massive Dirac Hamiltonian of the form (2.10d) which is of minimum rank $r_{\min}$ (not necessarily unique in that more than one distinct mass matrix may be possible).

To which AZ symmetry class the Dirac Hamiltonian

$$\mathcal{H} = \sum_{i=1}^{d} \alpha_i\,\frac{\partial}{\mathrm{i}\partial x_i} + \beta\,m(\boldsymbol{x}) \tag{2.11}$$

belongs depends on whether it is possible to construct a combination from the triplet of operations

$$T \equiv \mathcal{T}\,\mathsf{K}, \quad C \equiv \mathcal{C}\,\mathsf{K}, \quad \Gamma, \tag{2.12a}$$

for time-reversal symmetry (TRS), particle-hole symmetry (PHS), and chiral symmetry (CHS), respectively (K denotes the operation of complex conjugation and $\mathcal{T}$, $\mathcal{C}$, and Γ are matrices sharing the same rank as the Dirac matrices $\boldsymbol{\alpha}$), such that

$$T^2 = \pm 1, \quad C^2 = \pm 1, \quad [T,C] = 0, \quad \Gamma^2 = 1, \tag{2.12b}$$

and

$$\text{TRS:} \quad [T,\mathcal{H}] = 0, \tag{2.13a}$$

$$\text{PHS:} \quad \{C,\mathcal{H}\} = 0, \tag{2.13b}$$

$$\text{CHS:} \quad \{\Gamma,\mathcal{H}\} = 0. \tag{2.13c}$$

(We have performed a global choice of gauge for which $[T,C] = 0$ holds.) Equations (2.13) are equivalent to

$$\text{TRS:} \quad [T,\beta] = \{T,\boldsymbol{\alpha}\} = 0, \tag{2.14a}$$

$$\text{PHS:} \quad \{C,\beta\} = [C,\boldsymbol{\alpha}] = 0, \tag{2.14b}$$

$$\text{CHS:} \quad \{\Gamma,\beta\} = \{\Gamma,\boldsymbol{\alpha}\} = 0. \tag{2.14c}$$

Observe here that the antiunitarity of T and C interchanges the action of commutators and anticommutators when acting on the mass relative to the kinetic part of the Dirac Hamiltonian (2.11).

C. The tenfold way for the Clifford algebras

We are ready to combine the Clifford algebras and their classifying spaces from Sec. II A with the AZ classification of massive Dirac Hamiltonians from Sec. II B. We associate with each AZ symmetry class, with each dimension d of space, and with any rank of the Dirac matrices $\boldsymbol{\alpha} \equiv (\alpha_1,\ldots,\alpha_d)$ equal to or larger than the minimal rank as defined below Eq. (2.10d), a Clifford algebra according to the following rules.

The symmetry classes A and AIII are associated with the complex Clifford algebra

$$\text{A:} \quad Cl_{d+1} = \{\beta,\boldsymbol{\alpha}\}, \tag{2.15a}$$

$$\text{AIII:} \quad Cl_{d+2} = \{\beta,\Gamma,\boldsymbol{\alpha}\}, \tag{2.15b}$$

respectively.

For the remaining eight symmetry classes, it is always possible to define the operation J that satisfies the relations

$$\{T,J\} = \{C,J\} = [\Gamma,J] = [\boldsymbol{\alpha},J] = [\beta,J] = 0, \quad (2.16)$$

and plays the role of an imaginary unit for the real Clifford algebras as $J^2 = -1$. The symmetry classes AI, BDI, D, DIII, AII, CII, C, and CI are associated with the real Clifford algebras [35]

$$\text{AI:} \quad Cl_{1,d+2} = \{J\,\beta; T, TJ, \boldsymbol{\alpha}\}, \quad (2.17a)$$
$$\text{BDI:} \quad Cl_{d+1,3} = \{J\,\boldsymbol{\alpha}, TCJ; C, CJ, \beta\}, \quad (2.17b)$$
$$\text{D:} \quad Cl_{d,3} = \{J\,\boldsymbol{\alpha}; C, CJ, \beta\}, \quad (2.17c)$$
$$\text{DIII:} \quad Cl_{d,4} = \{J\,\boldsymbol{\alpha}; C, CJ, TCJ, \beta\}, \quad (2.17d)$$
$$\text{AII:} \quad Cl_{3,d} = \{J\,\beta, T, TJ; \boldsymbol{\alpha}\}, \quad (2.17e)$$
$$\text{CII:} \quad Cl_{d+3,1} = \{J\,\boldsymbol{\alpha}, C, CJ, TCJ; \beta\}, \quad (2.17f)$$
$$\text{C:} \quad Cl_{d+2,1} = \{J\,\boldsymbol{\alpha}, C, CJ; \beta\}, \quad (2.17g)$$
$$\text{CI:} \quad Cl_{d+2,2} = \{J\,\boldsymbol{\alpha}, C, CJ; TCJ, \beta\}, \quad (2.17h)$$

respectively.

D. The tenfold way for the classifying spaces V

The definition of the classifying space V associated with the Dirac Hamiltonian (2.11) depends on the AZ symmetry class to which it belongs, the dimensionality d of space, and the rank r of the Dirac matrices $\boldsymbol{\alpha} = (\alpha_1, \ldots, \alpha_d)$, which is assumed larger than the minimal rank $r_{\min}$ defined in Sec. II B. The classifying space V encodes the fact that the mass matrix β in Eq. (2.11) might not be unique for given d and the rank of the Dirac matrices $\boldsymbol{\alpha} \equiv (\alpha_1, \ldots, \alpha_d)$. The construction of the classifying space V proceeds in the following steps.

Step 1. To each AZ symmetry class, we assign the following pair of Clifford algebras differing by one generator, holding the dimensionality d of space fixed and the rank of the Dirac Hamiltonian fixed. The Clifford algebra to the left of the arrow in the fifth column "extension" from Table I is obtained after removing from the tenfold list of Clifford algebras defined by Eqs. (2.15) and (2.17) one generator, namely, the mass matrix $J\,\beta$ for the symmetry classes AI and AII and the mass matrix β otherwise. This gives the tenfold list

$$\text{A:} \quad Cl_d = \{\boldsymbol{\alpha}\}, \quad (2.18a)$$
$$\text{AIII:} \quad Cl_{d+1} = \{\Gamma, \boldsymbol{\alpha}\}, \quad (2.18b)$$

and

$$\text{AI:} \quad Cl_{0,d+2} = \{; T, TJ, \boldsymbol{\alpha}\}, \quad (2.19a)$$
$$\text{BDI:} \quad Cl_{d+1,2} = \{J\,\boldsymbol{\alpha}, TCJ; C, CJ\}, \quad (2.19b)$$
$$\text{D:} \quad Cl_{d,2} = \{J\,\boldsymbol{\alpha}; C, CJ\}, \quad (2.19c)$$
$$\text{DIII:} \quad Cl_{d,3} = \{J\,\boldsymbol{\alpha}; C, CJ, TCJ\}, \quad (2.19d)$$
$$\text{AII:} \quad Cl_{2,d} = \{T, TJ; \boldsymbol{\alpha}\}, \quad (2.19e)$$
$$\text{CII:} \quad Cl_{d+3,0} = \{J\,\boldsymbol{\alpha}, C, CJ, TCJ; \}, \quad (2.19f)$$
$$\text{C:} \quad Cl_{d+2,0} = \{J\,\boldsymbol{\alpha}, C, CJ; \}, \quad (2.19g)$$
$$\text{CI:} \quad Cl_{d+2,1} = \{J\,\boldsymbol{\alpha}, C, CJ; TCJ\}. \quad (2.19h)$$

Step 2. For each AZ symmetry class, we seek *all* distinct Hermitian matrices sharing the same rank as the Dirac matrices $\boldsymbol{\alpha} \equiv (\alpha_1, \ldots, \alpha_d)$ such that they can be added to the list of generators entering the corresponding Clifford algebra from the tenfold list defined by Eqs. (2.18) and (2.19) so as to deliver the corresponding Clifford algebra from the tenfold list defined by Eqs. (2.15) and (2.17). These mass matrices form a set V, the classifying space. Determining V is an example of the extension problem in K theory. A characterization of the classifying space V can be deduced from K theory [34,45]. The outcome of this exercise is listed in the second column of Table II (owing to the Bott periodicity) for the case when the rank r of the Dirac matrices $\boldsymbol{\alpha} \equiv (\alpha_1, \ldots, \alpha_d)$ is

$$r = r_{\min} N, \quad (2.20)$$

where $r_{\min}$ is the rank of the minimal representation for the Dirac Hamiltonian (2.11) and N is an integer. Explicit examples for the construction of V can be found in Ref. [35].

The zeroth homotopy group of the classifying spaces is given in the third column of Table II. This homotopy group has the following physical consequences, as shown by Kitaev in Ref. [34]. Imagine that d-dimensional space is divided into two halves. Both halves share a $(d-1)$-dimensional boundary. Whenever the zeroth homotopy group of the classifying space in the tenfold way is nonvanishing, consider the Dirac Hamiltonian (2.11) with the mass term interpolating smoothly across the $(d-1)$-dimensional boundary between two fixed elements in the classifying space characterized by distinct values of the zeroth homotopy group. By the very definition of a homotopy group, this is only possible if the mass term vanishes along the $(d-1)$-dimensional boundary separating the two halves of d-dimensional space. As was shown by Jackiw and Rebbi for the symmetry class BDI when $d = 1$ [46], the Dirac Hamiltonian (2.11) must then support a zero mode that is extended along the $(d-1)$-dimensional boundary but exponentially localized away from it. This is the defining property of a topological insulator (superconductor). Hence, by combining the zeroth homotopy group of the classifying spaces given in the third column of Table II with the Bott periodicity (2.8), one infers which of the AZ symmetry classes allows a topological (superconductor) insulator for any given dimensionality d of space. The periodic table for topological (superconductors) insulators follows [30,34].

Another application of the zeroth homotopy groups associated with the classifying spaces is relegated to Appendix A, where we show in which sense one may declare that a mass matrix is "unique."

All higher homotopy groups of the classifying spaces are given in column four to ten of Table II, for they obey the periodicities

$$\pi_p(C_j) = \pi_{p+2}(C_j), \quad p = 0,1,2,\ldots, \quad (2.21a)$$

for the complex classes $j = 0,1$ and

$$\pi_p(R_j) = \pi_{p+8}(R_j), \quad p = 0,1,2,\ldots, \quad (2.21b)$$

for the real classes $j = 0,1,\ldots,7$. They also obey the translation rules

$$\pi_p(C_j) = \pi_{p+1}(C_{j+1}), \quad p = 0,1,2,\ldots, \quad (2.22a)$$

for the complex classes with the integers j and $j+1$ defined modulo 2 and

$$\pi_p(R_j) = \pi_{p+1}(R_{j-1}), \quad p = 0,1,2,\ldots, \tag{2.22b}$$

for the real classes with the integers j and $j-1$ defined modulo 8. If we combine these translations rules with the definition of V_d given in Table I, we find the relation

$$\pi_D(V_d) = \pi_0(V_{d-D}) \tag{2.23}$$

for any $D = 0,1,2,\ldots,d$.

E. Existence and uniqueness of normalized Dirac masses

We summarize the properties of d-dimensional Dirac Hamiltonians that follow from the topology of the classifying spaces V_d for the ten AZ symmetry classes. (1) For each symmetry class, there exists a minimum rank $r_{\min}(d)$, an even integer equal to or larger than the integer 2, for which the d-dimensional Dirac Hamiltonian supports a mass matrix and below which either no mass matrix or no Dirac kinetic contribution are allowed by symmetry.

(2) Suppose that the rank of the d-dimensional massive Dirac Hamiltonian is $r = r_{\min}(d)\,N$. When there exists a mass matrix squaring to unity (up to a sign) that commutes with all other symmetry-allowed mass matrices, we call it the unique mass matrix. There are the following three cases depending on the entries in the $\pi_0(V_d)$ column of Table I.

(i) $\pi_0(V_d) = \mathbb{Z}$: there is always a unique mass matrix for $N \geqslant 1$.

(ii) $\pi_0(V_d) = \mathbb{Z}_2$: there is a unique mass matrix $\beta_{\min}$ only when $N = 1$. When N is an even integer, for any given mass matrix, there exists another matrix that anticommutes with it. When N is an odd integer larger than 1, the matrix $\beta_{\min} \otimes \mathbb{1}_N$ plays a role similar to that of the unique mass matrix in that the two matrices $\pm\beta_{\min} \otimes \mathbb{1}_N$ belong to different connected components of V_d, even though there exists a normalized mass matrix that neither commutes nor anticommutes with $\beta_{\min} \otimes \mathbb{1}_N$.

(iii) $\pi_0(V_d) = 0$: for any given mass matrix, there exists another mass matrix that anticommutes with it. That is, there is no unique mass matrix for $N \geqslant 1$.

When (i) $N = 1$, (ii) the Dirac Hamiltonian has a unique mass matrix that realizes topologically distinct ground states for different signs of its mass, and (iii) the mass is varied smoothly in space, then domain boundaries along which the mass vanishes are accompanied by massless Dirac fermions, whose low-energy Hamiltonian is of rank $r_{\min}(d)/2$. It follows that $r_{\min}(d-1) = r_{\min}(d)$.

We illustrate in Appendix A these properties for 1D Dirac Hamiltonians in the ten AZ symmetry classes.

F. Relationship to higher homotopy groups

The zeroth homotopy group of a topological space indicates if it is path connected and, if not, how to index all its distinct subspaces that are path connected. Equation (2.23) relates the zeroth to the higher homotopy groups of the classifying spaces V_d defined in Table I. Equation (2.23) can be given the following interpretation.

We recall that the homotopy group $\pi_n(X)$ is the set of homotopy classes of maps $f : S^n \to X$ between the unit sphere S^n in $(n+1)$-dimensional Euclidean space and the topological space X. Following Teo and Kane in Ref. [47], we identify D in Eq. (2.23) as the dimensionality of the sphere S^D that surrounds a defect in d-dimensional space. For point, line, and surface defects, $D = d-1$, $d-2$, and $d-3$, respectively. In other words, $D+1$ is the codimension of such defects in d-dimensional space. A homotopy group $\pi_D(V_d)$ with more than one element signals that defects of codimension $D+1$ in the normalized Dirac masses can be indexed by a topological number. For given D and d, Eq. (2.23) [both d and $d-D$ on the left- and right-hand sides of $\pi_D(V_d) = \pi_0(V_{d-D})$, respectively, are defined either modulo 2 or modulo 8 depending on the AZ symmetry class] dictates through the homotopy reduction $D \to D-D = 0$ and the dimensional reduction $d \to d-D$ which five of the ten AZ symmetry classes support topological defects in their normalized Dirac masses. In particular, point defects inherit the topological numbers from the zeroth homotopy group of V_1. Any Dirac Hamiltonian with a defective normalized Dirac mass of topological character supports eigenstates with a vanishing energy eigenvalue (zero modes) that are bound to the defect in the directions transverse to it. These zero modes are robust to any local perturbation as long as they respect the AZ symmetry class and they are not too strong.

III. ANDERSON LOCALIZATION AND THE ZEROTH HOMOTOPY GROUP OF THE CLASSIFYING SPACES

We assume space to be d-dimensional. Furthermore, we assume that a microscopic lattice model with lattice spacing $\mathfrak{a}$ describing noninteracting fermions propagating in a static random environment respecting one of the ten symmetry constraints from the AZ symmetry classes is captured by the Dirac Hamiltonian

$$\mathcal{H} = \sum_{i=1}^{d} \alpha_i \frac{\partial}{\mathrm{i}\partial x_i} + V(\boldsymbol{x}) + \cdots, \tag{3.1a}$$

in the low-energy and long-wavelength limit. The rank of the Dirac matrices is

$$r = r_{\min} N, \tag{3.1b}$$

where $r_{\min}$ is the smallest rank that admits a Dirac mass matrix and $N = 1,2,\ldots$. Hence, for any $\boldsymbol{x} \in \mathbb{R}^d$, there exists a Dirac mass matrix $V(\boldsymbol{x})$ of rank r that competes with the kinetic contribution parameterized by the Dirac matrices $\boldsymbol{\alpha} = (\alpha_1, \ldots \alpha_d)$ [i.e., $V(\boldsymbol{x})$ anticommutes with $\boldsymbol{\alpha}$]. The matrix elements of the Dirac mass matrix $V(\boldsymbol{x})$ in Eq. (3.1a) are random functions of $\boldsymbol{x} \in \mathbb{R}^d$. The dots represent all other static random vector and scalar potentials allowed by the AZ symmetry class. We fix the chemical potential μ to be $\mu = 0$.

The matrix elements of the Dirac mass matrix $V(\boldsymbol{x})$ are assumed to be random functions that change smoothly in space on the length scale of ξ_{dis} ($\gg\mathfrak{a}$). Their correlations are assumed local in that these matrix elements that are not related by the AZ symmetries are uncorrelated up to an exponential precision beyond the finite length scale $\xi_{\mathrm{dis}} \gg \mathfrak{a}$, e.g., (disorder

averaging is denoted by an overline)

$$\overline{V(\boldsymbol{x})} =: \mathsf{m}\,\beta_0 \tag{3.1c}$$

and

$$\frac{1}{r}\overline{\mathrm{tr}[V(\boldsymbol{x})-\mathsf{m}\,\beta_0][V(\boldsymbol{y})-\mathsf{m}\,\beta_0]} =: \mathsf{g}^2\, e^{-|\boldsymbol{x}-\boldsymbol{y}|/\xi_{\mathrm{dis}}}, \tag{3.1d}$$

with all higher cumulants vanishing. The choice of the normalized Dirac mass matrix β_0 from the classifying space $V_{d,r}$ will be done in Secs. III A–III C in such a way that the parameter space $(\mathsf{m},\mathsf{g}) \in \mathbb{R} \times [0,\infty[$ captures the phase diagram representing the competition between delocalized and all topologically distinct localized phases of noninteracting fermions in a given d-dimensional AZ symmetry class. The former phase is favored by the Dirac kinetic contribution. The latter phase is favored by the Dirac masses. In other words, localized (insulating) phases are favored by large $|\mathsf{m}|$, whereas increasing g generates more density of states in the band (mass) gap and, in doing so, helps delocalization.

The main result of this section is captured by Fig. 1, a consequence of Table I, and Fig. 2. Let $V_{d,r}$ be the classifying space associated with any typical realization of the random Dirac Hamiltonian (3.1). We then have the following phases (at the band center $\varepsilon = 0$ of the quasiparticle dispersion). (a) If $\lim_{N\to\infty} \pi_0(V_{d,r_{\mathrm{min}}N}) = \mathbb{Z}$, there are $N+1$ topologically distinct insulating phases that are separated pairwise by either a critical point or a metallic phase. (b) If $\pi_0(V_{d,r_{\mathrm{min}}N}) = \mathbb{Z}_2$, there are two topologically distinct insulating phases that are separated by either a critical point or a metallic phase. (c) If $\pi_0(V_{d,r_{\mathrm{min}}N}) = 0$, there is only a topologically trivial insulating phase. When $d \geqslant 2$ (where the equality holds for class AII, CII, D, and DIII), the ground state is metallic for sufficiently large g.

The key intuition to support items (a) and (b) is the following. Since the spatial variation of $V(\boldsymbol{x})$ is assumed to be smooth for any realization of the disorder, d-dimensional space can be decomposed into open sets (domains) with the characteristic size ξ_{dis} such that (1) for each domain the values taken in it by $V(\boldsymbol{x})$ can be assigned an index from the zeroth homotopy group $\pi_0(V_{d,r})$ and (2) $\det[V(\boldsymbol{x})] = 0$ along the boundary of each domain.

Figure 2 is an illustration of this decomposition of d-dimensional space when either $\pi_0(V_{d,r}) = \mathbb{Z}$ or $\pi_0(V_{d,r}) = \mathbb{Z}_2$. There are then gapless modes bound to the boundaries of these domains. We use a semiclassical picture in analogy with the Chalker-Coddington network model of the IQHE. When no connected boundaries defined by the condition $\det[V(\boldsymbol{x})] = 0$ percolate across d-dimensional space, we expect an insulating phase. However, if a connected boundary along which $\det[V(\boldsymbol{x})] = 0$ percolates across d-dimensional space, we expect departure from an insulating phase. Quantum mechanics modifies this percolating picture by turning it into that of a Chalker-Coddington-like (quantum) network model in dimension d, whereby the scattering matrix at each node of the network is fixed by the AZ symmetry class and $r = r_{\mathrm{min}}\,N$.

A. Case of the zeroth homotopy group $\mathbb{Z}$

In each dimension d of space, there are three AZ symmetry classes whose classifying spaces $V_{d,r_{\mathrm{min}}N}$ are the unions of

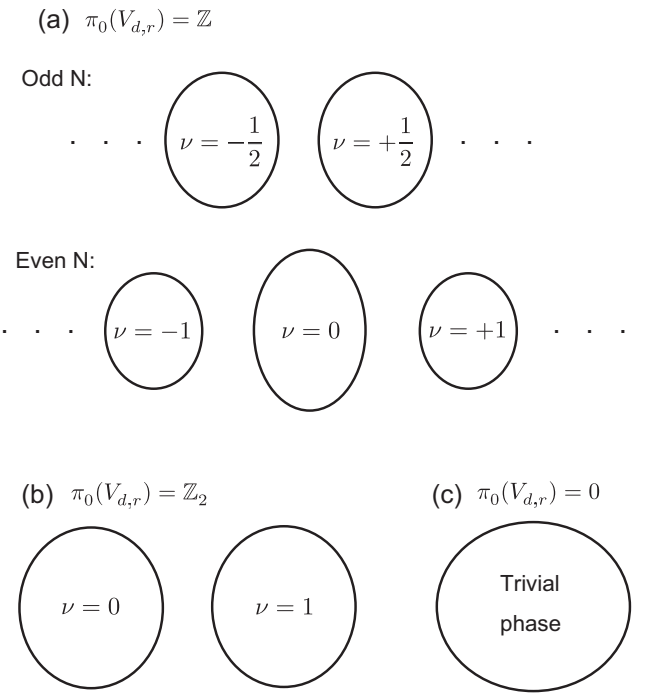

FIG. 1. Connectedness of the compact topological space $V_{d,r}$ parameterized by the normalized Dirac masses. The zeroth homotopy groups $\pi_0(V_{d,r})$ index the disconnected parts of the compact topological space $V_{d,r}$. The zeroth homotopy group $\pi_0(V_{d,r_{\mathrm{min}}N})$ is either (a) $\mathbb{Z}$ (in the limit $N \to \infty$), (b) $\mathbb{Z}_2$, or (c) $\{0\} \equiv 0$ according to Table II. (a) When $\pi_0(\lim_{N\to\infty} V_{d,r_{\mathrm{min}}N}) = \mathbb{Z}$, $V_{d,r_{\mathrm{min}}N}$ is disconnected and given by the union of path-connected and compact topological subspaces indexed by the half-integers or integers defined in Eq. (3.8c). For odd N, $V_{d,r_{\mathrm{min}}N}$ is the union of path-connected and compact topological subspaces labeled by negative and positive half integers. The total "volume" of the union of all subspaces with negative half-integer labels equals that of the union of all subspaces with positive half-integer labels when the mean values for the Dirac masses vanish. For even N, $V_{d,r_{\mathrm{min}}N}$ is the union of path-connected and compact topological subspaces labeled by the integers (3.8c). The total "volume" of the union of all subspaces with strictly negative integer labels equals that of the union of all subspaces with strictly positive integer labels when the mean values for the Dirac masses vanish. The subspace labeled by the integer 0 has a distinct (larger) "volume" when the mean values for the Dirac masses vanish. (b) When $\pi_0(V_{d,r}) = \mathbb{Z}_2$, $V_{d,r}$ is the union of two path-connected and compact topological subspaces that are indexed by the integers (3.15d) and are of equal "volume" when the mean values for the Dirac masses vanish. (c) When $\pi_0(V_{d,r}) = \{0\} \equiv 0$, $V_{d,r}$ is a path-connected and compact topological space.

one of the three Grassmannian manifolds, i.e., the classifying spaces are any one of

$$\bigcup_{n=0,\ldots,N} \{\mathrm{U}(N)/[\mathrm{U}(n)\times\mathrm{U}(N-n)]\}, \tag{3.2a}$$

$$\bigcup_{n=0,\ldots,N} \{\mathrm{O}(N)/[\mathrm{O}(n)\times\mathrm{O}(N-n)]\}, \tag{3.2b}$$

$$\bigcup_{n=0,\ldots,N} \{\mathrm{Sp}(N)/[\mathrm{Sp}(n)\times\mathrm{Sp}(N-n)]\}. \tag{3.2c}$$

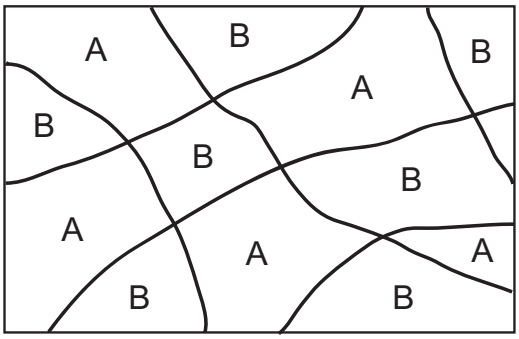

FIG. 2. For each realization of a random potential perturbing the massless Dirac Hamiltonian defined in d-dimensional Euclidean space $\mathbb{R}^d$, we may decompose $\mathbb{R}^d$ into open sets (domains) of linear size $\xi_{\rm dis}$. In each of these domains, the normalized Dirac masses correspond to a unique value of their zeroth homotopy group. At the boundary between domains differing by the values taken by their zeroth homotopy group, the Dirac masses must vanish. Such boundaries support quasi-zero-energy boundary states. When it is possible to classify the elements of the zeroth homotopy group by the pair of indices A and B, we may assign the letters A or B to any one of these domains as is illustrated. When the typical "volume" of a domain of type A equals that of type B, quasizero modes undergo quantum percolation through the sample and thus establish either a critical or a metallic phase of quantum matter in d-dimensional space.

These unions of Grassmannian manifolds are realized by the topological space of normalized Dirac masses whenever there exists a unique (up to a sign) normalized mass matrix that commutes with all other allowed normalized mass matrices. In the limit $N \to \infty$, the zeroth homotopy group of either one of these Grassmannian manifolds is $\mathbb{Z}$.

When the rank (3.1b) of the Dirac Hamiltonian (3.1a) belonging to any one of these AZ symmetry classes is the minimal one, $N = 1$ and there is a unique (up to a sign) normalized Dirac mass matrix β_0 of rank $r_{\rm min}$ such that

$$V(\boldsymbol{x}) = m(\boldsymbol{x})\,\beta_0 \tag{3.3}$$

in Eq. (3.1a). The Dirac Hamiltonian (3.1a) with the uniform mass $m > 0$ is topologically distinct from the Dirac Hamiltonian (3.1a) with the uniform mass $m < 0$. Correspondingly, the classifying spaces (3.2) reduce to

$$\bigcup_{n=0,1} \mathrm{U}(1)/[\mathrm{U}(n) \times \mathrm{U}(1-n)] \simeq \{-1,+1\}, \tag{3.4a}$$

$$\bigcup_{n=0,1} \mathrm{O}(1)/[\mathrm{O}(n) \times \mathrm{O}(1-n)] \simeq \{-1,+1\}, \tag{3.4b}$$

$$\bigcup_{n=0,1} \mathrm{Sp}(1)/[\mathrm{Sp}(n) \times \mathrm{Sp}(1-n)] \simeq \{-1,+1\}. \tag{3.4c}$$

If the Dirac mass matrix $V(\boldsymbol{x})$ of minimal rank is random with the statistical correlation (3.1c) and (3.1d), we may decompose d-dimensional space in disjoint domains as depicted in Fig. 2. A typical domain has the linear size $\xi_{\rm dis}$. In it $m(\boldsymbol{x}) \neq 0$ with a given sign, along its boundary $m(\boldsymbol{x}) = 0$, and a sign change is only permissible across this boundary into another domain with opposite and constant sign of the mass $m(\boldsymbol{x}) \neq 0$. Any boundary separating two domains with opposite signs of $m(\boldsymbol{x}) \neq 0$ binds gapless boundary states. Whenever two boundaries approach each other within a distance much smaller than $\xi_{\rm dis}$, boundary states undergo an elastic quantum scattering process dictated by the AZ symmetry class. In other words, Fig. 2 defines a quantum network model, whereby incoming plane waves along the boundaries defined by the condition $m(\boldsymbol{x}) = 0$ scatter off each other elastically at the nodes of this network of boundaries. The mean value m of the random Dirac mass $m(\boldsymbol{x})$ dictates the relative volume occupied by the domains with $\mathrm{sgn}[m(\boldsymbol{x})] = +1$ relative to the volume occupied by the domains with $\mathrm{sgn}[m(\boldsymbol{x})] = -1$. When $\mathsf{m} = 0$, both volume are typically equal, in which case the domain boundaries percolate across the system and the boundary states are delocalized and signal either a critical or a metallic phase.

The situation is different when $N = 2$. Indeed, the unions of Grassmannian manifolds (3.2) are now comprised of the pair of Grassmannians:

$$\mathrm{U}(2)/[\mathrm{U}(2) \times \mathrm{U}(0)], \quad \mathrm{U}(2)/[\mathrm{U}(0) \times \mathrm{U}(2)], \tag{3.5a}$$

$$\mathrm{O}(2)/[\mathrm{O}(2) \times \mathrm{O}(0)], \quad \mathrm{O}(2)/[\mathrm{O}(0) \times \mathrm{O}(2)], \tag{3.5b}$$

$$\mathrm{Sp}(2)/[\mathrm{Sp}(2) \times \mathrm{Sp}(0)], \quad \mathrm{Sp}(2)/[\mathrm{Sp}(0) \times \mathrm{Sp}(2)], \tag{3.5c}$$

with the dimensions 0, 0, and 0, respectively, and the Grassmannians

$$\mathrm{U}(2)/[\mathrm{U}(1) \times \mathrm{U}(1)], \tag{3.6a}$$

$$\mathrm{O}(2)/[\mathrm{O}(1) \times \mathrm{O}(1)], \tag{3.6b}$$

$$\mathrm{Sp}(2)/[\mathrm{Sp}(1) \times \mathrm{Sp}(1)], \tag{3.6c}$$

with the dimensions 2, 1, and 4, respectively. Accordingly, there are three topologically distinct insulating phases when $N = 2$. To derive the dimensions of these Grassmannian manifolds, we used the fact that $\mathrm{U}(n)$, $\mathrm{O}(n)$, and $\mathrm{Sp}(n)$ have the dimensions n^2, $n(n-1)/2$, and $n(2n+1)$, respectively.

Imagine that d-dimensional space is randomly decomposed into three types of domains according to the rule that the random Dirac mass matrix $V(\boldsymbol{x})$ is associated with only one of the three path-connected Grassmannian manifolds making up the classifying space (3.6) in each domain. The domain boundaries bind gapless states, percolation of which leads to delocalization or criticality between localized phases as in the case of $N = 1$. The transitions can be induced by changing the parameter m. Unlike the $N = 1$ case, however, the ground state at $\mathsf{m} = 0$ and for any nonvanishing g not too strong is most likely a localized phase. Indeed, localization is most likely to occur because d-dimensional space is randomly partitioned into domains such that most of the domains are characterized by a random Dirac mass matrix $V(\boldsymbol{x})$ associated with the path-connected Grassmannian manifolds of largest dimension in Eq. (3.6).

This difference between the $N = 1$ and 2 cases is not accidental. The same difference holds between the cases of odd N and even N integers, namely that the tuning $\mathsf{m} = 0$ delivers typically a critical or metallic phase of quantum matter in d-dimensional space when N is odd, while it delivers typically a localized phase of quantum matter in d-dimensional space when N is even, as we now explain.

When the classifying space $V_{d,r_{\min}N}$ is any one of the three unions of Grassmannian manifolds (3.2), we can always choose to represent the Dirac Hamiltonian (3.1a) with

$$\boldsymbol{\alpha} = \boldsymbol{\alpha}_{\min} \otimes \mathbb{1}_N \tag{3.7a}$$

for the Dirac kinetic contribution and

$$V(\boldsymbol{x}) = \beta_{\min} \otimes M(\boldsymbol{x}) \tag{3.7b}$$

for the Dirac mass contribution, whereby $\boldsymbol{\alpha}_{\min}$ and $\beta_{\min}$ represent the Clifford algebra with rank $r_{\min}$, while $\mathbb{1}_N$ is a unit $N \times N$ matrix and $M(\boldsymbol{x})$ is a random $N \times N$ Hermitian matrix which is a smooth continuous function of $\boldsymbol{x}$. For a given realization of the random matrix $M(\boldsymbol{x})$, we may partition d-dimensional space into domains whose boundaries are defined by $\det[M(\boldsymbol{x})] = 0$. Each domain can be assigned a topological index as follows. We may index each element of $\pi_0(V_{d,r_{\min}N})$ with the values of ν defined by

$$\nu := \frac{1}{2}\,\mathrm{tr}\{\mathrm{sgn}[M(\boldsymbol{x})]\} \in \begin{cases} \{-1/2,+1/2\}, & \text{if } N = 1, \\ \{-1,0,+1\}, & \text{if } N = 2, \\ \text{and so on}, & \text{if } N > 2, \end{cases} \tag{3.8a}$$

where the Hermitian matrix $M(\boldsymbol{x})$ is diagonalized by the unitary matrix $\mathrm{U}(\boldsymbol{x})$,

$$M =: U^\dagger\,\mathrm{diag}\,(\lambda_1,\ldots,\lambda_N)\,U \tag{3.8b}$$

and

$$\mathrm{sgn}[M(\boldsymbol{x})] := U^\dagger\,\mathrm{diag}\left(\frac{\lambda_1}{|\lambda_1|},\ldots,\frac{\lambda_N}{|\lambda_N|}\right)U. \tag{3.8c}$$

Each domain with $V(\boldsymbol{x})$ a smooth function of $\boldsymbol{x}$ has thereby been assigned the topological index ν.

We still need to *choose* the parameter space $(\mathsf{m},\mathsf{g}) \in \mathbb{R} \times [0,\infty[$ announced in Eqs. (3.1c) and (3.1d), when the zeroth homotopy group of the classifying space is $\mathbb{Z}$. We must distinguish two cases.

Case when $\mathsf{g} > 0$ *is a relevant perturbation to the clean critical point.* We select the normalized Dirac mass matrix

$$\beta_0 := \beta_{\min} \otimes \mathbb{1}_N, \tag{3.9a}$$

that anticommutes with all the components of $\boldsymbol{\alpha}$ and commutes with all Dirac mass matrices allowed for given r and symmetry constraints (see also Appendix A 3 a). The matrix β_0 is the unique mass matrix introduced in Sec. II E. We define the parameter space $(\mathsf{m},\mathsf{g}) \in \mathbb{R} \times [0,\infty[$ through the probability distribution of the Dirac mass matrix $V(\boldsymbol{x})$ given by

$$\overline{V(\boldsymbol{x})} =: \mathsf{m}\,\beta_0 \tag{3.9b}$$

and

$$\frac{1}{r}\,\overline{\mathrm{tr}\{[V(\boldsymbol{x}) - \mathsf{m}\,\beta_0][V(\boldsymbol{y}) - \mathsf{m}\,\beta_0]\}} =: \mathsf{g}^2\,e^{-|\boldsymbol{x}-\boldsymbol{y}|/\xi_{\mathrm{dis}}}, \tag{3.9c}$$

with all higher cumulants vanishing. With the definitions (3.9b) and (3.9c) for the probability distribution of $V(\boldsymbol{x})$, the point $\mathsf{m} = \mathsf{g} = 0$ is a massless Dirac critical point. The critical point $\mathsf{m} = \mathsf{g} = 0$ separates two insulating phases with $\nu = \pm N/2$ along the horizontal axis $\mathsf{g} = 0$ in parameter space. By assumption, $\mathsf{g} > 0$ is relevant in the vicinity of the clean critical point at $\mathsf{m} = \mathsf{g} = 0$. This is the rule when $d = 1$, in which case there appears for $\mathsf{g} > 0$ $N - 1$ additional localized phases, with $\nu = -(N/2)+1,-(N/2)+2,\ldots,(N/2)-1$ that are pairwise separated by lines of critical points, all of which emerge from the critical point $\mathsf{m} = \mathsf{g} = 0$, as was demonstrated in Ref. [36]. (It is the dimerization denoted by f in Ref. [36] that plays the role of m.) For those symmetry classes in $d = 2$ for which $\mathsf{g} > 0$ is (marginally) relevant in the vicinity of the clean critical point at $\mathsf{m} = \mathsf{g} = 0$, we conjecture that $N - 1$ additional localized phases that we may again label with $\nu = -(N/2)+1,-(N/2)+2,\ldots,(N/2)-1$ are stabilized when $\mathsf{g} > 0$. Consecutive localized phases are either separated by a line of critical points or by a metallic phase. The relevant symmetry classes are AIII, BDI, and CII in $d = 1$ and A and C in $d = 2$.

Case when $\mathsf{g} > 0$ *is an irrelevant perturbation to a clean critical point.* We define the parameter space $(\mathsf{m},\mathsf{g}) \in \mathbb{R} \times [0,\infty[$ through the probability distribution of the Dirac mass matrix $V(\boldsymbol{x})$ given by

$$\overline{V(\boldsymbol{x})} =: \mathsf{m}\,\beta_0 + V_0, \tag{3.10a}$$

where β_0 again commutes with all other mass matrices permitted by the symmetry class, and

$$\frac{1}{r}\,\overline{\mathrm{tr}\{[V(\boldsymbol{x}) - \overline{V(\boldsymbol{x})}][V(\boldsymbol{y}) - \overline{V(\boldsymbol{y})}]\}} =: \mathsf{g}^2\,e^{-|\boldsymbol{x}-\boldsymbol{y}|/\xi_{\mathrm{dis}}}. \tag{3.10b}$$

Here, V_0 is any mass matrix permitted by the symmetry that satisfies the condition

$$V_0 = \beta_{\min} \otimes M_0, \tag{3.10c}$$

where the $N \times N$ Hermitian matrix M_0 has N nondegenerate eigenvalues. The existence of the $r \times r$ Hermitian matrix V_0 is required to obtain $N + 1$ distinct localized phases in the phase diagram by changing the parameter m in the clean limit $\mathsf{g} = 0$. The prescription (3.10) applies to the symmetry class D in $d = 2$ and all symmetry classes with $\pi_0(V) = \mathbb{Z}$ in $d \geqslant 3$.

More discussions on the relationship between the RG flow of g and the probability distribution of the Dirac mass matrix $V(x)$ are presented in Sec. VI B for 3D disordered systems and in Appendix B 3 c for the 2D systems of the symmetry class D.

The zeroth homotopy group of the topological space $V_{d,r_{\min}N}$ encodes the connectedness of $V_{d,r_{\min}N}$. The "volume" of each path-connected component

$$\mathrm{U}(N)/[\mathrm{U}(n) \times \mathrm{U}(N-n)], \tag{3.11a}$$

$$\mathrm{O}(N)/[\mathrm{O}(n) \times \mathrm{O}(N-n)], \tag{3.11b}$$

$$\mathrm{Sp}(N)/[\mathrm{Sp}(n) \times \mathrm{Sp}(N-n)], \tag{3.11c}$$

of $V_{d,r_{\min}N}$ is measured by the dimension

$$2n(N-n) = N^2 - n^2 - (N-n)^2, \tag{3.12a}$$

$$n(N-n) = \frac{N(N-1) - n(n-1)}{2} - \frac{(N-n)(N-n-1)}{2}, \tag{3.12b}$$

$$4n(N-n) = N(2N+1) - (N-n)[2(N-n)+1] - n(2n+1), \tag{3.12c}$$

respectively, as is depicted schematically in Fig. 1(a).

When N is odd, one can always write

$$V_{d,r_{\min}N} = \mathrm{A} \cup \mathrm{B}, \tag{3.13a}$$

where

$$\mathrm{A} := \bigcup_{n=0,\ldots,\frac{N-1}{2}} \{\mathrm{U}(N)/[\mathrm{U}(N-n)\times\mathrm{U}(n)]\} \tag{3.13b}$$

and

$$\mathrm{B} := \bigcup_{n=\frac{N+1}{2},\ldots,N} \{\mathrm{U}(N)/[\mathrm{U}(n)\times\mathrm{U}(N-n)]\}, \tag{3.13c}$$

and similarly with the substitutions $\mathrm{U}\to\mathrm{O},\mathrm{Sp}$. The existence of a critical or metallic phase of quantum matter when $\mathsf{m}=0$ in the parametrization (3.9) follows from repeating the argumentation for the $N=1$ case that is captured by Fig. 2.

When N is even, one can always write

$$V_{d,r_{\min}N} = V_- \cup V_0 \cup V_+, \tag{3.14a}$$

where

$$V_- := \bigcup_{n=0,\ldots,\frac{N}{2}-1} \{\mathrm{U}(N)/[\mathrm{U}(N-n)\times\mathrm{U}(n)]\}, \tag{3.14b}$$

$$V_0 := \mathrm{U}(N)/[\mathrm{U}(N/2)\times\mathrm{U}(N/2)], \tag{3.14c}$$

and

$$V_+ := \bigcup_{n=\frac{N}{2}+1,\ldots,N} \{\mathrm{U}(N)/[\mathrm{U}(n)\times\mathrm{U}(N-n)]\}, \tag{3.14d}$$

and similarly with the substitutions $\mathrm{U}\to\mathrm{O},\mathrm{Sp}$. Since the index ν assigned to localized phases is an odd function of m, the ground state at $\mathsf{m}=0$ and g nonvanishing but not too large in the parametrization (3.9) is expected to be in the localized phase, for d-dimensional space is partitioned into domains of Dirac mass matrices, which are predominantly drawn from V_0.

B. Case of the zeroth homotopy group $\mathbb{Z}_2$

In each dimension d of space, there are two AZ symmetry classes whose classifying spaces $V_{d,r_{\min}N}$ are homeomorphic to either the orthogonal group $\mathrm{O}(N)$ or the quotient space $\mathrm{O}(2N)/\mathrm{U}(N)$ and thus have the zeroth homotopy group $\mathbb{Z}_2$. The former case is called the first descendant $\mathbb{Z}_2$. The second case is called the second descendant $\mathbb{Z}_2$. If so, we can always choose to represent the Dirac Hamiltonian (3.1a) with

$$\boldsymbol{\alpha} = \boldsymbol{\alpha}_{\min}\otimes\mathbb{1}_N \tag{3.15a}$$

for the Dirac kinetic contribution and

$$V(\boldsymbol{x}) = \rho_{\min}\otimes M(\boldsymbol{x}) \tag{3.15b}$$

for the Dirac mass contribution in each domain where the Dirac mass matrix $V(\boldsymbol{x})$ is continuous and invertible. Here, $\rho_{\min}$ is a $r_{\min}/2\times r_{\min}/2$ matrix such that, when tensored with the antisymmetric Pauli matrix σ_2, $\boldsymbol{\alpha}_{\min}$ and $\rho_{\min}\otimes\sigma_2$ deliver a representation of the Clifford algebra of rank $r_{\min}$. Finally, $\mathbb{1}_N$ is a unit $N\times N$ matrix and $M(\boldsymbol{x})$ is a $2N\times 2N$ Hermitian matrix which is also antisymmetric, i.e.,

$$M(\boldsymbol{x}) = M^\dagger(\boldsymbol{x}), \quad M(\boldsymbol{x}) = -M^{\mathsf{T}}(\boldsymbol{x}). \tag{3.15c}$$

Each domain in the partition of d-dimensional space into domains defined by the boundaries where $\det[M(\boldsymbol{x})]=0$ can be assigned a topological index as follows. We may index each element of $\pi_0(V_{d,r_{\min}N})$ with the values of $\nu=0,1$ defined by

$$(-1)^\nu := \frac{\mathrm{Pf}\,[\mathrm{i}M(\boldsymbol{x})]}{\sqrt{\det\,[\mathrm{i}M(\boldsymbol{x})]}}. \tag{3.15d}$$

This topological number ν is well-defined because $\mathrm{i}M(\boldsymbol{x})$ is a real-valued antisymmetric matrix and $\det\,[\mathrm{i}M(\boldsymbol{x})]$ is positive. Each domain has thereby been assigned the $\mathbb{Z}_2$-valued topological index ν.

When N is odd, we choose the parameter space $(\mathsf{m},\mathsf{g})\in\mathbb{R}\times[0,\infty[$ by selecting

$$\beta_0 := \rho_{\min}\otimes\sigma_2\otimes\mathbb{1}_N \tag{3.16a}$$

in the probability distribution of the Dirac mass matrix $V(\boldsymbol{x})$ given by

$$\overline{V(\boldsymbol{x})} =: \mathsf{m}\,\beta_0 \tag{3.16b}$$

and

$$\frac{1}{r}\,\overline{\mathrm{tr}\{[V(\boldsymbol{x})-\mathsf{m}\,\beta_0][V(\boldsymbol{y})-\mathsf{m}\,\beta_0]\}} =: \mathsf{g}^2\,e^{-|\boldsymbol{x}-\boldsymbol{y}|/\xi_{\mathrm{dis}}}, \tag{3.16c}$$

with all higher cumulants vanishing. In the clean limit $\mathsf{g}=0$, the point $\mathsf{m}=0$ is a massless Dirac critical point separating the two insulating phases with $\nu=0$ ($\mathsf{m}>0$) and $\nu=1$ ($\mathsf{m}<0$). Given $\mathsf{g}>0$, the d-dimensional space is decomposed into domains, and we may identify the domains labeled by A in Fig. 2 with $\nu=0$ and the domains labeled by B in Fig. 2 with $\nu=1$ for any realization of the random Dirac mass matrix $V(\boldsymbol{x})$. Hence, tuning the mean value m to some critical value (e.g., $\mathsf{m}=0$) realizes a situation where the domains A and B appear with equal probability and the domain boundaries percolate. This tuning stabilizes either a critical point or a metallic phase in d-dimensional space.

When N is even, we do not adopt the probability distribution (3.16), for it leads to the massless Dirac point $\mathsf{m}=\mathsf{g}=0$ separating two insulating phases belonging to the same topological phase with $\nu=0$ in the clean limit $\mathsf{g}=0$. For example, when we consider $N=2$ and the first descendant $\mathbb{Z}_2$ (see Appendix A 3 a), we may choose

$$\begin{aligned} M(\boldsymbol{x}) = {} & m_{2,0}(\boldsymbol{x})\,\sigma_2\otimes\tau_0 + m_{2,1}(\boldsymbol{x})\,\sigma_2\otimes\tau_1 \\ & + m_{2,3}(\boldsymbol{x})\,\sigma_2\otimes\tau_3 + m_{1,2}(\boldsymbol{x})\,\sigma_1\otimes\tau_2, \end{aligned} \tag{3.17}$$

where the quadruplets σ_μ and τ_μ, $\mu=0,1,2,3$, are made of the unit 2×2 matrix and the three Pauli matrices, respectively. In this case

$$(-1)^\nu = \mathrm{sgn}\big(m_{2,0}^2 + m_{1,2}^2 - m_{2,1}^2 - m_{2,3}^2\big). \tag{3.18}$$

If we define the controlling parameter m as in Eq. (3.16), we have $\overline{m_{2,0}}=\mathsf{m}$ and $\overline{m_{1,2}}=\overline{m_{2,1}}=\overline{m_{2,3}}=0$, for which the localized phase with $\nu=0$ always appear for nonvanishing m with sufficiently small g. Instead, we choose a probability distribution such that the massless Dirac point $\mathsf{m}=\mathsf{g}=0$ in the parameter space $(\mathsf{m},\mathsf{g})\in\mathbb{R}\times[0,\infty[$ separates two

TABLE III. Interplay between the topology of the normalized Dirac masses in a given AZ symmetry class and Anderson localization when space is one-dimensional. For each AZ symmetry class from the first column, (i) the second column gives the minimal rank $r_{\min}$ of the Dirac matrices for which a Dirac mass is allowed by the symmetries, (ii) the third column gives the corresponding topological space for the normalized Dirac masses $V_{d=1,r=r_{\min}N}$, (iii) the fourth column gives the corresponding zeroth homotopy group $\pi_0(V_{d=1,r=r_{\min}N})$, and (iv) the fifth column gives the corresponding panel from Fig. 3. Each panel from Fig. 3 is a phase diagram for quasiparticles at the Fermi energy, which is fixed to $\varepsilon = 0$ in the cases of the three chiral classes (AIII, BDI, and CII) and the four BdG classes (C, CI, D, and DIII). Parameter space is two-dimensional with the mean value $\mathsf{m} \in \mathbb{R}$ of the characteristic Dirac masses as horizontal axis and the characteristic disorder strength $\mathsf{g} \geqslant 0$ as vertical axis. The last column characterizes transport through the dependence of the mean conductance as a function of the length L of the disordered region when the random masses are identically distributed with a vanishing mean value $\mathsf{m} = 0$. Insulating and critical phases are characterized by a mean conductance that decays exponentially and algebraically fast with $L/(N\ell)$, respectively, where ℓ is the mean free path. The entries "even-odd" indicate that the conductance decays algebraically for odd N and exponentially fast for even N. In each of the zeroth homotopy column, the three entries $\mathbb{Z}$ hold in the limit $N \to \infty$, while the entry 0 is a short hand for the group $\{0\}$ made of the single element 0.

AZ symmetry class	$r_{\min}$	$V_{d=1,r}$	$\pi_0(V_{d=1,r})$	Phase diagram from Fig. 3	Cut at $\mathsf{m} = 0$
A	2	C_1	0	(c)	insulating
AIII	2	C_0	$\mathbb{Z}$	(a)	even-odd
AI	2	R_7	0	(c)	insulating
BDI	2	R_0	$\mathbb{Z}$	(a)	even-odd
D	2	R_1	$\mathbb{Z}_2$	(b)	critical
DIII	4	R_2	$\mathbb{Z}_2$	(b)	critical
AII	4	R_3	0	(c)	insulating
CII	4	R_4	$\mathbb{Z}$	(a)	even-odd
C	4	R_5	0	(c)	insulating
CI	4	R_6	0	(c)	insulating

insulating phases with $\nu = 0$ and $\nu = 1$ in the clean limit $\mathsf{g} = 0$. For the above example of $N = 2$, such a choice is given by

$$\overline{V(\boldsymbol{x})} = 0, \tag{3.19a}$$

$$\overline{m_{2,0}^2} + \overline{m_{1,2}^2} - \overline{m_{2,1}^2} - \overline{m_{2,3}^2} =: \mathsf{m}, \tag{3.19b}$$

and

$$\frac{1}{r}\,\overline{\mathrm{tr}\,[V(\boldsymbol{x})\,V(\boldsymbol{y})]} =: \mathsf{g}^2\, e^{-|\boldsymbol{x}-\boldsymbol{y}|/\xi_{\mathrm{dis}}}. \tag{3.19c}$$

For general values of N, we may adopt $\mathsf{m} := \overline{\mathrm{Pf}\,[\mathrm{i}M(\boldsymbol{x})]}$ instead of Eq. (3.16).

C. Case of the zeroth homotopy group {0}

In each dimension d of space, there are five AZ symmetry classes whose classifying spaces $V_{d,r}$ are compact and path-connected topological spaces and have thus a vanishing zeroth homotopy groups. We can always choose to represent the Dirac Hamiltonian (3.1a) with

$$\boldsymbol{\alpha} = \boldsymbol{\alpha}_{\min} \otimes \mathbb{1}_N \tag{3.20}$$

for the Dirac kinetic contribution, and then we choose $\beta_{\min}$ arbitrarily from the allowed $r_{\min} \times r_{\min}$ normalized Dirac mass matrices which anticommutes with all the components of $\boldsymbol{\alpha}_{\min}$.

For any of these five AZ symmetry classes, we choose the parameter space $(\mathsf{m},\mathsf{g}) \in \mathbb{R} \times [0,\infty[$ by selecting

$$\beta_0 := \beta_{\min} \otimes \mathbb{1}_N \tag{3.21a}$$

in the probability distribution of the Dirac mass matrix $V(\boldsymbol{x})$ given by

$$\overline{V(\boldsymbol{x})} =: \mathsf{m}\,\beta_0, \tag{3.21b}$$

$$\frac{1}{r}\,\overline{\mathrm{tr}\{[V(\boldsymbol{x}) - \mathsf{m}\,\beta_0][V(\boldsymbol{y}) - \mathsf{m}\,\beta_0]\}} =: \mathsf{g}^2\, e^{-|\boldsymbol{x}-\boldsymbol{y}|/\xi_{\mathrm{dis}}}, \tag{3.21c}$$

with all higher cumulants vanishing.

In these five AZ symmetry classes, the phase diagram has only a single localized phase that is adiabatically connected to a topologically trivial band insulator with reducing disorder.

Nevertheless, there can be anomalies of the conductivity and of the density of states at $\varepsilon = 0$ when higher than the zeroth homotopy group of $V_{d,r}$ have more than one elements, as we shall illustrate in Sec. V.

IV. APPLICATION TO 1D SPACE

The effects of static and local disorder are always strong in 1D space. The ballistic transport for a finite number N of 1D channels is unstable to disorder; Anderson localization rules. However, there are exceptions to the rule, i.e., the localization length and the density of states are divergent at the boundaries of insulating phases in the phase diagrams of the symmetry classes AIII, BDI, CII, D, and DIII. The main result of this section is that, according to Sec. III, these anomalies are caused by the nature of the disconnectedness of the topological space parameterized by the normalized Dirac mass as encoded by the zeroth homotopy group of the relevant classifying space in the third column of Table III.

We can apply the lessons from Sec. III to deduce the qualitative phase diagram for disordered 1D wires in any

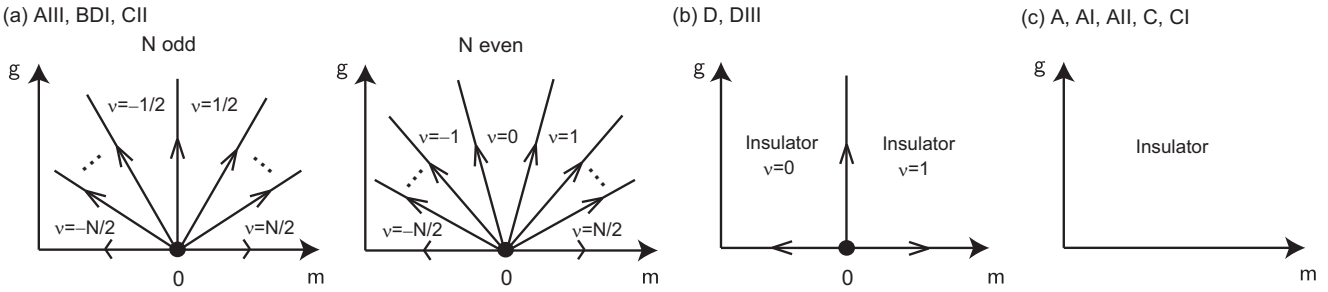

FIG. 3. Qualitative quantum phase diagrams for 1D disordered wires with the quasiparticle energy fixed at $\varepsilon = 0$. The horizontal axis is parameterized by the characteristic value $\mathsf{m} \in \mathbb{R}$ of the disorder-averaged Dirac masses allowed by the symmetry class. The vertical axis is parameterized by the characteristic value $\mathsf{g} \geqslant 0$ taken by the strength of the generic static and local random mass disorder allowed by the symmetry class. Arrows on the phase boundaries and on the horizontal axis indicate flows under renormalization group transformations.

symmetry class. The phase diagram is spanned by the control parameters m and g defined in Sec. III, as shown in Fig. 3.

We note that, regarding transport of quasiparticles of any nonvanishing energy ε, there are only three relevant symmetry classes, the standard symmetry classes A, AI, and AII. The chiral symmetry classes AIII, BDI, and CII and the BdG symmetry classes C, CI, D, and DIII show their characteristic transport properties at the band center $\varepsilon = 0$ of their quasiparticle spectra. In other words, a nonvanishing ε induces a crossover from one chiral or BdG class to one standard symmetry class [48].

Before presenting our results, we review the relevant literature.

A. A brief review

For one-dimensional lattice models with local random potentials, analytical results for the conductance and density of states have been obtained using the Fokker-Planck (FP) equation obeyed by the Lyapunov exponents of the 1D transfer matrix [36–39,48–55].

These results establish that the metallic phase (in the so-called quasi-one-dimensional (1D) limit defined by taking the number N of one-dimensional channels to infinity in a suitable way [56]) is always unstable to disorder away from the band center. Upon increasing the length of the 1D geometry, disorder drives a crossover to an (Anderson) insulating phase [49,50]. However, the band center $\varepsilon = 0$ is anomalous for seven of the ten AZ symmetry classes [36–39,48,51–55].

On the one hand, the chiral symmetry classes AIII, BDI, and CII display an even-odd effect in the parity of the number N of 1D transverse channels by which the disorder-averaged conductance at the band center alternates between exponential decay for even N and algebraic decay for odd N [36]. On the other hand, the disorder-averaged thermal conductance at the band center for any one of the superconducting symmetry classes D and DIII shows a mean conductance with algebraic decay for any N [51]. These results hold for Gaussian disorder with vanishing mean.

The density of states in the neighborhood of the band center also signals that the band center is a critical energy for the symmetry classes AIII, BDI, CII, D, and DIII separating two 1D Anderson insulating phases, as it fails to follow the dependence predicted by random matrix theory (i.e., a suppression of the density of states resulting from the enhanced level repulsion caused by the spectral symmetry about the band center) [38,52,54]. In contrast, the disorder-averaged conductance is exponentially suppressed with the length of the wire in the symmetry classes C, CI, A, AI, and AII for all energies while the density of states does not deviate from its expected behavior at the diffusive (unstable) fixed point.

The Fokker-Planck equation (the DMPK equation) obeyed by the Lyapunov exponents describing the transfer matrix in 1D contains universal data of geometric origin [39,57]. In each of the ten AZ symmetry classes, the 1D transfer matrix defines a noncompact symmetric space, of which the Lyapunov exponents are the radial coordinates [58,59]. An infinitesimal increase in the length of the disordered region for one of the ten symmetry classes induces an infinitesimal Brownian motion of the Lyapunov exponents that is solely controlled by the multiplicities of the ordinary, long, and short roots of the corresponding classical semi-simple Lie algebra under suitable assumptions on the disorder (locality, weakness, and isotropy between all channels). The long and short roots have a very special meaning with regard to Anderson localization. When the 1D transfer matrix describes the stability of the metallic phase of noninteracting fermions perturbed by one-body local random potentials in the bulk of a 1D lattice model, the multiplicity of the short root entering the Brownian motion of the Lyapunov exponents always vanish [36–39,48–55]. Moreover, the multiplicities of the long roots also vanish for the five 1D symmetry classes AIII, BDI, D, DIII, and CII [36,51]. This vanishing is the signature of the existence of critical points separating topological insulating phases in 1D wires. However, when the 1D transfer matrix describes the 1D boundary of a 2D topological band insulator moderately perturbed by local random potentials, the multiplicities of the short roots is nonvanishing in the Brownian motions of the Lyapunov exponents in the five AZ symmetry classes A, AII [60] D, DIII, and C. Correspondingly, the conductance is of order one along the infinitely long boundary, i.e., the insulating bulk supports extended edge states. These extended edge states can be thought of as realizing a 1D ballistic phase robust to disorder. The interpretation of a DMPK equation with nonvanishing multiplicity of the short root is that it describes transport along the boundary of a 2D topological insulator.

The same conclusions for the stability of a bulk 1D metallic phase [61–64], and for the stability of a 1D ballistic phase

along the boundary of a 2D band insulator perturbed by moderate disorder [28–30] also follow from describing these disordered noninteracting fermionic models with NLSMs. The role played by the multiplicities of the short roots in order to evade Anderson localization within the 1D transfer matrix approach is played by the presence of a topological term in the NLSM with the target spaces corresponding to the symmetry classes A, AII, D, DIII, and C [28–30].

B. $\pi_0(V_{d=1,r}) = \mathbb{Z}$

According to the third column of Table III, the topological space $V_{d=1,r=r_{\min}N}$ that parameterizes the space of Dirac masses is the union of the Grassmannian manifolds indexed by the number of 1D channels N for the symmetry classes AIII, BDI, and CII.

Figure 3(a) is the schematic phase diagram for the chiral symmetry classes AIII, BDI, and CII at the band center $\varepsilon = 0$. A 1D disordered wire with N channels is characterized by $N + 1$ distinct insulating phases that are indexed by the set of half-integers and integers with N odd and even, respectively. The flow of g along the phase boundary separating two neighboring insulating phases in Fig. 3(a) is to the infinitely strong disorder fix points $\mathsf{g} \to \infty$ [65,66]. The topological argument for this property is the following. The topological space $V_{d=1,r=r_{\min}N}$ parameterized by the Dirac masses allowed in any one of the three chiral symmetry classes is disconnected. One Dirac mass is singled out, the Dirac mass whose Dirac matrix commutes with all other Dirac masses present when $N > 1$: β_0 defined in Eq. (3.9a). The value m taken by averaging this mass over its probability distribution is the control parameter m that triggers a quantum phase transition between two distinct neighboring insulating phases in Fig. 3(a). At $\mathsf{m} = 0$, a disordered wire is in the $\nu = 0$ localized phase when N is even and on the phase boundary between the $\nu = \pm\frac{1}{2}$ insulating phases when N is odd. This qualitative even-odd effect in N that originates with the parity of the number of disconnected components $N + 1$ of $V_{d=1,r=r_{\min}N}$ is captured quantitatively by the Fokker-Planck approach [36–39,48,51–54], the NLSM approach [62–64,67], or the application of noncommutative geometry [68–71] and quantum-entanglement techniques [72]. One-parameter scaling is lost at the phase boundaries in the vicinity of the band center [36–39]. Recently, analytic results encoding a two-parameter scaling similar to that characterizing the integer quantum Hall effect were obtained for the symmetry classes AIII and BDI from the supersymmetric NLSM approach [64]. Moreover, the fanlike phase diagram depicted in Fig. 4(a), in which $N + 1$ localized phases emerge from $\mathsf{m} = \mathsf{g} = 0$, has been confirmed for the symmetry class BDI from a numerical study of the Lyapunov exponents of transfer matrices [64]. Note that a nonlinearity in the band dispersion makes the fanlike diagram asymmetric about $\mathsf{m} = 0$ in tight-binding models.

The anomalous behavior at the phase boundaries can be deduced from the results obtained previously by the Fokker-Planck approach [36–39,48,51–54]. At any phase boundary, the dimensionless Landauer conductance g shows anomalous dependence on the wire length L ($\gg N\ell$),

$$\overline{\ln g} \propto -\sqrt{\frac{L}{N\ell}}, \quad \ln \overline{g} \propto -\frac{1}{2}\ln\left(\frac{L}{N\ell}\right), \tag{4.1a}$$

and the density of states near $\varepsilon = 0$ has the strongest divergence, the Dyson singularity,

$$\rho(\varepsilon) \propto \frac{1}{|\varepsilon\tau\,[\ln(|\varepsilon|\tau)]^3\,|}, \tag{4.1b}$$

where $\tau = N^2\,\ell$, ℓ is the mean free path, and the Fermi velocity has been set to unity. The universal critical behavior (4.1) is a manifestation of an (unstable) infinite-disorder quantum critical point controlled by Griffiths effects [73–77].

In an insulating phase, the dimensionless conductance has exponential dependence on L,

$$\overline{\ln g} \propto -\frac{L}{\xi}, \tag{4.2}$$

where the localization length ξ is of order $N\,\ell$ and diverges at phase boundaries. The exponent in the power-law ε dependence of $\rho(\varepsilon)$ increases from -1 as m is changed from its value at a phase boundary. Half way between two consecutive transitions, the density of states is the closest to the prediction from random matrix theory,

$$\rho(\varepsilon) \propto (\varepsilon\tau)^{m_o-1}\,|\ln(\varepsilon\tau)|, \tag{4.3}$$

where $m_o = 1,2,4$ are the multiplicities of the ordinary roots for the chiral symmetry classes BDI, AIII, and CII, respectively [38]. However, the density of states (4.3) is not quite the one expected from random matrix theory, for it acquires a multiplicative logarithmic correction, as shown in Ref. [38]. The density of states interpolates between these two limiting functions as a function of the control parameter m [78].

C. $\pi_0(V_{d=1,r}) = \mathbb{Z}_2$

According to the third column of Table III, the topological space $V_{d=1,r=r_{\min}N}$ that parameterizes the normalized random Dirac mass in 1D has two disconnected components for the BdG symmetry classes D and DIII. Accordingly, there should be two topologically distinct insulating phases separated by a phase-boundary line, at which the localization length and the density of states diverge. Tuning the control parameter m defined in Sec. III B to zero selects the phase-boundary line [51,52,54], around which one-parameter scaling is broken [53,55,77].

Figure 3(b) is the phase diagram for the BdG symmetry classes D and DIII at the Fermi level $\varepsilon = 0$. A 1D disordered wire is characterized by two insulating phases that are separated by a phase boundary along which the disorder strength g flows to the infinitely strong disorder fix point, the Dyson fix point. This phase boundary is located at $\mathsf{m} = 0$. The topological argument for this property is the following. The topological space $V_{d=1,r=r_{\min}N}$ parameterized by the Dirac masses allowed in any one of these two BdG symmetry classes is made of two disconnected components. For any realization of the random potential these two components are indexed by the $\mathbb{Z}_2$ index defined in Eq. (3.8). Hence the control parameter m that drives the quantum phase transition between the two distinct insulating phases can be chosen to be the disorder-averaged value over this Pfaffian. On the other hand, had we started from the symmetry class BDI and weakly broken the time-reversal and chiral symmetries

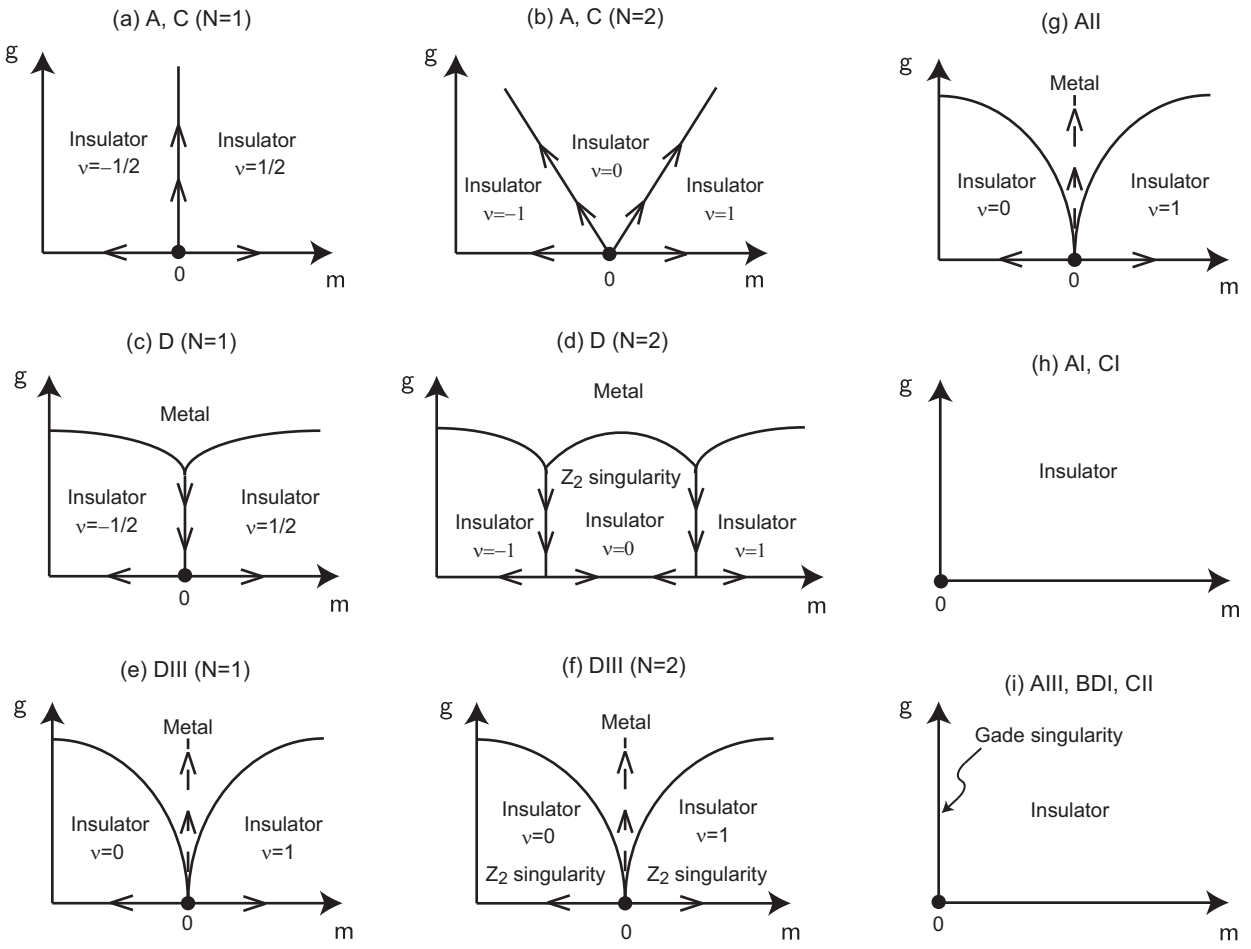

FIG. 4. Qualitative quantum phase diagrams for 2D random Dirac Hamiltonians with the quasiparticle energy fixed at $\varepsilon = 0$. The horizontal axis is parameterized by the characteristic value $\mathsf{m} \in \mathbb{R}$ of the disorder-averaged Dirac masses allowed by the symmetry class. We choose the probability distribution (3.10) for the case of $N = 2$ in the symmetry class D. The vertical axis is parameterized by the characteristic value $\mathsf{g} \geqslant 0$ taken by the strength of the generic local disorder allowed by the 2D AZ symmetry class. The zeroth homotopy group associated with the space of normalized Dirac mass fixes the indexing of the topologically distinct insulating phases. The first homotopy group of the normalized Dirac masses determines if the density of states is regular or singular at the band center. The existence of a metallic phase, the flows along phase boundaries, and the dimensionality of the phase boundaries all follow from perturbative renormalization-group calculations.

by the addition of weak perturbations that bring the Dirac Hamiltonian to one in the symmetry class D, we may then keep the control parameter m of the symmetry class BDI along the horizontal axis in parameter space. There follows the same phase diagram as in Fig. 4(a) with the caveat that the $N + 1$ unperturbed localized phases with the $\mathbb{Z}$ topological numbers ν become $N + 1$ localized phases with alternating $\mathbb{Z}_2$ topological numbers ν after perturbation [78].

The anomalous behavior at the phase boundary can be deduced from the results obtained previously by the Fokker-Planck approach [51–54]. The anomalous dependence on the wire length L of the dimensionless Landauer conductance g is the same as Eq. (4.1a), and the density of states $\rho(\varepsilon)$ exhibits the Dyson singularity (4.1b). In the insulating phases the conductance has the exponential dependence on L, Eq. (4.2). The density of states $\rho(\varepsilon)$ has the power-law dependence on the excitation energy ε with the exponent continuously varying from -1 of the Dyson singularity to the exponent of the random matrix theory [33] (0 and 1 for class D and DIII, respectively), as $|\mathsf{m}|$ is increased from the critical point $\mathsf{m} = 0$. The fact that the symmetry classes D and DIII share with the chiral symmetry classes the same Dyson singularity is known as "superuniversality" [55,78].

D. $\pi_0(V_{d=1,r}) = \{0\}$

According to the third column of Table III, the topological space $V_{d=1,r=r_{\min} N}$ that parameterizes the normalized random Dirac masses is path-connected for the symmetry classes A, AI, AII, C, and CI. Figure 3(c) is the schematic phase diagram for the symmetry classes A, AI, AII, C, and CI at $\varepsilon = 0$ and to all symmetry classes away from $\varepsilon = 0$. A 1D disordered wire is always localized in these symmetry classes. The topological argument for this property is the following. The topological space $V_{d=1,r}$ parameterized by the Dirac masses allowed in any one of these five symmetry classes is path connected. Consequently, the sign of m has no topological meaning. The allowed Dirac masses select a unique insulating phase.

The density of states in the vicinity of the quasiparticle energy $\varepsilon = 0$ is affected by the enhanced level repulsion in the

BdG symmetry classes C and CI, but this effect is captured by random matrix theory [33] since the localization length is never divergent [51,52]; $\rho_{\rm C}(\varepsilon) \propto \varepsilon^2$ and $\rho_{\rm CI}(\varepsilon) \propto |\varepsilon|$.

V. APPLICATION TO 2D SPACE

This section is dedicated to Anderson localization in the ten 2D AZ symmetry classes when a local disorder is present. First, we review known facts about these 2D disordered systems. Unlike the Fokker-Planck approach for which we only know how to extract controlled analytical results in 1D [79], the NLSM approach delivers perturbative renormalization-group (RG) results in any dimensions close to 2D [80]. We then show how the topology of classifying spaces combined with perturbative RG flows allow to deduce the phase diagram that delimits the topologically distinct localized and metallic phases for each 2D AZ symmetry class. This analysis delivers a unifying explanation for many past analytical and numerical results regarding Anderson localization in the 2D symmetry classes when the disorder is local.

A. A brief review

In the symmetry classes AI, all the single-particle states are exponentially localized upon perturbation by a random potential. This result is understood perturbatively as the phenomenon of weak localization by which the first nonvanishing quantum correction to the longitudinal conductivity caused by a disorder is negative [81]. This result is also understood nonperturbatively as a consequence of the fact that the 2D NLSM that encodes the physics of Anderson localization in the symmetry class AI has a coupling, the inverse of the value of the longitudinal conductivity in the diffusive regime, that flows to strong coupling [82,83].

In the symmetry class A, the phase diagram of single-particle states consists of multiple of localized phases that are distinguished by their quantized Hall conductivity and are separated by phase boundaries at which the localization length diverges [6,7,11–13,84]. The existence of critical points separating neighboring localized phases can be understood as a result of the topological term which can be added to the 2D NLSM for class A [13]. These critical states levitate with increasing disorder strength until they "annihilate" upon merging [84,85].

In the 2D symmetry class AII, only the single-particle states close to the edges of the Bloch bands are exponentially localized in the presence of a weak disorder [82,83]. As the disorder strength is increased, the lower and upper mobility edges separating in energy the Lifshitz tails from the extended single-particle states approach each other until they merge and all single-particle states are exponentially localized for sufficiently strong disorder.

Consequently, the metallic phase for noninteracting electrons propagating in 2D space is unstable to the presence of any local disorder in the symmetry classes A and AI, while it is stable for a sufficiently weak disorder in the symmetry class AII, as long as the chemical potential is sufficiently far from the unperturbed band edges.

These three outcomes for the competition between the kinetic energy and the local random potential in 2D space are not exhaustive in the presence of a particle-hole or a chiral symmetry, as it does in the symmetry classes AIII, BDI, D, DIII, CII, C, and CI. Among the BdG symmetry classes, symmetry class CI is insulating very much in the same way as symmetry class AI is [86]. Symmetry class C can display a spin IQHE very much in the same way as symmetry class A can display the charge IQHE [86]. The metallic phases in the symmetry classes D and DIII are stable to weak disorder [87–89]. Symmetry class D can display a thermal IQHE very much in the same way as symmetry class A can display the charge IQHE [88,90–92]. Symmetry class DIII can realize a thermal $\mathbb{Z}_2$ topological insulator very much in the same way as symmetry class AII can [28,93]. Finally, the chiral classes AIII, BDI, and CII are anomalous at the band center with diverging localization length and density of states, while they crossover to the symmetry classes A, AI, and AII, respectively, for any nonvanishing value of the chemical potential [40,41].

All of these features that are of topological origin can be understood qualitatively from the zeroth and first homotopy groups from Table IV, as we now explain below.

B. Implications of the topology of the classifying spaces

Equation (3.1) with $d = 2$ and with the rank $r = r_{\rm min} N$ is our starting point. It is assumed that the local random disorder entering the Dirac Hamiltonian is the most general $r \times r$ Hermitian matrix with random identically independently distributed (iid) matrix elements up to the constraints imposed by the selected AZ symmetry classes. We fix the chemical potential $\mu = 0$ and discuss transport properties of quasiparticles of energy $\varepsilon = 0$ for all ten symmetry classes.

For each AZ symmetry class in the first column of Table IV, we give the minimum rank $r_{\rm min}$ for which the Dirac Hamiltonian admits a Dirac mass, the classifying space $V_{d=2,r}$, its zeroth homotopy group $\pi_0(V_{d=2,r_{\rm min}N})$, its first homotopy group $\pi_1(V_{d=2,r_{\rm min}N})$, and its phase diagram for $N = 1$ and $N = 2$. All other entries hold for any N. Each panel from Fig. 4 is a phase diagram in a two-dimensional parameter space. The horizontal and vertical axes are the characteristic mean value m of the Dirac masses and the characteristic disorder strength g, respectively, introduced in Sec. III. The last column characterizes transport through the dependence of the mean conductivity as a function of the linear length L of the disordered region when $\mathsf{m} = 0$ and $\varepsilon = 0$. Insulating phases are characterized by a mean conductivity that decays exponentially with L. A metallic phase has a mean conductivity that grows with L. Critical phases have a mean conductivity that is nonvanishing but finite for $L \to \infty$. The entry "even-odd" indicates that the parity of N selects either an insulating or a critical phase, depending on whether N is even or odd, respectively. The new entry "Gade singularity" compared to the 1D Table III signals a conductivity that is independent of the disorder strength and a divergence of the density of states upon approaching the band center. This new entry is a signature of $\pi_1(V_{d=2,r}) = \mathbb{Z}$, as we are going to explain.

The main result of this section is that, according to Sec. III, there are deviations in Table IV away from the insulating behavior found in the 2D symmetry classes AI and CI. These deviations are attributed to the zeroth and first homotopy

TABLE IV. Interplay between the topology of the normalized Dirac masses in a given AZ symmetry class and Anderson localization when space is two-dimensional. For each AZ symmetry class from the first column, (i) the second column gives the minimal rank $r_{\min}$ of the Dirac matrices for which a Dirac mass is allowed by the symmetries, (ii) the third column gives the corresponding topological space for the normalized Dirac masses $V_{d=2,r=r_{\min}N}$, (iii) the fourth column gives the corresponding zeroth homotopy group $\pi_0(V_{d=2,r=r_{\min}N})$, (iv) the fifth column gives the corresponding first homotopy group $\pi_1(V_{d=2,r=r_{\min}N})$, and (v) the sixth column gives the corresponding panel from Fig. 4. Each panel from Fig. 4 is a phase diagram for quasiparticles at the Fermi energy, which is fixed to $\varepsilon = 0$. Parameter space is two-dimensional with the mean value $\mathsf{m} \in \mathbb{R}$ for the characteristic Dirac masses as horizontal axis and the characteristic disorder strength $\mathsf{g} \geqslant 0$ as vertical axis. The last column characterizes transport through the dependence of the mean conductivity as a function of the linear length L of the disordered region when $\mathsf{m} = 0$. Insulating phases are characterized by a mean conductivity that decays exponentially with L. A metallic phase has a mean conductivity that grows with L. A critical phase has a mean conductivity of the order of e^2/h. The entries "even-odd" indicate a critical or metallic phase for odd N and an insulating phase for even N. The entries "Gade singularity" indicate a diverging density of state associated with $\pi_1(V_{d=2,r}) = \mathbb{Z}$. In each homotopy column, the three entries $\mathbb{Z}$ hold for N larger than an integer (infinity included) that depends on the order of the homotopy group and the classifying space, the two entries $\mathbb{Z}_2$ hold for N larger than an integer that also depends on the order of the homotopy group and the classifying space. The entry 0 is a short hand for the group {0} made of the single element 0.

AZ symmetry class	$r_{\min}$	$V_{d=2,r}$	$\pi_0(V_{d=2,r})$	$\pi_1(V_{d=2,r})$	Phase diagram from Fig. 4	Cut at $\mathsf{m} = 0$
A	2	C_0	$\mathbb{Z}$	0	(a) and (b)	even-odd
AIII	4	C_1	0	$\mathbb{Z}$	(i)	Gade singularity
AI	4	R_6	0	0	(h)	insulating
BDI	4	R_7	0	$\mathbb{Z}$	(i)	Gade singularity
D	2	R_0	$\mathbb{Z}$	$\mathbb{Z}_2$	(c) and (d)	even-odd
DIII	4	R_1	$\mathbb{Z}_2$	$\mathbb{Z}_2$	(e) and (f)	metallic
AII	4	R_2	$\mathbb{Z}_2$	0	(g)	metallic
CII	8	R_3	0	$\mathbb{Z}$	(i)	Gade singularity
C	4	R_4	$\mathbb{Z}$	0	(a) and (b)	even-odd
CI	8	R_5	0	0	(h)	insulating

groups of the normalized Dirac masses being either $\mathbb{Z}_2$ or $\mathbb{Z}$.

C. $\pi_0(V_{d=2,r}) = \mathbb{Z}$

According to Table IV, the 2D AZ symmetry classes A, D, and C are associated with Grassmannian manifolds. Hence the zeroth homotopy group of the topological spaces associated with the normalized Dirac masses in these AZ symmetry classes is $\mathbb{Z}$. According to Sec. III, their phase diagrams must host $N + 1$ topologically distinct insulating phases and N transition lines separating them.

The arguments of Sec. III follow from the zeroth homotopy group of the Grassmannian manifolds. The 2D symmetry classes A and C share the same trivial first homotopy group. In view of the fact that the 2D metallic phase is perturbatively unstable (due to weak localization) in both symmetry classes (a fact not encoded in the homotopy groups of Table IV), we expect 2D phase diagrams in the 2D symmetry classes A and C that are similar to the one in the 1D chiral symmetry classes, the one shown in Figs. 4(a) and 4(b) for $N = 1$ and $N = 2$, respectively.

Contrary to the 2D symmetry classes A and C, the metallic phase of the 2D symmetry class D is stable (due to weak antilocalization) to weak disorder. Hence the 2D symmetry class D is expected to host a (thermal) metallic phase when the characteristic disorder strength g is sufficiently large, in addition to $N + 1$ topologically distinct insulating phases. When the metallic phase is robust to weak disorder, topologically distinct localized phases can be separated by a metallic phase rather than by a mere phase boundary line. It is the RG flow of the random Dirac mass in the Dirac Hamiltonian that determines which of the metallic phase or the critical boundary separates two topologically distinct insulating phases. Now, the characteristic coupling g for the disorder is marginally irrelevant in the vicinity of the critical point $\mathsf{m} = 0$, $\mathsf{g} = 0$ for the symmetry class D with $N = 1$, as is reviewed in Appendix B. Consequently, there is a RG flow along the phase boundary between topologically distinct insulating phases into the critical point $\mathsf{m} = 0$, $\mathsf{g} = 0$ when $N = 1$. More generally, phase boundaries separate topologically distinct insulating phases at small g. Thus, starting from any of the $N + 1$ insulating phase separated by phase boundaries, we have a transition driven by increasing g into the metallic phase of the 2D symmetry class D, as shown in Figs. 4(c) ($N = 1$) and 4(d) ($N = 2$). With regard to the case of $N > 1$, say $N = 2$ as depicted in Fig. 4(d), we are choosing the probability distribution (3.10) to parametrize the horizontal axis of the phase diagram instead of the probability distribution (3.9) used to parametrize the horizontal axis of the phase diagram 4(c) when $N = 1$. (See Appendix B 3 c for a more detailed discussion of the relationship between the irrelevant RG flow of g and the expectation values of mass terms.) Moreover, the Grassmannian manifold for the 2D symmetry class D also differs from that for the symmetry classes A and C in that its first homotopy group is nontrivial and given by $\mathbb{Z}_2$. In the $N = 2$ case, it is the path-connected component $\mathrm{O}(2)/\mathrm{O}(1) \times \mathrm{O}(1)$ from the space of Dirac masses (the $\nu = 0$ insulating phase) that has a nontrivial first homotopy group and can thus host $\mathbb{Z}_2$ vortices, each supporting a Majorana zero mode. Such zero modes would lead to a Griffiths-like singularity at $\varepsilon = 0$ in the density of states. However, $\mathbb{Z}_2$ vortices are not expected to exist in any insulating phase whose space of Dirac masses has a trivial first homotopy group. For example, in the $N = 2$ case, the pointlike components

$O(2)/O(2) \times O(0)$ or $O(2)/O(0) \times O(2)$ from the space of Dirac masses (the $\nu = \pm 1$ insulating phases) have a trivial first homotopy group. Hence, if it is the $\nu = \pm 1$ insulating phases of Dirac fermions in the symmetry class D with $N = 2$ that are realized in the vicinity of $\varepsilon = 0$, then no Griffiths-like singularity is expected at $\varepsilon = 0$ in the density of states. In other words, we expect a density of states that deviates from the one predicted by random matrix theory in the symmetry class D for any insulating phase supporting Majorana zero modes bound to $\mathbb{Z}_2$ Dirac mass vortices [94].

These predictions are consistent with the following numerical studies of 2D quantum network models. The cases $N = 1$ and $N = 2$ in the symmetry class A are the best known applications of quantum network models. Chalker and Coddington studied numerically in Ref. [14] the 2D quantum network model corresponding to the case $N = 1$ in the symmetry class A [15,95]. Lee and Chalker studied numerically in Ref. [96] the 2D quantum network model corresponding to the case $N = 2$ in the symmetry class A with their investigation of spin-degenerate Landau levels and found two quantum phase transitions separating three insulating phases of 2D quantum matter. Two-dimensional quantum network models for the symmetry class C have also been studied analytically and numerically [97–100]. They deliver the same phase diagrams as for the 2D symmetry class A. The case of $N = 1$ in the symmetry class D can also be regularized by a 2D quantum network model with nodal scattering matrices of appropriate symmetry and rank [91], or by two-band lattice models for Majorana fermions [101]. The former model shows a critical boundary with the attractive fixed point corresponding to the Dirac Hamiltonian at $\mathsf{m} = \mathsf{g} = 0$ that separates two insulating phases of 2D quantum matter for not too strong g, as shown in Fig. 4(c) when $N = 1$. The two insulating phases are unstable to the metallic phase upon increasing g, as shown in Fig. 4(c). There have been numerical studies on the critical properties around the multicritical point where the two insulating and one metallic phases meet at $\mathsf{g} > 0$ [92,93]. For $N = 2$, there are three insulating phases on top of which sits a metallic phase, as shown in Fig. 4(d). Moreover, quasizero modes bound to $\mathbb{Z}_2$ vortices in the Dirac masses are present in any insulating phase for which the first homotopy group is $\mathbb{Z}_2$, the $\nu = 0$ phase in Fig. 4(d) when $N = 2$.

D. $\pi_0(V_{d=2,r}) = \mathbb{Z}_2$

According to Table IV, the 2D AZ symmetry classes DIII and AII are associated with disconnected topological spaces with two path-connected components, i.e., the zeroth homotopy group of the topological spaces associated with the normalized Dirac masses in these AZ symmetry classes is $\mathbb{Z}_2$. According to Sec. III, their phase diagrams must host two topologically distinct insulating phases and one critical boundary or one metallic phase separating them at $\mathsf{m} = 0$.

From the point of view of topology, the normalized Dirac masses in the 2D symmetry class DIII differ from those in the 2D symmetry class AII in that the former has the first homotopy group $\mathbb{Z}_2$ when $N \geqslant 2$, while the latter has a trivial first homotopy group for all $N = 1,2,\ldots$. This difference manifests itself through a density of states that deviates from the one predicted from random matrix theory in the 2D insulating phases of the symmetry class DIII when $N = 2,3,\ldots$ [Fig. 4(f)]. The metallic phase is stable (due to weak antilocalization) to the presence of weak disorder in both 2D symmetry classes. Now, the characteristic coupling g for the disorder is marginally relevant in the vicinity of the critical point $\mathsf{m} = \mathsf{g} = 0$ for symmetry classes DIII and AII, as is reviewed in Appendix B. Consequently, the metallic phase separates two topologically distinct insulating phases for any nonvanishing $\mathsf{g} > 0$ all the way down to the critical point $\mathsf{m} = \mathsf{g} = 0$ and sits on top of the insulating phases as depicted in Figs. 4(e)–4(g).

These predictions are consistent with the following published works. Studies of random Dirac Hamiltonians [102–104] and a network model [105] in the 2D symmetry class AII have confirmed the robustness of the metallic phase all the way down to the critical point $\mathsf{m} = \mathsf{g} = 0$ in Fig. 4(g). The numerical study in Ref. [93] of a 2D quantum network model for the symmetry class DIII is also consistent with Fig. 4(e).

E. $\pi_0(V_{d=2,r}) = \{0\}$

According to Table IV, the 2D AZ symmetry classes AIII, AI, BDI, CII, and CI are associated with path-connected topological spaces, i.e., the zeroth homotopy group of the topological spaces associated with the normalized Dirac masses in these AZ symmetry classes is the trivial group $\{0\}$. According to Sec. III, their phase diagrams must host no more than one insulating phases.

The symmetry classes AI and CI do not support a 2D metallic phase, as it is unstable due to weak localization. For this reason, their phase diagrams in Fig. 4(h) consist of a single insulating phase. An example of a localized phase in class CI is a dirty $d_{x^2-y^2}$ superconductor with TRS and spin SU(2) rotation symmetry [86,87].

The chiral symmetry classes AIII, BDI, and CII stand out in 2D space because (i) the quantum corrections to their longitudinal Drude conductivities vanish to any order in perturbation theory precisely at the band center, and (ii) their density of states diverges at the band center $\varepsilon = 0$, as was shown by Gade and Wegner for a sublattice model perturbed by disorder with chiral symmetry in Refs. [40,41]. Items (i) and (ii) are also true for random Dirac Hamiltonians in the 2D symmetry classes AIII, BDI, and CII at the band center [42,43,106].

On the one hand, the topology of the classifying spaces of the 2D chiral symmetry classes AIII, BDI, and CII is not predictive regarding item (i). On the other hand, the fact that the first homotopy group of the normalized Dirac masses in the 2D symmetry classes AIII, BDI, and CII is $\mathbb{Z}$ provides an explanation for the diverging density of states upon approaching the band center alternative to the one based on the RG calculations from Refs. [40–43,106] or to the one based on Griffith effects from Ref. [44]. The physical interpretation of $\pi_1(V^{\mathrm{AIII}}_{d=2,r=4}) = \pi_1(V^{\mathrm{BDI}}_{d=2,r=4}) = \pi_1(V^{\mathrm{CII}}_{d=2,r=8}) = \mathbb{Z}$ is that one finds the (noncontractible) unit circle S^1 in the topological space of normalized Dirac masses from the 2D symmetry classes AIII, BDI, and CII. This subspace is generated by two anticommuting mass matrices as was pointed out in the studies of charge fractionalization in graphene [107–113]. Such a unit

circle, corresponding as it is to a pair of normalized masses, supports pointlike defects, U(1) vortices, which can bind an integer number of zero modes if isolated [114]. A finite but dilute density of vortices binds midgap states resulting in the singular density of states at the band center. We show the phase diagrams of the 2D chiral symmetry classes at $\epsilon = 0$ in Fig. 4(i). In the insulating phase, the density of states exhibits a Griffiths singularity $\rho(\varepsilon) \propto |\varepsilon|^{\alpha}$ at the band center $\varepsilon = 0$ with the exponent α varying continuously with $|\mathsf{m}|$ from $\alpha = -1$ at $\mathsf{m} = 0$ (Gade singularity) to the value expected from random matrix theory $\alpha = 1,0,3$ for class AIII, BDI, and CII, respectively. We note that the 2D symmetry class CII differs from the 2D symmetry classes AIII and BDI when $\varepsilon \neq 0$ and the disorder is weak. Indeed, any deviation of the chemical potential away from the band center is a relevant symmetry-breaking perturbation that drives a crossover between the symmetry class CII to the symmetry class AII. As spin-orbit coupling favors antiweak localization, the metallic phase is stable to weak disorder in the symmetry class AII.

VI. APPLICATION TO 3D SPACE

In this section, we are going to employ the machinery of classifying spaces in order to deduce the qualitative phase diagrams capturing the physics of Anderson localization when the effects of local disorder are not always strong, or marginally strong as they were in 1D and 2D, respectively. The lowest dimension in which such disorder can be treated perturbatively in all ten AZ symmetry classes is $d = 3$. We shall show that the machinery of the classifying spaces applied to the normalized Dirac masses is predictive regarding the phase diagrams when combined with the fact that the characteristic coupling g for the disorder is irrelevant at the critical Dirac point for any $d \geqslant 3$. Before doing so, however, we briefly review salient past results on Anderson localization in 3D.

The metallic phase is stable in 3D space for the standard symmetry classes A, AI, and AII. A sufficiently strong disorder is required to stabilize the insulating phase [115–117]. The same is true for all chiral and symmetry classes at the band center.

The insulating phases in 3D space for the standard symmetry classes A and AI are topologically trivial. There are two topologically distinct insulating phases in the 3D symmetry class AII [118–120]. At the band center, four more nonstandard symmetry classes support topologically distinct insulating phases [28–30].

A. Higher homotopy groups and topological defects

More interestingly from the point of view of this paper, we predict that there are 3D symmetry phases with topologically trivial insulating phases that support a singular density of states at the band center due to the fact that their normalized Dirac masses support topological defects, as we are going to explain now.

To investigate this possibility, we start from the Dirac Hamiltonian (3.1) with $d = 3$ and the rank $r = r_{\min} N$. It is assumed that the local disorder entering the Dirac Hamiltonian is the most general $r \times r$ Hermitian matrix with random iid matrix elements up to the constraints imposed by the selected AZ symmetry classes. We fix the chemical potential $\mu = 0$ and discuss transport properties of quasiparticles of energy $\varepsilon = 0$ for all ten symmetry classes.

According to Sec. II F, when $\pi_{d-1}(V_d)$ has a nontrivial entry, point defects in the normalized Dirac masses may bound zero modes. If so, they contribute to a singular density of states. From the transition rule in Eq. (2.23), in any dimension d of space, $\pi_{d-1}(V_d) = \mathbb{Z}$ for the chiral symmetry classes AIII, BDI, and CII, while $\pi_{d-1}(V_d) = \mathbb{Z}_2$ in the BdG symmetry classes D and DIII. Hence, in any dimension d of space, a random Dirac Hamiltonian of the form (3.1) displays a singular density of states at the band center in the chiral symmetry classes AIII, BDI, and CII and in the BdG symmetry classes D and DIII due to the proliferation of midgap states bound to $\mathbb{Z}$ and $\mathbb{Z}_2$ point defects, respectively. Topological defects of higher dimensions $d_{\text{def}} = 1, \ldots, d-1$ also bind midgap states that contribute to the density of states around $\varepsilon = 0$. However, they are not expected to cause a singularity of the density of states at $\varepsilon = 0$. Indeed, either the density of extended defects scales with the linear size L of space as $L^{-d_{\text{def}}}$ and is thus subextensive, or the midgap states bound to compact extended defects with the characteristic linear length L_{def} are a level spacing of order $1/L_{\text{def}}$ away from $\varepsilon = 0$. Above the dimensionality of space $d = 3$, all AZ symmetry classes support at least one nontrivial homotopy group. The form of the singularity of the density of states at the band center depends parametrically on the statistical distribution of the Dirac masses. It is generically nonuniversal, except at the critical points that govern the transition between distinct phases.

B. $\pi_0(V_{d=3,r}) = \mathbb{Z}$

The normalized Dirac masses realize the Grassmannian manifolds in the 3D symmetry classes AIII, DIII, and CI according to Table V. We deduce that these 3D symmetry classes support $N + 1$ topologically distinct insulating phases separated by N boundaries by combining the arguments of Sec. III with the fact that the characteristic coupling g for the disorder is irrelevant at the critical Dirac point for any $d \geqslant 3$, see Fig. 5(a). Since the characteristic coupling g is irrelevant, we must distinguish the case when $N = 1$ from the case when $N > 1$. When $N = 1$, we choose the probability distribution (3.9). When $N > 1$, we choose the probability distribution (3.10). Indeed, we recall that if we label the horizontal axis (the clean limit) of the phase diagram with m defined by Eq. (3.9b), then the horizontal axis supports no more than two insulating phases with $\nu = \pm\frac{N}{2}$, respectively. Given that g is irrelevant in the vicinity of $\mathsf{m} = \mathsf{g} = 0$, the choice (3.9b) delivers two localized phases below the metallic dome. In other words, the phase diagram when $N > 1$ with the choice (3.9) is identical to that of Fig. 5(a) with the caveat that the index $\nu = \pm\frac{1}{2}$ is to be replaced with the index $\nu = \pm\frac{N}{2}$ for the two localized phases. To display $N + 1 > 2$ localized phases in the phase diagram, it is necessary to have $N + 1 > 2$ insulating phases along the horizontal axis (the clean limit) of the phase diagram. This is achieved with the choice (3.10) that insures that the eigenvalues of the Dirac mass matrix β_0 in Eq. (3.10a) competes with N nondegenerate eigenvalues of the matrix M_0 in Eq. (3.10c) The second homotopy group of the normalized Dirac masses is $\mathbb{Z}$ in the 3D symmetry class AIII according to Table V. The first and second homotopy groups

TABLE V. Interplay between the topology of the normalized Dirac masses in a given AZ symmetry class and Anderson localization when space is three-dimensional. For each AZ symmetry class from the first column, (i) the second column gives the minimal rank $r_{\min}$ of the Dirac matrices for which a Dirac mass is allowed by the symmetries, (ii) the third column gives the corresponding topological space for the normalized Dirac masses $V_{d=3,r=r_{\min}N}$, (iii) the fourth column gives the corresponding zeroth homotopy group $\pi_0(V_{d=3,r=r_{\min}N})$, (iv) the fifth column gives the corresponding first homotopy group $\pi_1(V_{d=3,r=r_{\min}N})$, (v) the sixth column gives the corresponding second homotopy group $\pi_2(V_{d=3,r=r_{\min}N})$, (vi) the seventh column gives the corresponding panel from Fig. 5, and (vii) the last column signals if the density of states per unit energy and per unit volume is singular at the Fermi energy, which is fixed to $\varepsilon = 0$. A singular density of states is associated with nontrivial point defects characterized by $\pi_2(V_{d=3,r=r_{\min}N})$. In each homotopy column, the three entries $\mathbb{Z}$ hold for N larger than an integer (infinity included) that depends on the order of the homotopy group and the classifying space, the two entries $\mathbb{Z}_2$ hold for N larger than an integer that also depends on the order of the homotopy group and the classifying space. The entry 0 is a short hand for the group $\{0\}$ made of the single element 0.

AZ symmetry class	$r_{\min}$	$V_{d=3,r}$	$\pi_0(V_{d=3,r})$	$\pi_1(V_{d=3,r})$	$\pi_2(V_{d=3,r})$	Phase diagram from Fig. 5	Density of states
A	4	C_1	0	$\mathbb{Z}$	0	(c)	Nonsingular
AIII	4	C_0	$\mathbb{Z}$	0	$\mathbb{Z}$	(a)	Singular
AI	8	R_5	0	0	0	(c)	Nonsingular
BDI	8	R_6	0	0	$\mathbb{Z}$	(c)	Singular
D	4	R_7	0	$\mathbb{Z}$	$\mathbb{Z}_2$	(c)	Singular
DIII	4	R_0	$\mathbb{Z}$	$\mathbb{Z}_2$	$\mathbb{Z}_2$	(a)	Singular
AII	4	R_1	$\mathbb{Z}_2$	$\mathbb{Z}_2$	0	(b)	Nonsingular
CII	8	R_2	$\mathbb{Z}_2$	0	$\mathbb{Z}$	(b)	Singular
C	8	R_3	0	$\mathbb{Z}$	0	(c)	Nonsingular
CI	8	R_4	$\mathbb{Z}$	0	0	(a)	Nonsingular

of the normalized Dirac masses are $\mathbb{Z}_2$ in the 3D symmetry class DIII according to Table V. Hence the density of states (the number of states per unit energy and per unit volume) is singular at the band center due to the proliferations of midgap states that are bound to point-defects of the normalized Dirac masses for the 3D symmetry classes AIII and DIII. The 3D symmetry class CI has trivial first and second homotopy groups so that the density of states is nonsingular at the band center.

C. $\pi_0(V_{d=3,r}) = \mathbb{Z}_2$

The normalized Dirac masses are the union of two path-connected compact topological spaces in the 3D symmetry classes AII and CII according to Table V. We deduce that these 3D symmetry classes support two topologically distinct insulating phases separated by one boundary by combining the arguments of Sec. III with the fact that the characteristic coupling g for the disorder is irrelevant at the critical Dirac point for any $d \geqslant 3$. A metallic phase sits on top of these two topologically distinct insulating phases. Thus we deduce the phase diagram for classes AII and CII shown in Fig. 5(b). This phase diagram is consistent with the self-consistent Born approximation [121] and nonperturbative numerical studies in the symmetry class AII [117]. On the other hand, had we started from the symmetry class DIII and weakly broken the particle-hole and chiral symmetries by the addition of weak perturbations that bring the Dirac Hamiltonian to one in the symmetry class AII, we may then keep the control parameter m of the symmetry class DIII along the horizontal axis in parameter space. This would give the same phase diagram as in Fig. 5(a) for $N > 1$ with the caveat that the $N + 1$ unperturbed localized phases with the $\mathbb{Z}$ topological numbers become $N + 1$ localized phases with alternating $\mathbb{Z}_2$ topological numbers after perturbation.

The first and second homotopy groups of the normalized Dirac masses from the 3D symmetry classes AII and CII differ.

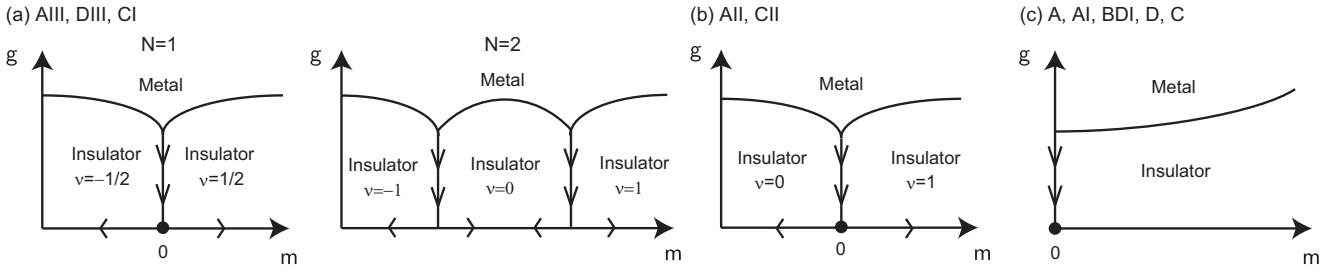

FIG. 5. Qualitative quantum phase diagrams for 3D random Dirac Hamiltonians with the quasiparticle energy fixed at $\varepsilon = 0$. The horizontal axis is parameterized by the characteristic value $\mathsf{m} \in \mathbb{R}$ of the disorder-averaged Dirac masses allowed by the symmetry class. We choose the probability distribution (3.10) for the case of $N = 2$ in the symmetry classes AIII, DIII, and CI. The vertical axis is parameterized by the characteristic value $\mathsf{g} \geqslant 0$ taken by the strength of the generic local disorder allowed by the 3D AZ symmetry class. The zeroth homotopy group of the topological space associated with the normalized Dirac mass fixes the indexing of the topologically distinct insulating phases. The existence of a metallic phase, the flows along phase boundaries, and the dimensionality of the phase boundaries all follow from perturbative renormalization-group calculations.

The second homotopy group is trivial in the 3D symmetry classes AII according to Table V. Hence the density of states is not singular in the 3D symmetry classes AII. The second homotopy group is $\mathbb{Z}$ in the 3D symmetry classes CII according to Table V. Hence the density of states is singular in the 3D symmetry classes CII. The first homotopy groups of the 3D symmetry classes AII and CII are $\mathbb{Z}_2$ and trivial, respectively. In the former case, the density of states receives a contribution from midgap states bound to the line defects. This contribution need not be singular at $\varepsilon = 0$.

D. $\pi_0(V_{d=3,r}) = \{0\}$

The normalized Dirac masses are path-connected compact topological spaces in the 3D symmetry classes A, AI, BDI, D, and C according to Table V. These symmetry classes support a single insulating phase, see Fig. 5(c). Of these, only the 3D symmetry class AI has the trivial group for its three homotopy groups. The normalized Dirac masses in the 3D symmetry classes BDI and D have the second homotopy groups $\mathbb{Z}$ and $\mathbb{Z}_2$ for N sufficiently large, respectively. Thus the 3D symmetry classes BDI and D have densities of states that are singular at the band center because of the proliferation of midgap states bound to $\mathbb{Z}$ and $\mathbb{Z}_2$ pointlike defects in the normalized Dirac masses, respectively. Line defects of the normalized Dirac masses are also allowed in the 3D symmetry classes A, D, and C. They also contribute to the density of states, but they need not give rise to a singularity at $\varepsilon = 0$. We note that the density of states computed for a network model from the symmetry class C was found to be nonsingular in Ref. [100].

VII. BOUNDARIES OF TOPOLOGICAL INSULATORS

So far, we have been concerned with the interplay between topology, local symmetries, and Anderson localization for d-dimensional random massive Dirac Hamiltonians that capture the effects of local, and smooth disorder of d-dimensional lattice models such as quantum network models at low energies and long wavelengths. We have explained in Sec. II D how Table I can be used to identify in each dimension d of space the five AZ symmetry classes that support topologically distinct insulating phases of d-dimensional quantum matter. There is an alternative road to the classification of TIs and TSCs that was explained in Sec. II D, which we now review for the sake of completeness.

Any $(d-1)$-dimensional boundary of a d-dimensional topological insulators or superconductors is immune to Anderson localization [28]. This immunity is captured by the presence of a topological term in the NLSM that captures the physics of Anderson localization on the $(d-1)$-dimensional boundary subject to the symmetry constraint imposed by one of the ten AZ symmetry classes [28]. Alternatively, this property holds for those AZ symmetry constraints that prohibit the existence of any Dirac mass matrix of rank $r = \widetilde{r}_{\min} < r_{\min}$ entering the random Dirac Hamiltonian that encodes single-particle transport at low energies and long wavelength on any $(d-1)$-dimensional boundary. In Appendix A 4, we formulate the conditions for the presence (or absence) of Dirac mass matrices. We show that the conditions for the absence of normalized Dirac masses in $(d-1)$-dimensions are equivalent to the conditions for a nontrivial zeroth homotopy group of the topological spaces associated with the normalized Dirac masses in d-dimensions. This alternative derivation of the tenfold way for TI/TSCs is captured by Table VI for 2D and 3D spaces.

TABLE VI. Immunity to Anderson localization in five out of the ten AZ symmetry classes along any boundary of a topological insulator (TI) or a topological superconductors (TSC). This immunity is a consequence of the absence of any Dirac mass matrix with the rank $r = \widetilde{r}_{\min} < r_{\min}$ (see Appendix A 4) for a random Dirac Hamiltonian capturing the low-energy and long-wavelength effects of local disorder on the boundary in the corresponding AZ symmetry class.

class	edge of 2D TI/TSC	surface of 3D TI/TSC
A	ballistic	–
AIII	–	metallic
AI	–	–
BDI	–	–
D	ballistic	–
DIII	ballistic	metallic
AII	ballistic	metallic
CII	–	metallic
C	ballistic	–
CI	–	metallic

VIII. SURFACE STABILITY OF TOPOLOGICAL INSULATORS WITH REFLECTION SYMMETRY

A. General discussions

This section is devoted to the stability of topological crystalline insulators (TCIs) with a reflection symmetry when perturbed by a local random potential that retains the reflection symmetry on average. The disorder is assumed weak in the bulk in that its characteristic strength is much smaller than the band gap from the d-dimensional bulk. In this limit, the $(d-1)$-dimensional boundary may be treated in isolation and represented in terms of massless Dirac fermions perturbed by local random potentials obeying appropriate symmetries. The material SnTe is an example of a TCI and the alloying with Pb in $Sn_{1-x}Pb_xTe$ can be modeled by a weak local random potential.

By definition, a d-dimensional TCI is a band insulator that supports on any one of its $(d-1)$-dimensional boundaries that is invariant under the crystalline symmetry, here a reflection symmetry, boundary states that disperse across the bulk gap with a linear (Dirac) dispersion relation in the close vicinity to their band crossing [122]. In other words, the reflection symmetry protects $(d-1)$-dimensional boundary massless Dirac cones.

A classification of d-dimensional TCI with reflection symmetry has been obtained in Ref. [35] (see also Ref. [123]) from studying the zeroth homotopy groups of the topological spaces associated with the normalized Dirac masses entering d-dimensional massive Dirac Hamiltonians obeying nonlocal reflection symmetries in addition to the AZ local symmetries. For each of the AZ symmetry classes ordered as in the first columns of Tables VII and VIII, the results from Ref. [35] are summarized in columns three to six when space is two- and three-dimensional, respectively. For completeness,

TABLE VII. Topological classification of crystalline insulators (TCIs) in 2D with reflection symmetry and their edge stability when the reflection symmetry is retained on average, a situation for which we use the acronym STCI (statistical topological crystalline insulator). For each AZ symmetry class, we give in the second column the topological classification of insulators (TIs). Columns three to six are the TCIs for the symmetry classes BDI, DIII, CII, and CI with the reflection symmetry R^{η_T,η_C}, where the superscripts $\eta_T = \pm$ and $\eta_C = \pm$ specify if the operation for reflection commutes (+ sign) or anticommutes (− sign) with reversal of time T and exchange of particles and holes C, respectively. Here, we choose the convention $(R^{\eta_T,\eta_C})^2 = +1$. The third and fourth columns for the symmetry class AIII/(AI, AII)/(D, C) are the topological classification of the TCIs with the reflection symmetry $R^{\eta,\eta}$, where the superscript η specifies if the operation for reflection commutes (+) or anticommutes (−) with chiral/time-reversal/particle-hole transformation, respectively. The quotation marks for the entry "$\mathbb{Z}_2$" corresponding to a TCI with the $R^{-,-}$ symmetry in class CII indicates instability to interavalley scattering [35,123]. The last column gives the STCIs. The superscript † over the trivial zeroth homotopy groups in the STCI column signals when the edge states of a TCI are unstable to the presence of disorder that respects the reflection symmetry on average.

	2D TI	2D TCI				
AZ symmetry class	–	$R^{+,+}$	$R^{-,-}$	$R^{+,-}$	$R^{-,+}$	2D STCI
A	$\mathbb{Z}$	0	–	–	–	0
AIII	0	$\mathbb{Z}$	0	–	–	$\mathbb{Z}$
AI	0	0	0	–	–	0
BDI	0	$\mathbb{Z}$	0	0	0	$\mathbb{Z}$
D	$\mathbb{Z}$	$\mathbb{Z}_2$	0	–	–	$\mathbb{Z}_2$
DIII	$\mathbb{Z}_2$	$\mathbb{Z}_2$	$\mathbb{Z}$	0	$\mathbb{Z}_2$	$\mathbb{Z}_2$
AII	$\mathbb{Z}_2$	0	$\mathbb{Z}_2$	–	–	$0^\dagger$
CII	0	$\mathbb{Z}$	"$\mathbb{Z}_2$"	0	0	$\mathbb{Z}$
C	$\mathbb{Z}$	0	0	–	–	0
CI	0	0	$\mathbb{Z}$	0	0	$0^\dagger$

TABLE VIII. Topological classification of crystalline insulators (TCIs) in 3D with reflection symmetry and their surface stability when the reflection symmetry is retained on the average, a situation for which we use the acronym STCI (statistical topological crystalline insulator). For each AZ symmetry class, we give in the second column the topological classification of insulators (TIs). Columns three to six are the TCIs for the symmetry classes BDI, DIII, CII, and CI with the reflection symmetry R^{η_T,η_C}, where the superscripts $\eta_T = \pm$ and $\eta_C = \pm$ specify if the operation for reflection commutes (+ sign) or anticommutes (− sign) with reversal of time T and exchange of particles and holes C, respectively. The third column for symmetry class A indicates the $\mathbb{Z}$ classification of TCIs with reflection symmetry. Here, we choose the convention $(R^{\eta_T,\eta_C})^2 = +1$. The third and fourth columns for the symmetry class AIII/(AI, AII)/(D, C) are the topological classification of the TCIs with the reflection symmetry $R^{\eta,\eta}$, where the superscript η specifies if the operation for reflection commutes (+) or anticommutes (−) with the chiral/time-reversal/particle-hole transformation, respectively. The quotation marks for the entry "$\mathbb{Z}_2$" corresponding to a TCI with the $R^{-,-}$ symmetry in class C indicates instability to intervalley scattering [35,123]. The last column gives the STCIs. The superscript † over the trivial zeroth homotopy groups in the STCI column signals when the surface states of a TCI are unstable to the presence of disorder that respects the reflection symmetry on the average.

	3D TI	3D TCI				
AZ symmetry class	–	$R^{+,+}$	$R^{-,-}$	$R^{+,-}$	$R^{-,+}$	3D STCI
A	0	$\mathbb{Z}$	–	–	–	$\mathbb{Z}$
AIII	$\mathbb{Z}$	0	$\mathbb{Z}$	–	–	$0^\dagger$
AI	0	0	$\mathbb{Z}$	–	–	$0^\dagger$
BDI	0	0	0	0	$\mathbb{Z}$	$0^\dagger$
D	0	$\mathbb{Z}$	0	–	–	$\mathbb{Z}$
DIII	$\mathbb{Z}$	$\mathbb{Z}_2$	0	$\mathbb{Z}$	$\mathbb{Z}$	$\mathbb{Z}_2$
AII	$\mathbb{Z}_2$	$\mathbb{Z}_2$	$\mathbb{Z}$	–	–	$\mathbb{Z}_2$
CII	$\mathbb{Z}_2$	0	$\mathbb{Z}_2$	$\mathbb{Z}_2$	$\mathbb{Z}$	$0^\dagger$
C	0	$\mathbb{Z}$	"$\mathbb{Z}_2$"	–	–	$\mathbb{Z}$
CI	$\mathbb{Z}$	0	0	$\mathbb{Z}$	$\mathbb{Z}$	$0^\dagger$

the second columns of Tables VII and VIII are the same as in Table I when $d = 2$ and $d = 3$, respectively. Hence, for the AZ symmetry classes BDI, DIII, CII, and CI, the zeroth homotopy group of the topological space associated with the normalized Dirac masses when reflection symmetry is not imposed (column two) is supplemented by the zeroth homotopy group of the topological space associated with the normalized Dirac masses when the reflection symmetry R^{η_T,η_C} holds (columns three to six). We choose the convention $(R^{\eta_T,\eta_C})^2 = +1$. Here, any one of the superscripts $\eta_T = \pm$ and $\eta_C = \pm$ takes the value + (−) if the operation of reflection commutes (anticommutes) with the operation T for the reversal of time and the operation C for the exchange of particles and holes, respectively. For the AZ symmetry classes AIII/(AI, AII)/(D,C), the third and fourth columns indicate the topological classification with the reflection symmetry $R^{\eta,\eta}$, where the superscript η takes the value + (−) if the reflection operator commutes (anticommutes) with the operation for chiral/time-reversal/particle-hole transformation, respectively. For the symmetry class A, the third column shows the classification in the presence of a reflection symmetry. Any entry "−" indicates the absence of the symmetries under reversal of time T or under exchange of particles and holes C.

The question we want to address is what is the fate of those boundary massless Dirac cones protected by a combination of AZ and reflection symmetries if a boundary is perturbed by a local random potential belonging to a statistical ensemble such that (i) there exist realizations of the random potential that break the reflection symmetry, (ii) even though the reflection symmetry holds on average. The acronym STCI for statistical topological crystalline insulator is used when items (i) and (ii) are met.

The answer is found in the last columns of Tables VII and VIII in 2D and 3D space, respectively. Each entry of the column STCI from the Tables VII and VIII gives the zeroth homotopy group of the topological space associated with the normalized Dirac masses in $(d-1)$-dimensional space that are allowed by imposing no other symmetries than the ones from the AZ symmetry class to which the d-dimensional STCI belongs. The intuition for this result is that a d-dimensional STCI supports either a metallic or critical phase on any of its $(d-1)$-dimensional boundary that is invariant under the crystalline operation if Anderson localization in the corresponding $(d-1)$-dimensional AZ symmetry class is preempted for topological reasons.

The interpretation of the nonvanishing zeroth homotopy groups in the columns three to six from Tables VII and VIII is the following. Whenever the representation of the d-dimensional TCI in terms of a Dirac Hamiltonian with Dirac matrices of rank r is the minimal one,

$$r = r_{\text{min}}, \tag{8.1a}$$

i.e., no mass matrix is compatible with the symmetries for any smaller rank of the Dirac matrices (the actual value of r_{min} depends on the AZ class and the type of the R symmetry), then there exists a normalized mass matrix β with the following two properties. First, β is unique up to a sign. Second, β is invariant under the reflection represented by R,

$$R\,\beta\,R^{-1} = \beta. \tag{8.1b}$$

Two Dirac Hamiltonians that differ through the sign $\pm\beta$ with which β enters select two topologically distinct crystalline insulating phases in d-dimensional space. The topologically nontrivial TCI phase is the one that supports a massless Dirac cone on any one of the $(d-1)$-dimensional boundaries that are invariant under the reflection symmetry. Such a massless Dirac cone is derived from the Dirac Hamiltonian $\widetilde{\boldsymbol{\alpha}}\cdot\widetilde{\boldsymbol{p}}$ with the Dirac matrices $\widetilde{\boldsymbol{\alpha}} \equiv (\widetilde{\alpha}_1,\ldots,\widetilde{\alpha}_{d-1})$ of rank $r_{\text{min}}/2$ and the boundary momentum $\widetilde{\boldsymbol{p}} \in \mathbb{R}^{d-1}$.

Assume that a topologically nontrivial phase of a d-dimensional TCI is selected by the sign with which the mass matrix β enters a Dirac Hamiltonian of minimal rank. Furthermore, assume that, without the protection arising from the reflection symmetry, this TCI is a topologically trivial band insulator. This implies that a normalized mass matrix β' must exist such that β' anticommutes with β,

$$\{\beta,\beta'\} = 0, \tag{8.2a}$$

and β' is odd under the transformation

$$R\,\beta'\,R^{-1} = -\beta' \tag{8.2b}$$

by the operation R.

Consider a d-dimensional Dirac Hamiltonian with the pair of mass terms $m\,\beta$ and $m'\,\beta'$ that satisfies Eqs. (8.1) and (8.2). Assume that the breaking of the reflection symmetry by $m'\,\beta'$ is small,

$$|m'| \ll |m|. \tag{8.3}$$

If the sign of m selects a topologically nontrivial crystalline insulating phase in the limit $m' = 0$, then any $(d-1)$-dimensional boundary left invariant under the reflection symmetry must support a massive Dirac cone with the gap proportional to $|m'|$. Such a massive Dirac cone is derived from the Dirac Hamiltonian $\widetilde{\boldsymbol{\alpha}}\cdot\widetilde{\boldsymbol{p}} + \widetilde{m}'\,\widetilde{\beta}'$ with the Dirac matrices $\widetilde{\boldsymbol{\alpha}} \equiv (\widetilde{\alpha}_1,\ldots,\widetilde{\alpha}_{d-1})$ and $\widetilde{\beta}'$ of rank $r_{\text{min}}/2$ and the boundary momentum $\widetilde{\boldsymbol{p}} \in \mathbb{R}^{d-1}$. The Dirac mass matrix $\widetilde{\beta}'$ at the boundary originates from the Dirac mass matrix β' in the bulk.

Assume that β' is multiplied by a random function

$$m' : \mathbb{R}^d \to \mathbb{R}, \boldsymbol{x} \mapsto m'(\boldsymbol{x}) \tag{8.4a}$$

that satisfies the bound

$$\sup_{\boldsymbol{x}\in\mathbb{R}^d} |m'(\boldsymbol{x})| < |m|, \tag{8.4b}$$

where m selects a topologically nontrivial crystalline insulating phase in the limit for which the reflection symmetry is recovered. The fate of the boundary states that are protected by the reflection symmetry in the presence of the weak reflection-symmetry-breaking perturbation (8.4) is the same as the fate of massless Dirac fermions in $(d-1)$ dimensions perturbed by a generic local random potential with vanishing mean [by item (ii)] that obeys no other symmetries than the ones from the AZ symmetry class to which the d-dimensional TCI belongs. The latter stability analysis can be done with the methods from Secs. II–VII. When the classifying space of the normalized Dirac masses in $(d-1)$-dimensions has nontrivial zeroth homotopy group (listed in the last columns of Tables VII and VIII), it has two path-connected compact subspaces indexed by the ambiguity to assign a sign to the unique normalized Dirac mass matrix $\widetilde{\beta}'$ of the minimal rank (half the minimal rank of the bulk TCI, i.e., $r_{\text{min}}/2$). The anticommutation relation (8.2b) implies that this pair of path-connected compact subspaces are homeomorphic to each other by the reflection transformation R.

Assume now that we are given a statistical ensemble of random Dirac Hamiltonians of rank $r = r_{\text{min}}$, each realization of which would be the same d-dimensional TCI, perturbed by reflection-symmetry-breaking random potentials, with the reflection symmetry R obeying Eq. (8.1b). We may then decompose any $(d-1)$-dimensional boundary that is invariant under the reflection symmetry into patches labeled by the sign of the Dirac mass $\widetilde{m}'(\widetilde{\boldsymbol{x}})$ multiplying the $\widetilde{\beta}'$ matrix that smoothly varies along this boundary, say A if the sign is $+$ and B if the sign is $-$, as was done in Fig. 2. The relative size of all the regions labeled A compared to all the regions labeled B in Fig. 2 is fixed by the mean value of the mass term with the mass matrix $\widetilde{\beta}'$. This difference in sizes vanishes if the reflection symmetry holds on average. The existence of a $(d-2)$-dimensional submanifold between regions A and regions B that (i) percolates across the $(d-1)$-dimensional boundary and (ii) binds a midgap state signals a metallic or critical phase of $(d-1)$-dimensional boundary.

The argument of the previous paragraph breaks down if we relax the assumption $r = r_{\text{min}}$ to $r = r_{\text{min}}\,N$ with $N = 2,3,\ldots$. Indeed, when the rank of the Dirac matrices is the integer multiple $N = 2,3,\ldots$ of the minimum rank r_{min}, the operation for reflection does not need to interchange regions A and B from Fig. 2 anymore. Imposing the reflection symmetry on average is not sufficient anymore to ensure that the difference in the sizes of all regions labeled A and all regions labeled B in Fig. 2 vanishes. Stronger assumptions obeyed by the statistical ensemble of random masses must be fulfilled to guarantee the existence of a $(d-2)$-dimensional path between all regions A and B that percolates across the $(d-1)$-dimensional boundary depicted in Fig. 2 and binds a midgap state. To appreciate this point, we consider the following two cases.

Consider first the case of the zeroth homotopy group $\mathbb{Z}_2$ and $N = 2$. We can then make the choice (3.15) with M a 4×4 matrix. The reflection transformation R still anticommutes with the mass matrix (3.15b), as assumed in Eq. (8.2b). However, it leaves the Pfaffian (3.15d) used to index the topological sector of the mass term unchanged. Hence R cannot be used to construct a homeomorphism between the subspaces belonging to distinct topological sectors when

$N = 2$. Imposing that the randomness preserves the reflection symmetry on average is not sufficient to enforce a metallic or critical phase of $(d-1)$-dimensional boundary.

We can generalize this argument to arbitrary N. For odd N, preserving the reflection symmetry on average leads to a vanishing value for the disorder average of the $\mathbb{Z}_2$ topological number (3.15d). Either a metallic or critical phase follows at the boundary of a STCI. For even N, preserving the reflection symmetry on average does not constrain the disorder average of the topological number (3.15d). We thus expect an even-odd effect (a sensitivity to the parity of N) with regard to the stability of surface states of a STCI when the zeroth homotopy group is $\mathbb{Z}_2$.

In the case of $\mathbb{Z}$ for the zeroth homotopy group of the topological space associated with the normalized Dirac masses in $(d-1)$ dimensions, there exists a unique normalized Dirac mass matrix, up to a sign, that commutes with all other permissible mass matrices. This Dirac matrix corresponds to β_0 in Eq. (3.9a). The disorder average value of this mass term vanishes (i.e., $\mathsf{m} = 0$) due to statistical (average) reflection symmetry of the STCI. According to Tables III and IV, we have the following even-odd effect. The $(d-1)$-dimensional boundary of a STCI is metallic or critical for odd N, while it is localized for even N, as depicted in Figs. 3(a) and 4(a)–4(d). Next, we consider two examples of a three-dimensional TCI.

B. Example in the 3D symmetry class AII

First, we consider a 3D TI in the symmetry class AII. We then impose a crystalline symmetry by demanding invariance under the reflection

$$\boldsymbol{x} \equiv (x,y,z) \mapsto (-x,y,z), \tag{8.5a}$$

$$\boldsymbol{s} \equiv (s_x,s_y,s_z) \mapsto (s_x,-s_y,-s_z), \tag{8.5b}$$

for the space and spin degrees of freedom, respectively.

To this end, we choose the 4×4 massive Dirac Hamiltonian

$$\mathcal{H}(\boldsymbol{k}) := (k_x\, s_y - k_y\, s_x) \otimes \sigma_x + k_z\, s_0 \otimes \sigma_y + m\, s_0 \otimes \sigma_z. \tag{8.6}$$

The 2×2 unit matrix s_0 and the Pauli matrices $\boldsymbol{s}$ act on the spin-1/2 degrees of freedom. They enter the kinetic energy through a spin-orbit coupling. The 2×2 unit matrix σ_0 and the Pauli matrices $\boldsymbol{\sigma}$ act on the orbital degrees of freedom. Reversal of time is represented by conjugation of $\mathcal{H}(\boldsymbol{k})$ with

$$T := \mathrm{i} s_y \otimes \sigma_0\, \mathsf{K}, \tag{8.7}$$

where complex conjugation is denoted by K. The massive Dirac Hamiltonian (8.6) realizes a 3D insulator in the symmetry class AII with the Dirac matrices

$$\boldsymbol{\alpha} \equiv (s_y \otimes \sigma_x, -s_x \otimes \sigma_x, s_0 \otimes \sigma_y), \quad \beta \equiv s_0 \otimes \sigma_z, \tag{8.8}$$

as

$$T\, \mathcal{H}(-\boldsymbol{k})\, T^{-1} = \mathcal{H}(\boldsymbol{k}). \tag{8.9}$$

The rank $r = 4$ of the Dirac matrices is the minimal one for 3D topological insulators from the symmetry class AII represented by single-particle massive Dirac Hamiltonians,

$$r_{\mathrm{min}} = 4. \tag{8.10}$$

According to Ref. [19], the 3D Dirac Hamiltonian (8.6) of rank $r = r_{\mathrm{min}} = 4$ captures the low-energy and long-wavelength limit in the vicinity of *one out of four inequivalent* L points from the face-centered-cubic (fcc) Brillouin zone of the band insulator SnTe for one sign of m or the band insulator PbTe for the opposite sign of m. The rank $r = r_{\mathrm{min}} = 4$ arises because (1) both SnTe and PbTe have a simple rocksalt structure (two atoms in the unit cell), (2) both display a spin-orbit coupling, and (3) because the splitting in energy between the conduction and valence bands is minimum at the center of the eight hexagonal faces of the fcc Brillouin zone, the so-called L points. SnTe and PbTe belong to the same trivial insulating phase in the entry AII from the second column of Table VIII, because this phase supports an even number of gapless surface states. However, the plane

$$(k_x,k_y,k_z) = (0,k_y,k_z) \tag{8.11}$$

from the face centered cubic Brillouin zone is invariant under the reflection (8.5b). On this so-called mirror plane, the massive 3D Dirac Hamiltonian (8.6) simplifies to the direct sum of two massive 2D Dirac Hamiltonians of rank $r = 2$ from the 2D symmetry class D whose relative Chern numbers differ by one.

The topological space of the normalized Dirac masses in the 3D symmetry class AII follows here from the extension problem

$$Cl_{2,3} \equiv \{T, TJ; \alpha_x,\alpha_y,\alpha_z\} \to Cl_{3,3} \equiv \{J\,\beta, T, TJ; \alpha_x,\alpha_y,\alpha_z\} \tag{8.12a}$$

with the classifying space

$$R_1 = \mathrm{O}(N) \tag{8.12b}$$

[see Eq. (2.5) and Table II], whose zeroth homotopy group is [124]

$$\pi_0(R_1) = \mathbb{Z}_2, \tag{8.12c}$$

as the solution. We recall that the topological number is $\mathbb{Z}_2$ rather than $\mathbb{Z}$ from the fact that the tensoring

$$\mathcal{H}(\boldsymbol{k}) \to \mathcal{H}(\boldsymbol{k}) \otimes \tau_0, \tag{8.13a}$$

where τ_0 is a 2×2 unit matrix and $\boldsymbol{\tau}$ are Pauli matrices, admits the normalized mass term

$$\beta' \equiv s_z \otimes \sigma_x \otimes \tau_y \tag{8.13b}$$

that anticommutes with

$$\beta \equiv s_0 \otimes \sigma_z \otimes \tau_0 \tag{8.13c}$$

and is invariant under the transformation $T = \mathrm{i} s_y \otimes \sigma_0 \otimes \tau_0\, \mathsf{K}$ that implements reversal of time.

We now impose the crystalline symmetry originating from the operation (8.5b) on the 3D massive Dirac Hamiltonian (8.13a). To this end, we define

$$R_x^- := s_x \otimes \sigma_0, \quad (R_x^-)^2 = s_0 \otimes \sigma_0, \quad \{R_x^-, T\} = 0, \tag{8.14a}$$

and demand that

$$R_x^-\, \mathcal{H}(-k_x,k_y,k_z)\, R_x^- = \mathcal{H}(k_x,k_y,k_z). \tag{8.14b}$$

One observes that the mass matrix β is compatible with the crystalline symmetry originating from the operation (8.5b).

However, the crystalline symmetry originating from the operation (8.5b) is not compatible with the mass matrix β' defined by Eq. (8.13b) if

$$R_x^- := s_x \otimes \sigma_0 \otimes \tau_0, \quad T := \mathrm{i} s_y \otimes \sigma_0 \otimes \tau_0 \mathsf{K}, \tag{8.15a}$$

is combined with the symmetry condition

$$R_x^- \mathcal{H}(-k_x,k_y,k_z) \otimes \tau_0 R_x^- = \mathcal{H}(k_x,k_y,k_z) \otimes \tau_0. \tag{8.15b}$$

This conclusion can be generalized in the following way.

If we impose the symmetry under the reflection (8.5b) that anticommutes with reversal of time to any single-particle 3D Dirac Hamiltonian belonging to the symmetry class AII, we must supplement the Clifford algebra for class AII [recall Eq. (2.17)] with a new generator $J\alpha_x R_x^-$ that squares to $+1$ times the identity operator. The topological space of the normalized Dirac masses in the 3D symmetry class AII obeying this reflection symmetry follows here from the extension problem

$$\begin{aligned} Cl_{2,4} &\equiv \{T, TJ; \alpha_x, \alpha_y, \alpha_z, J\alpha_x R_x^-\} \\ &\to Cl_{3,4} \equiv \{J\beta, T, TJ; \alpha_x, \alpha_y, \alpha_z, J\alpha_x R_x^-\} \end{aligned} \tag{8.16a}$$

with the classifying space

$$R_0 = \lim_{N\to\infty} \cup_{n=0}^{N} \{\mathrm{O}(N)/[\mathrm{O}(n) \times \mathrm{O}(N-n)]\} \tag{8.16b}$$

[see Eq. (2.5) and Table II], whose zeroth homotopy group is

$$\pi_0(R_0) = \mathbb{Z}, \tag{8.16c}$$

as the solution.

The zeroth homotopy group $\mathbb{Z}$ for the normalized Dirac masses in the 3D symmetry class AII obeying the crystalline symmetry under the operation (8.5b) is the reason why an even number of surface massless Dirac cones represented by rank two Dirac matrices is protected, when no such protection is operative if we relax this crystalline symmetry and deal with the 3D symmetry class AII. In other words, an insulator from the 3D symmetry class AII that would support an even number of surface Dirac cones in the clean limit is topologically trivial because a generic local random potential from the symmetry class AII gaps out any even number of surface Dirac cones. Since the clean limit of SnTe can be approximated at low energies by the massive Dirac Hamiltonian (8.6) tensored with the $N \times N$ unit matrix where $N = 4$ is the even number of Dirac cones centered around the $N = 4$ inequivalent L points in the fcc Brillouin zone [125], we conclude that SnTe is a topologically trivial insulator under a generic single-particle local perturbation belonging to the symmetry class AII, while SnTe is a topologically nontrivial insulator whose topologically distinct phases are indexed in $\mathbb{Z}$, if the crystalline symmetry under the operation (8.5b) is imposed. Accordingly, the corresponding entries in Table VIII are $\mathbb{Z}_2$ and $\mathbb{Z}$ in the second and fourth columns, respectively. It remains to explain the entry $\mathbb{Z}_2$ in the last column.

We now assume that the 8×8 Dirac Hamiltonian (8.13a) is perturbed by a local random potential that (1) belongs to the symmetry class AII, (2) may break the crystalline symmetry (8.14) for any given realization, (3) but preserves the crystalline symmetry (8.14) on the average. Hence the mass matrix β' defined in Eq. (8.13b) enters the random potential multiplied by a random function $m' : \mathbb{R}^3 \to \mathbb{R}, \boldsymbol{x} \mapsto m'(\boldsymbol{x})$ that varies smoothly in space but averages to zero everywhere in 3D space. This mass matrix anticommutes with the mass matrix (8.13c). Any surface of the TI that is invariant under the operation (8.5b) can be divided, for any realization of the random function m', into the regions A in which $\mathrm{sgn}\, m'(\boldsymbol{x})$ is $+$ and the regions B in which $\mathrm{sgn}\, m'(\boldsymbol{x})$ is $-$, as is done in Fig. 2. Along the one-dimensional boundary between two path-connected regions A and B, $m'(\boldsymbol{x}) = 0$. Such an edge binds a pair of midgap helical edge states. The typical difference between the area of all the regions A and the area of the regions B is fixed by the mean value of the random function m'. This typical difference is zero if the mean value of the random function m' vanishes everywhere on the surface. If so, a pair of helical midgap states are bound to a one-dimensional path that percolates across the surface. Hence they are extended.

The parameter x in the alloy $\mathrm{Sn}_{1-x}\mathrm{Pb}_x\mathrm{Te}$ is associated with a local random potential as the selection of the sites on which Sn is to be substituted by Pb is essentially a random Poisson process to a first approximation. In the clean limit $x \to 0$, the projection of the massive 3D Dirac cones (8.6) at the four inequivalent L points onto one of the mirror symmetric surface Brillouin zone delivers an even number of 2D massless Dirac cones. Specifically, four Dirac cones appear on the [001] surface ($N = 2$) [125], while six Dirac cones appear on the [111] surface ($N = 3$). The disorder in the alloy $\mathrm{Sn}_{1-x}\mathrm{Pb}_x\mathrm{Te}$ belongs to the symmetry class AII. It is also believed to preserve, on average, the reflection symmetry present in the clean limit (8.6). Thus the alloy $\mathrm{Sn}_{1-x}\mathrm{Pb}_x\mathrm{Te}$ is an example of the STCIs [19,126]. According to the even-odd effect in the case of the zeroth homotopy group $\mathbb{Z}_2$ discussed in Sec. VIII A, the gapless surface states of $\mathrm{Sn}_{1-x}\mathrm{Pb}_x\mathrm{Te}$ are stable (extended) on the [111] surface, but they are unstable (localized) on the [001] surface for generic disorder that preserves the reflection symmetry on average. Nevertheless, the four Dirac cones at the [001] surface can also be stable if the C_4 rotation symmetry interchanging four Dirac cones is preserved on average. Alternatively, if one of the two reflection symmetries, which are present at the [001] surface, is broken by a lattice distortion, only two out of the four Dirac cones remain massless. This pair of surviving massless Dirac cones is immune to Anderson localization in the presence of weak disorder that preserves one of the two reflection symmetries at the [001] surface on average.

C. Example in the 3D symmetry class AI

Second, we consider a 3D TI in the symmetry class AI upon which we impose a crystalline symmetry under

$$\boldsymbol{x} \equiv (x,y,z) \mapsto (-x,y,z) \tag{8.17}$$

that anticommutes with reversal of time. To this end, we choose the 8×8 massive Dirac Hamiltonian ($r_{\mathrm{min}} = 8$ in the 3D symmetry class AI)

$$\mathcal{H}(\boldsymbol{k}) := k_x X_{233} + k_y X_{023} + k_z X_{002} + \sum_I m_I X_I. \tag{8.18a}$$

Here,

$$X_{\mu\nu\rho} := s_\mu \otimes \sigma_\nu \otimes \tau_\rho, \quad \mu,\nu,\rho = 0,1,2,3, \tag{8.18b}$$

where each quartet (s_0,s_1,s_2,s_3), $(\sigma_0,\sigma_1,\sigma_2,\sigma_3)$, and $(\tau_0,\tau_1,\tau_2,\tau_3)$ of 2×2 Hermitian matrices is built out of the 2×2 unit matrix together with the three Pauli matrices, and I denotes the collective index taking the values

$$I = 001,013,133,333. \tag{8.18c}$$

Represent reversal of time T by complex conjugation K,

$$T := X_{000}\,\mathsf{K}. \tag{8.19}$$

Represent the reflection (8.17) that anticommutes with T by

$$R_x^- := X_{020}. \tag{8.20}$$

One verifies that

$$T\,\mathcal{H}(-\boldsymbol{k})\,T = \mathcal{H}(\boldsymbol{k}). \tag{8.21}$$

Furthermore, one verifies that imposing

$$R_x^-\,\mathcal{H}(-k_x,k_y,k_z)\,R_x^- = \mathcal{H}(k_x,k_y,k_z) \tag{8.22}$$

demands of the four masses entering the massive 8×8 Dirac Hamiltonian (8.18a) that three of them vanish,

$$m_{013} = m_{133} = m_{333} = 0. \tag{8.23}$$

Since only one normalized mass matrix is compatible with the AZ symmetry class AI and the reflection symmetry (8.22) in 3D space, it follows that the topological space of normalized Dirac masses in the minimal representation has two compact and path-connected components $\{\pm X_{001}\}$. Consequently, a boundary that is left invariant by the reflection symmetry (8.17) must host boundary states that are described by a massless 4×4 Dirac equation in the low-energy and long-wavelength limit. Accordingly, we must find a nonvanishing entry in the corresponding entry of the R^{--} column of Table VIII. In order to conclude that this entry is $\mathbb{Z}$, we must double the rank of the Dirac Hamiltonian (8.18a) and verify that one mass commutes with all other allowed masses. Alternatively, we may reach the same conclusion from the fact that, without the reflection symmetry, the extension problem $Cl_{0,5}\to Cl_{1,5}$ has the classifying space R_5 with $\pi_0(R_5)=0$ for solution according to Eq. (2.5), while with the reflection symmetry, the extension problem $Cl_{0,6}\to Cl_{1,6}$ has the classifying space R_4 with $\pi_0(R_4)=\mathbb{Z}$ for solution according to Eq. (2.5). The fact that the reflection symmetry (8.22) in the 3D symmetry class AI preempts more than one mass matrix is the reason for which a 3D STCI in the symmetry class AI has no protected surface states when the reflection symmetry holds only on average.

D. Relation to surface states of weak topological insulators

Surface states of weak topological insulators (WTIs) are robust to local disorder that preserves the translation symmetry on average [102–104,127]. This is understood in the same manner as with STCIs. In a STCI, the average reflection symmetry tunes the surface states to be on the critical boundary or in the metallic phase at $\mathsf{m}=0$ for odd N. In a WTI, the average translation symmetry tunes the surface states to be on the critical boundary or in the metallic phase at $\mathsf{m}=0$ for odd N, as was shown for $\mathbb{Z}_2$ WTI of $N=1$ in Ref. [104]. When N is an even integer, the average translation symmetry is not sufficient for the surface states of a WTI to evade Anderson localization, as in STCIs.

IX. SUMMARY

The problem of Anderson localization for noninteracting fermions realizing random Dirac Hamiltonians was revisited from the perspective of the topologies of the spaces associated with Dirac mass matrices allowed by symmetries. It was first shown that the topological space V of normalized Dirac masses can be characterized in a systematic fashion with the help of the homotopy groups $\pi_0(V)$, $\pi_1(V)$, ..., $\pi_{d-1}(V)$ by imposing on V the Altland-Zirnbauer (AZ) symmetries obeyed by all realizations of the local disorder. (The AZ symmetries are local.) For any spatial dimension d and for any $n=0,\ldots,d-1$, one finds three d-dimensional AZ symmetry classes for which $\pi_n(V)=\mathbb{Z}$ and two d-dimensional AZ symmetry classes for which $\pi_n(V)=\mathbb{Z}_2$. In particular, the zeroth homotopy group is nontrivial whenever the topological space V is disconnected. The zeroth homotopy group $\pi_0(V)$ indexes the path-connected subspaces of V and enumerates the topologically distinct insulating phases in d dimensions. By considering a mapping of conducting channels, formed along boundaries between topologically distinct insulating regions, to a d-dimensional random quantum network model, we showed (i) which pairs of topologically distinct insulating phases are separated by either a metallic or a critical phase and (ii) that the control parameter across this intervening metallic phase or critical boundary involves either the disorder-averaged value taken by the Dirac mass that commutes with all other Dirac masses when $\pi_0(V)=\mathbb{Z}$, or the disorder-averaged value over the Pfaffian of the Dirac mass when $\pi_0(V)=\mathbb{Z}_2$. Qualitative phase diagrams in a two-dimensional parameter space spanned by this control parameter and the characteristic disorder strength were deduced for each d-dimensional AZ symmetry when the chemical potential is at the band center by combining $\pi_0(V)$ with a one-loop RG calculation.

We have also explained under what conditions the self-averaging density of states per unit energy and per unit volume is singular in the vicinity of the band center and when this singularity becomes universal. A sufficient condition for a singular density of states is that the homotopy group $\pi_{d-1}(V)$ is nontrivial and point defects bounding zero-energy states may appear. However, topology alone is not sufficient to predict the nature of the singularity.

Finally, we have extended the study of the interplay between the AZ symmetry classes, topology, and Anderson localization by allowing crystalline (reflection) symmetries to hold on average, a situation for which we reserve the acronym STCI (statistical topological crystalline insulator). Thereto, we find protected boundary states in five out of ten AZ symmetry classes by demanding that it also obeys a nonlocal reflection symmetry on average. We have shown that the stability against disorder of $(d-1)$-dimensional boundary states of d-dimensional TCIs is understood from the phase diagram of $(d-1)$-dimensional Dirac Hamiltonians with random mass. We have also pointed out the existence of an even-odd dependence of the stability on the parameter N that specifies

the matrix dimension of Dirac Hamiltonians. Finally, we have shown that the alloy $Sn_{1-x}Pb_xTe$ is an example of a STCI in the 3D symmetry class AII with an average reflection symmetry such that its surface states are protected by the zeroth homotopy group $\pi_0(V) = \mathbb{Z}_2$ for surface normalized Dirac masses.

Before closing this section, we comment on two limitations of our approach. First, the random Dirac Hamiltonians that we have studied are low-energy effective models that should be derived from tight-binding models on regular lattices. In the context of topological insulators, Dirac Hamiltonians are only good effective models at energy scales below the band gap. Our phase diagrams for Dirac Hamiltonians with random masses indicate that the metallic phases are stable even in the limit of strong disorder, whereas strong disorder should generically result in localization in lattice models. There is no contradiction here, since there is an implicit assumption in our analysis of Dirac Hamiltonians that the disorder strength is always smaller than the energy scale below which Dirac Hamiltonians are valid approximations to the underlying lattice models. We note that several attempts were published to study within a NLSM approach the localization transitions in the strong-disorder regime (of lattice models) in the chiral and AII symmetry classes [128–130].

Second, our approach was based on K theory. K theory aims at identifying stable homotopy groups of topological spaces. From the perspective of band theory, stability is to be interpreted as a topological attribute that is robust against any addition of trivial bands. Thus there are cases to which our theory cannot be applied. An example is the localization problem of a band insulator characterized by a nontrivial Hopf map. A band insulator characterized by a Hopf map [28,131,132] [a nontrivial element of $\pi_3(S^2)$] is unstable to the addition of trivial bands. Hence such a Hopf map is not expected to be captured by the zeroth homotopy groups of the topological spaces of normalized Dirac masses $\pi_0(V)$. Indeed, one cannot write down a Dirac Hamiltonian with a constant mass term supporting a nontrivial Hopf map, i.e., no Dirac Hamiltonian with a constant mass term corresponds to a band insulator with a nontrivial Hopf map.

ACKNOWLEDGMENTS

This work was supported by Grants-in-Aid from the Japan Society for Promotion of Science (Grants No. 24840047 and No. 24540338) and by the RIKEN iTHES Project. C.M. and A.F. are grateful for the hospitality of the Advanced Study Group "Topological Band Structures and Their Instabilities" at the MPI-PKS (Dresden). C.M. would like to acknowledge useful discussions with A. Altland, D. Bagrets, and M. Zirnbauer.

APPENDIX A: EXPLICIT CONSTRUCTIONS OF THE COMPACT TOPOLOGICAL SPACES V IN 1D

The properties of Sec. II are central to this paper. They are applications of deep results in algebraic topology. They can be verified through explicit constructions of massive Dirac Hamiltonians for any given dimension d of space, as we are going to do when $d = 1$ in Appendices A 1 and A 2. We shall then motivate why the properties of Sec. II hold in any $d = 1,2,\ldots$ in Appendix A 3. We close Appendix A with a discussion of massless Dirac Hamiltonians in Appendix A 4.

1. Examples of Dirac Hamiltonian of rank 2

For simplicity, we represent a generic Dirac Hamiltonian of rank $r = 2$ that obeys periodic boundary (ring geometry) conditions by

$$\mathcal{H}(k) := \tau_3 k + \tau_3 A_1 + \tau_2 M_2 + \tau_1 M_1 + \tau_0 A_0. \tag{A1}$$

The Fermi velocity and the Planck constants have been set to unity. The unit 2×2 matrix is denoted by τ_0 and $\boldsymbol{\tau} = (\tau_1,\tau_2,\tau_3)$ are three Pauli matrices. The real number A_1 couples as a vector potential induced by a magnetic flux at the center of a ring would do. The real number A_0 couples as a scalar potential would do, i.e., as the chemical potential. The real parameters M_1 and M_2 couple to the two available Pauli matrices that anticommute with the kinetic energy $\tau_3 k$. The four real parameters A_1, M_1, M_2, and A_0 furnish an exhaustive parametrization of a 2×2 Hermitian matrix.

When $A_1 = A_0 = 0$, the Dirac Hamiltonian (A1) has the eigenvalues

$$\varepsilon(k) = \pm\sqrt{k^2 + M^2}, \quad M^2 := M_1^2 + M_2^2. \tag{A2}$$

The real parameters M_1 and M_2 thus parametrize a Dirac mass. More precisely, we may write

$$\tau_2 M_2 + \tau_1 M_1 = M\,\beta(\theta), \tag{A3a}$$

where

$$M := \sqrt{M_1^2 + M_2^2}, \quad \theta := \arctan\frac{M_2}{M_1}, \qquad \beta(\theta) := \tau_1 \cos\theta + \tau_2 \sin\theta, \tag{A3b}$$

in which case ($\alpha \equiv \tau_3$)

$$\beta^2(\theta) = 1, \quad \{\beta(\theta),\alpha\} = 0. \tag{A4}$$

Thus the normalized Dirac mass $\beta(\theta)$ is parameterized by the angle $0 \leqslant \theta < 2\pi$. As a topological set, the normalized Dirac masses $\{\beta(\theta)|0 \leqslant \theta < 2\pi\}$ are homeomorphic to the circle S^1. They are also homeomorphic to U(1) through the map

$$\beta_{12} : [0,2\pi[\to \mathrm{U}(1), \theta \mapsto [\beta(\theta)]_{12}. \tag{A5}$$

Symmetry class A. The Dirac Hamiltonian (A1) with A_1, M_1, M_2, A_0 smooth and nonvanishing functions of the position x along the ring is said to belong to the AZ symmetry class A. As we have seen, the set

$$V^{\mathrm{A}}_{d=1,r=2} := \{\beta(\theta)|0 \leqslant \theta < 2\pi\} =: S^1, \tag{A6}$$

a circle, is the topological space of normalized Dirac masses associated with the Dirac Hamiltonian by adding to the kinetic contribution with the Dirac matrix α the normalized mass matrix $\beta(\theta)$ for $0 \leqslant \theta < 2\pi$. We note that $V^{\mathrm{A}}_{d=1,r=2}$ and U(1) are homeomorphic as topological spaces. Thus they share the same homotopy groups. On the other hand, $V^{\mathrm{A}}_{d=1,r=2}$ is not a group under matrix multiplication while U(1) is.

In addition to the conservation of the fermion number, we may impose TRS on the Dirac Hamiltonian (A1). There are two possibilities to do so.

Symmetry class AII. If charge conservation holds and TRS is imposed through

$$\mathcal{H}(k) = +\tau_2\,\mathcal{H}^*(-k)\,\tau_2, \tag{A7a}$$

then

$$\mathcal{H}(k) = \tau_3\,k + \tau_0\,A_0. \tag{A7b}$$

No mass matrix is permissible if TRS squares to minus the identity. The topological space of normalized Dirac masses in the symmetry class AII is the empty set

$$V^{\mathrm{AII}}_{d=1,r=2} = \emptyset. \tag{A7c}$$

Because of the fermion-doubling problem [133], the only way to realize (A7b) as the low-energy and long wavelength limit of a lattice model is on the boundary of a two-dimensional topological insulator in the symmetry class AII.

Symmetry class AI. If charge conservation holds and TRS is imposed through

$$\mathcal{H}(k) = +\tau_1\,\mathcal{H}^*(-k)\,\tau_1, \tag{A8a}$$

then

$$\mathcal{H}(k) = \tau_3\,k + \tau_2\,M_2 + \tau_1\,M_1 + \tau_0\,A_0. \tag{A8b}$$

The same mass matrix as in the symmetry class A is permissible if TRS squares to the identity. The homeomorphy between the allowed masses in the symmetry classes A and AI is accidental. It does not hold for larger representations of the Dirac matrix as we shall verify explicity when considering a rank 4 Dirac matrix below. The topological space of normalized Dirac masses obtained by augmenting the Dirac kinetic contribution by adding a mass matrix squaring to unity and obeying this TRS is

$$V^{\mathrm{AI}}_{d=1,r=2} := \{\beta(\theta)|0 \leqslant \theta < 2\pi\} =: S^1. \tag{A8c}$$

The topological spaces $V^{\mathrm{AI}}_{d=1,r=2}$ and U(1) are homeomorphic. (This homeomorphism is not a group homomorphism, for $V^{\mathrm{A}}_{d=1,r=2}$ is not a group while U(1) is.) Consequently, they share the same homotopy groups.

The standard symmetry classes A, AII, and AI can be further constrained by imposing the CHS. This gives the following three possibilities.

Symmetry class AIII. If charge conservation holds together with the CHS

$$\mathcal{H}(k) = -\tau_1\,\mathcal{H}(k)\,\tau_1, \tag{A9a}$$

then

$$\mathcal{H}(k) = \tau_3\,k + \tau_3\,A_1 + \tau_2\,M_2. \tag{A9b}$$

There is a unique mass matrix. The topological space of normalized Dirac masses obtained by adding to the Dirac kinetic contribution a mass matrix squaring to unity and obeying the CHS is

$$V^{\mathrm{AIII}}_{d=1,r=2} = \{\pm\tau_2\}. \tag{A9c}$$

Symmetry class CII. It is not possible to write down a 2×2 Dirac equation in the symmetry class CII. For example, imposing

$$\mathcal{H}(k) = -\tau_1\,\mathcal{H}(k)\,\tau_1, \quad \mathcal{H}(k) = +\tau_2\,\mathcal{H}^*(-k)\,\tau_2, \tag{A10}$$

enforces the symmetry class DIII, for composing the CHS with the TRS delivers a PHS that squares to the unity and not minus the unity. In order to implement the symmetry constraints of class CII, we need to consider a 4×4 Dirac equation (see Appendix A 2).

Symmetry class BDI. If charge conservation holds together with

$$\mathcal{H}(k) = -\tau_1\,\mathcal{H}(k)\,\tau_1, \quad \mathcal{H}(k) = +\tau_1\,\mathcal{H}^*(-k)\,\tau_1, \tag{A11a}$$

then

$$\mathcal{H}(k) = \tau_3\,k + \tau_2\,M_2. \tag{A11b}$$

There is a unique mass matrix. The topological space of normalized Dirac masses obtained by adding to the Dirac kinetic contribution a mass matrix squaring to unity while preserving TRS and PHS (a product of TRS and CHS), both of which square to unity, is

$$V^{\mathrm{BDI}}_{d=1,r=2} = \{\pm\tau_2\}. \tag{A11c}$$

Now, we move on to the four Bogoliubov-de-Gennes symmetry classes with PHS.

Symmetry class D. If we impose PHS through

$$\mathcal{H}(k) = -\mathcal{H}^*(-k), \tag{A12a}$$

then

$$\mathcal{H}(k) = \tau_3\,k + \tau_2\,M_2. \tag{A12b}$$

There is a unique mass matrix. The topological space of normalized Dirac masses obtained by adding to the Dirac kinetic contribution a mass matrix squaring to unity and preserving the PHS squaring to unity is

$$V^{\mathrm{D}}_{d=1,r=2} = \{\pm\tau_1\}. \tag{A12c}$$

Symmetry class DIII. If we impose PHS and TRS through

$$\mathcal{H}(k) = -\mathcal{H}^*(-k), \quad \mathcal{H}(k) = +\tau_2\,\mathcal{H}^*(-k)\,\tau_2, \tag{A13a}$$

respectively, then

$$\mathcal{H}(k) = \tau_3\,k. \tag{A13b}$$

No mass matrix is permissible if TRS squares to minus the identity. The topological space of normalized Dirac masses in the symmetry class DIII is the empty set

$$V^{\mathrm{DIII}}_{d=1,r=2} = \emptyset. \tag{A13c}$$

Because of the fermion-doubling problem [133], the only way to realize (A13b) as the low-energy and long wavelength limit of a lattice model is on the boundary of a two-dimensional topological superconductor in the symmetry class DIII.

Symmetry class C. If we impose PHS through

$$\mathcal{H}(k) = -\tau_2\,\mathcal{H}^*(-k)\,\tau_2, \tag{A14a}$$

then

$$\mathcal{H}(k) = \tau_3\,A_1 + \tau_2\,M_2 + \tau_1\,M_1. \tag{A14b}$$

PHS squaring to minus unity prohibits a kinetic energy in any Dirac Hamiltonian of rank 2 in the symmetry class C.

Symmetry class CI. If we impose PHS and TRS through

$$\mathcal{H}(k) = -\tau_2\,\mathcal{H}^*(-k)\,\tau_2, \quad \mathcal{H}(k) = +\tau_1\,\mathcal{H}^*(-k)\,\tau_1, \tag{A15a}$$

respectively, then

$$\mathcal{H}(k) = \tau_2 M_2 + \tau_1 M_1. \tag{A15b}$$

PHS squaring to minus unity prohibits a kinetic energy in the symmetry class CI.

2. Examples of Dirac Hamiltonian of rank 4

Consider the generic Dirac Hamiltonian of rank $r = 4$ that obeys periodic boundary conditions (ring geometry)

$$\begin{aligned}\mathcal{H}(k) := {} & \tau_3 \otimes \sigma_0 k + \tau_3 \otimes \sigma_\nu A_{1,\nu} + \tau_2 \otimes \sigma_\nu M_{2,\nu} \\ & + \tau_1 \otimes \sigma_\nu M_{1,\nu} + \tau_0 \otimes \sigma_\nu A_{0,\nu}.\end{aligned} \tag{A16}$$

The Fermi velocity and the Planck constants have been set to unity. The matrices τ_0 and $\boldsymbol{\tau}$ were defined in Eq. (A1). A second unit 2×2 matrix is denoted by σ_0 and $\boldsymbol{\sigma} = (\sigma_1,\sigma_2,\sigma_3)$ are another set of three Pauli matrices. The summation convention over the repeated index $\nu = 0,1,2,3$ is implied. There are four real-valued parameters for the components $A_{1,\nu}$ with $\nu = 0,1,2,3$ of an U(2) vector potential, eight for the components $M_{1,\nu}$ and $M_{2,\nu}$ with $\nu = 0,1,2,3$ of two independent U(2) masses, and four for the components $A_{0,\nu}$ with $\nu = 0,1,2,3$ of an U(2) scalar potential. As it should be there are 16 real-valued free parameters (functions if we opt to break translation invariance).

Symmetry class A. The Dirac Hamiltonian (A16) with $A_{1,\nu}$, $M_{1,\nu}$, $M_{2,\nu}$, $A_{0,\nu}$ smooth and nonvanishing functions of the position x along the ring is said to belong to the AZ symmetry class A. All eight mass matrices of rank $r = 4$ in the 1D symmetry class A can be arranged into the four pairs $(M_{1,\nu},M_{2,\nu})$ with $\nu = 0,1,2,3$ of anticommuting masses. The topological space of normalized Dirac masses obtained by adding to the kinetic energy a mass matrix squaring to the unit matrix is [35]

$$V^{\mathrm{A}}_{d=1,r=4} := \left\{\beta = \begin{pmatrix} 0 & U \\ U^\dagger & 0 \end{pmatrix} \middle| U \in \mathrm{U}(2)\right\}. \tag{A17a}$$

As a topological space, it is thus homeomorphic to $\mathrm{U}(2) \simeq \mathrm{U}(1) \times \mathrm{SU}(2) \simeq S^1 \times S^3$, an interpretation rendered plausible by the parametrization

$$\begin{aligned} V^{\mathrm{A}}_{d=1,r=4} &= \{\boldsymbol{M}\cdot\boldsymbol{X} + \boldsymbol{N}\cdot\boldsymbol{Y} | \boldsymbol{M}^2 = \cos^2\theta, \boldsymbol{N} = \tan\theta \boldsymbol{M}\} \\ &=: S^1 \times S^3, \\ \boldsymbol{M} &:= (M_{2,0},M_{1,1},M_{1,2},M_{1,3}), \\ \boldsymbol{N} &:= (-M_{1,0},M_{2,1},M_{2,2},M_{2,3}), \\ \boldsymbol{X} &:= (\tau_2 \otimes \sigma_0,\tau_1 \otimes \sigma_1,\tau_1 \otimes \sigma_2,\tau_1 \otimes \sigma_3), \\ \boldsymbol{Y} &:= (-\tau_1 \otimes \sigma_0,\tau_2 \otimes \sigma_1,\tau_2 \otimes \sigma_2,\tau_2 \otimes \sigma_3), \end{aligned} \tag{A17b}$$

We note that $V^{\mathrm{A}}_{d=1,r=4}$ is not closed under matrix multiplication so that it does not carry the group structure of U(2).

In addition to the conservation of the fermion number, we may impose TRS on the Dirac Hamiltonian (A16). There are two possibilities to do so.

Symmetry class AII. If charge conservation holds together with TRS through

$$\mathcal{H}(k) = +\tau_1 \otimes \sigma_2 \mathcal{H}^*(-k) \tau_1 \otimes \sigma_2, \tag{A18a}$$

then

$$\begin{aligned}\mathcal{H}(k) = {} & \tau_3 \otimes \sigma_0 k + \sum_{\nu=1,2,3} \tau_3 \otimes \sigma_\nu A_{1,\nu} + \tau_2 \otimes \sigma_0 M_{2,0} \\ & + \tau_1 \otimes \sigma_0 M_{1,0} + \tau_0 \otimes \sigma_0 A_{0,0}.\end{aligned} \tag{A18b}$$

Observe that by doubling the Dirac Hamiltonian (A7b), we went from no mass matrix to two anticommuting mass matrices. The topological space of normalized Dirac masses obtained by adding to the Dirac kinetic contribution a mass matrix squaring to unity and obeying this TRS is obtained by imposing the TRS (A18a) on Eq. (A17a) to be

$$V^{\mathrm{AII}}_{d=1,r=4} := \left\{\beta = \begin{pmatrix} 0 & U \\ U^\dagger & 0 \end{pmatrix} \middle| U = +\sigma_2 U^{\mathsf{T}} \sigma_2 \in \mathrm{U}(2)\right\}. \tag{A18c}$$

As a topological space, $V^{\mathrm{AII}}_{d=1,r=4}$ can be shown to be homeomorphic to $\mathrm{U}(2)/\mathrm{Sp}(1) \simeq \mathrm{U}(1) \times \mathrm{SU}(2)/\mathrm{SU}(2) \simeq \mathrm{U}(1)$, an interpretation rendered plausible by the parametrization

$$\begin{aligned} V^{\mathrm{AII}}_{d=1,r=4} &= \{\boldsymbol{M}\cdot\boldsymbol{X} | \boldsymbol{M}^2 = 1\} =: S^1, \\ \boldsymbol{M} &:= (M_{2,0},M_{1,0}), \\ \boldsymbol{X} &:= (\tau_2 \otimes \sigma_0,\tau_1 \otimes \sigma_0). \end{aligned} \tag{A18d}$$

Symmetry class AI. If charge conservation holds together with TRS through

$$\mathcal{H}(k) = +\tau_1 \otimes \sigma_0 \mathcal{H}^*(-k) \tau_1 \otimes \sigma_0, \tag{A19a}$$

then

$$\begin{aligned}\mathcal{H}(k) = {} & \tau_3 \otimes \sigma_0 k + \tau_3 \otimes \sigma_2 A_{1,2} + \sum_{\nu=0,1,3} (\tau_2 \otimes \sigma_\nu M_{2,\nu} \\ & + \tau_1 \otimes \sigma_\nu M_{1,\nu} + \tau_0 \otimes \sigma_\nu A_{0,\nu}).\end{aligned} \tag{A19b}$$

There are six mass matrices of rank $r = 4$ in the 1D symmetry class AI that can be arranged into the three pairs $(M_{1,\nu},M_{2,\nu})$ with $\nu = 0,1,3$ of anticommuting masses. The topological space of normalized Dirac masses obtained by adding to the Dirac kinetic contribution a mass matrix squaring to unity and obeying this TRS is

$$V^{\mathrm{AI}}_{d=1,r=4} := \left\{\beta = \begin{pmatrix} 0 & U \\ U^\dagger & 0 \end{pmatrix} \middle| U = +U^{\mathsf{T}} \in \mathrm{U}(2)\right\}. \tag{A19c}$$

As a topological space, $V^{\mathrm{AI}}_{d=1,r=4}$ can be shown to be homeomorphic to $\mathrm{U}(2)/\mathrm{O}(2) \simeq \mathrm{U}(1)/\{\pm 1\} \times \mathrm{SU}(2)/\mathrm{U}(1) \simeq S^1 \times S^2$, an interpretation rendered plausible by the parametrization

$$\begin{aligned} V^{\mathrm{AI}}_{d=1,r=4} &= \{\boldsymbol{M}\cdot\boldsymbol{X} + \boldsymbol{N}\cdot\boldsymbol{Y} | \boldsymbol{M}^2 = \cos^2\theta, \boldsymbol{N} = \tan\theta \boldsymbol{M}\} \\ &=: S^1 \times S^2, \\ \boldsymbol{M} &:= (M_{2,0},M_{1,1},M_{1,3}), \\ \boldsymbol{N} &:= (-M_{1,0},M_{2,1},M_{2,3}), \\ \boldsymbol{X} &:= (\tau_2 \otimes \sigma_0,\tau_1 \otimes \sigma_1,\tau_1 \otimes \sigma_3), \\ \boldsymbol{Y} &:= (-\tau_1 \otimes \sigma_0,\tau_2 \otimes \sigma_1,\tau_2 \otimes \sigma_3). \end{aligned} \tag{A19d}$$

The standard symmetry classes A, AII, and AI can be further constrained by imposing the CHS. This gives the following three possibilities.

Symmetry class AIII. If charge conservation holds together with the CHS,

$$\mathcal{H}(k) = -\tau_1 \otimes \sigma_0\, \mathcal{H}(k)\, \tau_1 \otimes \sigma_0, \tag{A20a}$$

then

$$\mathcal{H}(k) = \tau_3 \otimes \sigma_0\, k + \sum_{\nu=0,1,2,3} (\tau_3 \otimes \sigma_\nu\, A_{1,\nu} + \tau_2 \otimes \sigma_\nu\, M_{2,\nu}). \tag{A20b}$$

The Dirac mass matrix $\tau_2 \otimes \sigma_0\, M_{2,0}$ that descends from Eq. (A9b) commutes with the triplet of anticommuting mass matrices $\tau_2 \otimes \sigma_1\, M_{2,1}$, $\tau_2 \otimes \sigma_2\, M_{2,2}$, and $\tau_2 \otimes \sigma_3\, M_{2,3}$. The topological space of normalized Dirac masses obtained by adding to the Dirac kinetic contribution a mass matrix squaring to the unit matrix and obeying the CHS is [35]

$$V^{\mathrm{AIII}}_{d=1,r=4} := \Big\{ \beta = \tau_2 \otimes A | A := U\, I_{m,n}\, U^\dagger, \quad m,n = 0,1,2, \quad m+n=2, \quad U \in \mathrm{U}(2), \quad I_{m,n} := \mathrm{diag}(\overbrace{-1,\ldots,-1}^{m-\text{times}}, \overbrace{+1,\ldots,+1}^{n-\text{times}}) \Big\}. \tag{A20c}$$

As a topological space, it is thus homeomorphic to $\mathrm{U}(2)/[\mathrm{U}(2)\times\mathrm{U}(0)] \cup \mathrm{U}(2)/[\mathrm{U}(1)\times\mathrm{U}(1)] \cup \mathrm{U}(2)/[\mathrm{U}(0)\times\mathrm{U}(2)]$, as is also apparent from the parametrization

$$\begin{aligned} V^{\mathrm{AIII}}_{d=1,r=4} &= \{\pm\tau_2 \otimes \sigma_0\} \cup \{\boldsymbol{M}\cdot\boldsymbol{X} | \boldsymbol{M}^2 = 1\}, \\ \boldsymbol{M} &:= (M_{2,1}, M_{2,2}, M_{2,3}), \\ \boldsymbol{X} &:= (\tau_2 \otimes \sigma_1, \tau_2 \otimes \sigma_2, \tau_2 \otimes \sigma_3), \end{aligned} \tag{A20d}$$

(recall that $S^2 \simeq \mathrm{SU}(2)/\mathrm{U}(1)$ so that $\mathrm{U}(2)/[\mathrm{U}(1)\times\mathrm{U}(1)] \simeq S^2$).

Symmetry class CII. If charge conservation holds together with CHS and TRS,

$$\mathcal{H}(k) = -\tau_1 \otimes \sigma_0\, \mathcal{H}(k)\, \tau_1 \otimes \sigma_0, \tag{A21a}$$

$$\mathcal{H}(k) = +\tau_1 \otimes \sigma_2\, \mathcal{H}^*(-k)\, \tau_1 \otimes \sigma_2, \tag{A21b}$$

respectively, then

$$\mathcal{H}(k) = \tau_3 \otimes \sigma_0\, k + \sum_{\nu=1,2,3} \tau_3 \otimes \sigma_\nu\, A_{1,\nu} + \tau_2 \otimes \sigma_0\, M_{2,0}. \tag{A21c}$$

There is a unique mass matrix, as was the case in Eqs. (A9b) and (A11b). The topological space of normalized Dirac masses obtained by adding to the Dirac kinetic contribution a mass matrix squaring to the unit matrix and obeying CHS and TRS squaring to minus unity is

$$V^{\mathrm{CII}}_{d=1,r=4} := \big\{ \beta \in V^{\mathrm{AIII}}_{d=1,r=4} \big| \beta = (\tau_1 \otimes \sigma_2)\, \beta^*\, (\tau_1 \otimes \sigma_2) \big\}. \tag{A21d}$$

As a topological space, $V^{\mathrm{CII}}_{d=1,r=4}$ can be shown to be homeomorphic to $\mathrm{Sp}(1)/\mathrm{Sp}(1)\times\mathrm{Sp}(0) \cup \mathrm{Sp}(1)/\mathrm{Sp}(0)\times\mathrm{Sp}(1)$, an interpretation rendered plausible by the parametrization

$$V^{\mathrm{CII}}_{d=1,r=4} = \{\pm\tau_2 \otimes \sigma_0\}. \tag{A21e}$$

Symmetry class BDI. If charge conservation holds together with CHS and TRS,

$$\mathcal{H}(k) = -\tau_1 \otimes \sigma_0\, \mathcal{H}(k)\, \tau_1 \otimes \sigma_0, \tag{A22a}$$

$$\mathcal{H}(k) = +\tau_1 \otimes \sigma_0\, \mathcal{H}^*(-k)\, \tau_1 \otimes \sigma_0, \tag{A22b}$$

respectively, then

$$\mathcal{H}(k) = \tau_3 \otimes \sigma_0\, k + \tau_3 \otimes \sigma_2\, A_{1,2} + \sum_{\nu=0,1,3} \tau_2 \otimes \sigma_\nu\, M_{2,\nu}. \tag{A22c}$$

The Dirac mass matrix $\tau_2 \otimes \sigma_0\, M_{2,0}$ that descends from Eq. (A11b) commutes with the pair of anticommuting mass matrices $\tau_2 \otimes \sigma_1\, M_{2,1}$ and $\tau_2 \otimes \sigma_3\, M_{2,3}$. The topological space of normalized Dirac masses obtained by adding to the Dirac kinetic contribution a mass matrix squaring to the unit matrix and obeying CHS and TRS squaring to unity is

$$V^{\mathrm{BDI}}_{d=1,r=4} := \big\{ \beta \in V^{\mathrm{AIII}}_{d=1,r=4} \big| \beta = (\tau_1 \otimes \sigma_0)\, \beta^*\, (\tau_1 \otimes \sigma_0) \big\}. \tag{A22d}$$

As a topological space, $V^{\mathrm{BDI}}_{d=1,r=4}$ can be shown to be homeomorphic to $\mathrm{O}(2)/[\mathrm{O}(2)\times\mathrm{O}(0)] \cup \mathrm{O}(2)/[\mathrm{O}(1)\times\mathrm{O}(1)] \cup \mathrm{O}(2)/[\mathrm{O}(0)\times\mathrm{O}(2)]$, an interpretation rendered plausible from the parametrization

$$\begin{aligned} V^{\mathrm{BDI}}_{d=1,r=4} &= \{\pm\tau_2 \otimes \sigma_0\} \cup \{\boldsymbol{M}\cdot\boldsymbol{X} | \boldsymbol{M}^2 = 1\}, \\ \boldsymbol{M} &:= (M_{2,1}, M_{2,3}), \\ \boldsymbol{X} &:= (\tau_2 \otimes \sigma_1, \tau_2 \otimes \sigma_3), \end{aligned} \tag{A22e}$$

(recall that $S^1 \simeq \mathrm{O}(2)/[\mathrm{O}(1)\times\mathrm{O}(1)]$).

Now, we move on to the four BdG symmetry classes.

Symmetry class D. If we impose PHS through

$$\mathcal{H}(k) = -\mathcal{H}^*(-k), \tag{A23a}$$

then

$$\mathcal{H}(k) = \tau_3 \otimes \sigma_0\, k + \tau_3 \otimes \sigma_2\, A_{1,2} + \sum_{\nu=0,1,3} \tau_2 \otimes \sigma_\nu\, M_{2,\nu} + \tau_1 \otimes \sigma_2\, M_{1,2} + \tau_0 \otimes \sigma_2\, A_{0,2}. \tag{A23b}$$

There are four Dirac mass matrices. None commutes with all remaining ones. However, each of them is antisymmetric and so is their sum. The topological space of normalized Dirac masses obtained by adding to the Dirac kinetic contribution a mass matrix squaring to the unit matrix and obeying PHS squaring to unity is

$$\begin{aligned} V^{\mathrm{D}}_{d=1,r=4} &= \{\boldsymbol{M}\cdot\boldsymbol{X} | \boldsymbol{M}^2 = 1\} \cup \{\boldsymbol{N}\cdot\boldsymbol{Y} | \boldsymbol{N}^2 = 1\}, \\ \boldsymbol{M} &:= (M_{2,1}, M_{2,3}), \quad \boldsymbol{N} := (M_{2,0}, M_{1,2}), \\ \boldsymbol{X} &:= (\tau_2 \otimes \sigma_1, \tau_2 \otimes \sigma_3), \quad \boldsymbol{Y} := (\tau_2 \otimes \sigma_0, \tau_1 \otimes \sigma_2). \end{aligned} \tag{A24}$$

As a topological space, $V^{\mathrm{D}}_{d=1,r=4}$ is homeomorphic to O(2), as $V^{\mathrm{D}}_{d=1,r=4} \simeq S^1 \cup S^1 \simeq \mathrm{U}(1)\times\mathbb{Z}_2 \simeq \mathrm{O}(2)$.

Observe that $V^{\mathrm{D}}_{d=1,r=4}$ is not closed under matrix multiplication, i.e., it does not carry the group structure of O(2).

Symmetry class DIII. If we impose PHS and TRS through

$$\mathcal{H}(k) = -\mathcal{H}^*(-k), \quad \mathcal{H}(k) = +\tau_2 \otimes \sigma_0\, \mathcal{H}^*(-k)\, \tau_2 \otimes \sigma_0, \tag{A25a}$$

then

$$\mathcal{H}(k) = \tau_3 \otimes \sigma_0\, k + \tau_3 \otimes \sigma_2\, A_{1,2} + \tau_1 \otimes \sigma_2\, M_{1,2}. \quad \text{(A25b)}$$

Observe that there is only one Dirac mass matrix [there was none in Eq. (A13b)]. Moreover, this Dirac mass matrix is Hermitian and antisymmetric. The topological space of normalized Dirac masses obtained by adding to the Dirac kinetic contribution a mass matrix squaring to the unit matrix and obeying this PHS and this TRS is

$$V^{\mathrm{DIII}}_{d=1,r=4} = \{\pm\tau_1 \otimes \sigma_2\}. \quad \text{(A25c)}$$

As a topological space, $V^{\mathrm{DIII}}_{d=1,r=4}$ is homeomorphic to O(2)/U(1).

Symmetry class C. If we impose PHS through

$$\mathcal{H}(k) = -\tau_0 \otimes \sigma_2\, \mathcal{H}^*(-k)\, \tau_0 \otimes \sigma_2, \quad \text{(A26a)}$$

then

$$\mathcal{H}(k) = \tau_3 \otimes \sigma_0\, k + \sum_{\nu=1,2,3} \tau_3 \otimes \sigma_\nu\, A_{1,\nu} + \tau_2 \otimes \sigma_0\, M_{2,0} + \sum_{\nu=1,2,3} \tau_1 \otimes \sigma_\nu\, M_{1,\nu} + \sum_{\nu=1,2,3} \tau_0 \otimes \sigma_\nu\, A_{0,\nu}. \quad \text{(A26b)}$$

There are four mass matrices that anticommute pairwise. The topological space of normalized Dirac masses obtained by adding to the Dirac kinetic contribution a mass matrix squaring to the unit matrix and obeying this PHS is

$$\begin{aligned} V^{\mathrm{C}}_{d=1,r=4} &= \{\boldsymbol{M}\cdot\boldsymbol{X} | \boldsymbol{M}^2 = 1\} =: S^3, \\ \boldsymbol{M} &:= (M_{2,0}, M_{1,1}, M_{1,2}, M_{1,3}), \\ \boldsymbol{X} &:= (\tau_2 \otimes \sigma_0, \tau_1 \otimes \sigma_1, \tau_1 \otimes \sigma_2, \tau_1 \otimes \sigma_3). \end{aligned} \quad \text{(A26c)}$$

As a topological space, $V^{\mathrm{C}}_{d=1,r=4}$ is homeomorphic to Sp(1) since we have $\mathrm{Sp}(1) \simeq \mathrm{SU}(2) \simeq S^3$. Observe that $V^{\mathrm{C}}_{d=1,r=4}$ is not closed under matrix multiplication, i.e., it does not carry the group structure of Sp(1).

Symmetry class CI. If we impose PHS and TRS through

$$\mathcal{H}(k) = -\tau_0 \otimes \sigma_2\, \mathcal{H}^*(-k)\, \tau_0 \otimes \sigma_2, \quad \text{(A27a)}$$

$$\mathcal{H}(k) = +\tau_1 \otimes \sigma_0\, \mathcal{H}^*(-k)\, \tau_1 \otimes \sigma_0, \quad \text{(A27b)}$$

respectively, then

$$\mathcal{H}(k) = \tau_3 \otimes \sigma_0\, k + \tau_3 \otimes \sigma_2\, A_{1,2} + \tau_2 \otimes \sigma_0\, M_{2,0} + \sum_{\nu=1,3} (\tau_1 \otimes \sigma_\nu\, M_{1,\nu} + \tau_0 \otimes \sigma_\nu\, A_{0,\nu}). \quad \text{(A27c)}$$

There are three mass matrices that anticommute pairwise. The topological space of normalized Dirac masses obtained by adding to the Dirac kinetic contribution a mass matrix squaring to the unit matrix and obeying this PHS and this TRS is

$$\begin{aligned} V^{\mathrm{CI}}_{d=1,r=4} &= \left\{\boldsymbol{M}_i \cdot \boldsymbol{X}_i \middle| \boldsymbol{M}_i^2 = 1\right\} =: S^2, \\ \boldsymbol{M} &:= (M_{2,0}, M_{1,1}, M_{1,3}), \\ \boldsymbol{X} &:= (\tau_2 \otimes \sigma_0, \tau_1 \otimes \sigma_1, \tau_1 \otimes \sigma_3). \end{aligned} \quad \text{(A28)}$$

As a topological space, $V^{\mathrm{CI}}_{d=1,r=4}$ is homeomorphic to $\mathrm{Sp}(1)/\mathrm{U}(1)$ since we have the homeomorphism $\mathrm{Sp}(1)/\mathrm{U}(1) \simeq \mathrm{SU}(2)/\mathrm{U}(1) \simeq S^2$.

3. Interpretation of $\pi_0(V) = \mathbb{Z}, \mathbb{Z}_2, \mathbf{0}$

Assume that we have chosen the dimensionality d of space and the AZ symmetry class. We may then increase the rank r of the Dirac matrices until we reach the smallest rank r_{min} for which we may write the massive Dirac Hamiltonian

$$\mathcal{H}_{\mathrm{min}} = \boldsymbol{\alpha}_{\mathrm{min}} \cdot \frac{\partial}{\mathrm{i}\partial \boldsymbol{x}} + m\, \beta_{\mathrm{min}} + \cdots, \quad \text{(A29)}$$

where the $(d+1)$ matrices $\alpha_{\mathrm{min}\,1}, \ldots, \alpha_{\mathrm{min}\,d}, \beta_{\mathrm{min}}$ anticommute pairwise and square to the unit $r_{\mathrm{min}} \times r_{\mathrm{min}}$ matrix, m is a real-valued (mass) parameter, and "..." accounts for all scalar and vector gauge contributions as well as for the possibility of additional mass terms. Let $V_{d,r_{\mathrm{min}}}$ be the compact topological space associated with the normalized Dirac masses that enter on the right-hand side of Eq. (A29). There are then three possibilities when $\pi_0(V_{d,r_{\mathrm{min}}}) \neq 0$.

a. Case $\pi_0(V) \neq 0$

Assume that no other normalized $r_{\mathrm{min}} \times r_{\mathrm{min}}$ mass matrix than β_{min} enters the right-hand side of Eq. (A29). It then follows that

$$V_{d,r_{\mathrm{min}}} = \{\pm\beta_{\mathrm{min}}\}. \quad \text{(A30)}$$

Hence the ground state of $\mathcal{H}_{\mathrm{min}}$ for $m > 0$ cannot be smoothly deformed into the ground state of $\mathcal{H}_{\mathrm{min}}$ for $m < 0$ without closing the gap proportional to $|m|$. There are then three possible outcomes upon increasing the rank in Eq. (A29) from r_{min} to $r_{\mathrm{min}}\, N$ with $N = 2,3,\ldots$.

Case $\pi_0(V_d) = \mathbb{Z}$. There is one normalized Dirac mass matrix which commutes with all normalized Dirac mass matrices that have become available in the given AZ symmetry class upon increasing r from from r_{min} to $r_{\mathrm{min}}\, N$ with $N = 2,3,\ldots$. We may then write a generic Dirac mass term as

$$\beta_{\mathrm{min}} \otimes M \equiv \beta_{\mathrm{min}} \otimes \left(\frac{2\nu}{N}\mathbb{1}_N + A\right), \quad \text{(A31)}$$

where the $N \times N$ Hermitian matrix M squares to the unit $N \times N$ matrix $\mathbb{1}_N$, the $N \times N$ Hermitian matrix A is traceless, both M and A are restricted by the AZ symmetry class, and ν is the topological index defined in Eq. (3.8). The mass matrix $\beta_{\mathrm{min}} \otimes \mathbb{1}_N$ is unique up to a sign. The matrix M must obey the polar decomposition

$$\begin{aligned} M &= U_{N-n,n}\, I_{N-n,n}\, U^\dagger_{N-n,n}, \\ I_{N-n,n} &= \mathrm{diag}(+\mathbb{1}_{N-n}, -\mathbb{1}_n), \end{aligned} \quad \text{(A32)}$$

where the matrices $U_{N-n,n}$ form either $\mathrm{U}(N)$,$\mathrm{O}(N)$, or $\mathrm{Sp}(N)$ depending on the AZ symmetry class. (For the symplectic case, a matrix in $\mathrm{Sp}(N)$ has quaternions as matrix elements.) The representation (A32) is unique up to multiplication of $U_{N-n,n}$ from the right by the block diagonal matrix $\mathrm{diag}(U_{N-n}, U_n)$, where the $n \times n$ matrix U_n is taken from either $\mathrm{U}(n)$,$\mathrm{O}(n)$, or $\mathrm{Sp}(n)$ depending on the AZ symmetry class. The representations (3.7) and (3.8) follow.

Case of first descendant $\pi_0(V_d = R_1) = \mathbb{Z}_2$. There is a pair of two anticommuting normalized Dirac mass matrices that span $V_{d,2r_{\mathrm{min}}}$ upon increasing r from r_{min} to $2r_{\mathrm{min}}$. We can choose a representation of the Dirac mass matrix as follows. If $N = 2,3,\ldots$ and if we define the Hermitian $r_{\mathrm{min}}/2 \times r_{\mathrm{min}}/2$

matrix $\rho_{\min}$ by

$$\beta_{\min} =: \rho_{\min} \otimes \tau_2, \tag{A33a}$$

we may then write

$$\rho_{\min} \otimes M \equiv \rho_{\min} \otimes (\tau_2 A_2 + \tau_1 A_1) \tag{A33b}$$

for the generic normalized Dirac mass. Here, the $2N \times 2N$ matrix M is Hermitian and antisymmetric because the $N \times N$ matrix A_2 is Hermitian and symmetric (A_2 commutes with the operation K for complex conjugation), while the $N \times N$ matrix A_1 is Hermitian and antisymmetric (A_1 anticommutes with the operation K for complex conjugation). The matrix M is a solution of the extension problem

$$Cl_{1,2} = \{\mathrm{i}\tau_3; \mathsf{K}, \mathrm{i}\mathsf{K}\} \to Cl_{1,3} = \{\mathrm{i}\tau_3; \mathsf{K}, \mathrm{i}\mathsf{K}, M\}. \tag{A34}$$

Indeed, it is the matrix $\mathrm{i}\tau_3$ that enters in the kinetic contribution to the Dirac Hamiltonian in the example (A23b) for a one-dimensional Dirac Hamiltonian in the symmetry class D. The explicit representation of Eq. (3.15) for this example thus follows from solving with Eq. (A33) the extension problem (A34).

It is instructive to compare Eqs. (A33a) and (A33b) with the explicit representations (A12b) and (A23b) corresponding to the one-dimensional symmetry class D with $r = r_{\min}$ and $r = 2r_{\min}$, respectively. This comparison suggests that the choice $A_2 = \pm\mathbb{1}_N$ and $A_1 = 0$ is special for any odd N. Indeed, one may verify that it is impossible to construct an antisymmetric matrix A_1 of odd rank N that connects smoothly, without closing a gap, between the choices $A_2 = +\mathbb{1}_N$ and $A_1 = 0$ on the one hand, and $A_2 = -\mathbb{1}_N$ and $A_1 = 0$ on the other hand. Hence the choices $A_2 = \pm\mathbb{1}_N$ and $A_1 = 0$ represent two topologically distinct phases when N is odd.

Finally, we observe that there is no unique Dirac mass matrix that commutes with all other Dirac mass matrices for $N > 1$. For example, the Dirac mass matrix with $A_2 = \mathbb{1}_3$ and $A_1 = 0$ neither commutes nor anticommutes with the Dirac mass matrix for which

$$A_2 = \begin{pmatrix} \cos\theta & 0 & 0 \\ 0 & \cos\theta & 0 \\ 0 & 0 & 1 \end{pmatrix}, \quad A_1 = \sin\theta \begin{pmatrix} 0 & -\mathrm{i} & 0 \\ +\mathrm{i} & 0 & 0 \\ 0 & 0 & 0 \end{pmatrix}. \tag{A35}$$

Case of second descendant $\pi_0(V_d = R_2) = \mathbb{Z}_2$. There is a pair of three anticommuting normalized Dirac mass matrices that span $V_{d,2r_{\min}}$ upon increasing r from $r_{\min}$ to $2r_{\min}$. We can choose a representation of the Dirac mass matrix as follows. If $N = 2,3,\ldots$ and if we define the Hermitian $r_{\min}/2 \times r_{\min}/2$ matrix $\rho_{\min}$ by

$$\beta_{\min} =: \rho_{\min} \otimes \tau_2, \tag{A36a}$$

we may then write

$$\rho_{\min} \otimes M \equiv \rho_{\min} \otimes (\tau_2 A_2 + \tau_3 A_3 + \tau_1 A_1 + \tau_0 A_0) \tag{A36b}$$

for the generic Dirac mass matrix. Here, the $2N \times 2N$ matrix M is Hermitian and antisymmetric because the $N \times N$ matrix A_2 is Hermitian and symmetric (A_2 commutes with the operation K for complex conjugation), while the $N \times N$ matrix A_3, A_1, and A_0 are Hermitian and antisymmetric (A_3 and A_1 anticommute with the operation K for complex conjugation). The matrix M is a solution of the extension problem

$$Cl_{0,2} = \{;\mathsf{K}, \mathrm{i}\mathsf{K}\} \to Cl_{0,3} = \{;\mathsf{K}, \mathrm{i}\mathsf{K}, M\}, \tag{A37}$$

which constrains M to be pure imaginary, as can be verified for Eq. (A36b). The representation (3.15) follows.

The normalized Dirac mass matrix (A36a) should be compared with that in Eq. (A25) for the one-dimensional symmetry class DIII with $r = 4$, and Eq. (A36b) should be compared with the normalized Dirac masses for the one-dimensional symmetry class DIII with $r = 8$ that we now present. If we impose PHS and TRS through

$$\mathcal{H}(k) = -\mathcal{H}^*(-k), \tag{A38a}$$

$$\mathcal{H}(k) = +\tau_2 \otimes \sigma_0 \otimes \rho_0\, \mathcal{H}^*(-k)\, \tau_2 \otimes \sigma_0 \otimes \rho_0, \tag{A38b}$$

then

$$\begin{aligned} \mathcal{H}(k) = {} & \tau_3 \otimes \sigma_0 \otimes \rho_0\, k \\ & + \sum_{\nu=0,1,3} \tau_3 \otimes (\sigma_2 \otimes \rho_\nu\, A_{1,2,\nu} + \sigma_\nu \otimes \rho_2\, A_{1,\nu,2}) \\ & + \sum_{\nu=0,1,3} \tau_1 \otimes (\sigma_2 \otimes \rho_\nu\, M_{1,2,\nu} + \sigma_\nu \otimes \rho_2\, M_{1,\nu,2}). \end{aligned} \tag{A38c}$$

The topological space of normalized Dirac masses obtained by adding to the Dirac kinetic contribution a mass matrix squaring to the unit matrix and obeying PHS squaring to unity is

$$\begin{aligned} V^{\mathrm{DIII}}_{d=1,r=8} &= \{\boldsymbol{M} \cdot \boldsymbol{X} | \boldsymbol{M}^2 = 1\} \cup \{\boldsymbol{N} \cdot \boldsymbol{Y} | \boldsymbol{N}^2 = 1\}, \\ \boldsymbol{M} &:= (M_{1,2,0}, M_{1,1,2}, M_{1,3,2}), \\ \boldsymbol{N} &:= (M_{1,0,2}, M_{1,2,1}, M_{1,2,3}), \\ \boldsymbol{X} &:= (\tau_1 \otimes \sigma_2 \otimes \rho_0, \tau_1 \otimes \sigma_1 \otimes \rho_2, \tau_1 \otimes \sigma_3 \otimes \rho_2), \\ \boldsymbol{Y} &:= (\tau_1 \otimes \sigma_0 \otimes \rho_2, \tau_1 \otimes \sigma_2 \otimes \rho_1, \tau_1 \otimes \sigma_2 \otimes \rho_3). \end{aligned} \tag{A39}$$

As a topological space, $V^{\mathrm{DIII}}_{d=1,r=8} \simeq S^2 \cup S^2$ is homeomorphic to O(4)/U(2), for the homeomorphisms

$$\begin{aligned} \mathrm{O}(4)/\mathrm{U}(2) &\simeq \mathbb{Z}_2 \times \mathrm{SO}(4)/[\mathrm{U}(1) \times \mathrm{SU}(2)] \\ &\simeq \mathbb{Z}_2 \times [\mathrm{SO}(3) \times \mathrm{SU}(2)]/[\mathrm{SO}(2) \times \mathrm{SU}(2)] \\ &\simeq \mathbb{Z}_2 \times \mathrm{SO}(3)/\mathrm{SO}(2) \\ &\simeq S^2 \cup S^2 \end{aligned} \tag{A40}$$

hold between topological spaces. In order to compare the Dirac mass matrices entering Eq. (A38) with Eq. (A36b), notice first that $\rho_{\min} = \tau_1$ and second that σ_ν in Eq. (A39) plays the role of τ_ν in Eq. (A36b).

b. Case $\pi_0(V) = 0$

There is at least one $r_{\min} \times r_{\min}$ Hermitian matrix $\beta'_{\min}$ that enters "..." in Eq. (A29) such that it anticommutes with any one of the $(d+1)$ matrices $\alpha_{\min 1}, \ldots, \alpha_{\min d}, \beta_{\min}$ and it squares to the unit $r_{\min} \times r_{\min}$ matrix. For any $0 \leqslant \theta < 2\pi$, we may then define the normalized mass matrix

$$\beta_{\min}(\theta) := \cos\theta\, \beta_{\min} + \sin\theta\, \beta'_{\min} \tag{A41}$$

that provides a smooth path between $\beta_{\min}$ and $-\beta_{\min}$. Since $\beta_{\min}$ can be chosen arbitrarily in the compact topological

space V associated with the massive Dirac Hamiltonian (A29), we can rule out the existence of the disconnected subspace $\{\pm\beta_{\rm min}\}$ in $V_{d,r_{\rm min}}$. For general values of $N = 1,2,3,\ldots$, the trivial zeroth homotopy group $\pi_0(V_{d,r_{\rm min}}) = 0$ indicates that for any given pair $(\beta,\beta') \in V_{d,r_{\rm min}N} \times V_{d,r_{\rm min}N}$ (not necessarily anticommuting), we find the sequence of anticommuting pairs $(\beta,\beta_1) \in V_{d,r_{\rm min}N} \times V_{d,r_{\rm min}N}$, $(\beta_1,\beta_2) \in V_{d,r_{\rm min}N} \times V_{d,r_{\rm min}N}, \ldots, (\beta_n,\beta') \in V_{d,r_{\rm min}N} \times V_{d,r_{\rm min}N}$ as occurs in Eq. (A26).

4. Existence condition for the Dirac masses

Assume that we are given Eq. (A29). The question posed and solved in Sec. II was: (1) what is the compact topological space spanned by the normalized Dirac masses of rank $r = r_{\rm min}\,N$ in the limit $N \to \infty$?

By definition, the Dirac Hamiltonian (A29) realizes a topological insulator if the compact topological space V spanned by the normalized Dirac mass $\beta_{\rm min}$ consists of no more than the set $\{\pm\beta_{\rm min}\}$. It then follows that, on any $(d-1)$-dimensional boundary of d-dimensional space, the Dirac Hamiltonian (A29) reduces to a massless Dirac Hamiltonian of the form

$$\widetilde{\mathcal{H}} = \widetilde{\boldsymbol{\alpha}} \cdot \frac{\partial}{\mathrm{i}\partial \boldsymbol{x}} + \cdots, \tag{A42}$$

where the $(d-1)$ matrices $\widetilde{\alpha},\ldots,\widetilde{\alpha}$ anticommute pairwise and square to the unit, their rank is $r = r_{\rm min}/2$, and "..." accounts for scalar and vector gauge contributions, but "..." does not contain Dirac mass terms. Moreover, by the definition of the minimal rank $r_{\rm min}$, no Dirac mass is permissible upon lowering the rank of the Dirac matrices entering the Dirac Hamiltonian (A29) holding the dimensionality of space and the AZ symmetry class fixed. These observations motivate the following question: (2) given an AZ symmetry class and given the dimensionality d of space, is a Dirac mass of rank $\widetilde{r}_{\rm min}$ permissible or not?

Here, $\widetilde{r}_{\rm min}$ is the minimal rank for which it is possible to write down the kinetic contribution $-\mathrm{i}\widetilde{\boldsymbol{\alpha}} \cdot \partial/\partial \boldsymbol{x}$ to the Dirac Hamiltonian given the dimensionality d of space and the AZ symmetry class.

We want to know if a massless Dirac Hamiltonian belonging to some prescribed d-dimensional AZ symmetry class accommodates a Dirac mass. To answer this question, we recall that Eqs. (2.15) and (2.17) define for any AZ symmetry class and for any dimension d a Clifford algebra that supports at least one normalized Dirac mass, provided the rank r of the Dirac matrices is no less than the minimal rank $r_{\rm min}$. If we replace $r_{\rm min}$ by $\widetilde{r}_{\rm min}$, the answer to question 2 is given by the extension problems (the values of p and q are taken from Table I)

$$\begin{aligned} Cl_{q-1} &= \{e_1,\ldots,e_{q-1}\} \\ &\to \{e_1,\ldots,e_{q-1},e_q\} = Cl_q \end{aligned} \tag{A43a}$$

for the complex symmetry classes A and AIII;

$$\begin{aligned} Cl_{p,q-1} &= \{e_1,\ldots,e_p;e_{p+1},\ldots,e_{p+q-1}\} \\ &\to \{e_1,\ldots,e_p;e_{p+1},\ldots,e_{p+q-1},e_{p+q}\} = Cl_{p,q} \end{aligned} \tag{A43b}$$

for the real symmetry classes BDI, D, DIII, CII, C and CI; and

$$\begin{aligned} Cl_{p-1,q} &= \{e_1,\ldots,e_{p-1};e_p,\ldots,e_{p+q-1}\} \\ &\to \{e_1,\ldots,e_{p-1},e_p;e_{p+1},\ldots,e_{p+q}\} = Cl_{p,q} \end{aligned} \tag{A43c}$$

for the real symmetry classes AI and AII. In other words, for any given AZ symmetry class, we seek to enumerate all the distinct ways there are to construct the corresponding Clifford algebra from Eqs. (2.18) and (2.19) out of one in the same symmetry class but with one fewer generator. Recall here that the Clifford algebras (2.18) and (2.19) are obtained after removing the generator associated with the normalized Dirac mass in each of the Clifford algebras (2.15) and (2.17). The solutions to Eqs. (A43) are the classifying spaces (the values of p and q are taken from Table I)

$$\widetilde{V} = C_{q-1}, \quad \widetilde{V} = R_{q-p-1}, \quad \widetilde{V} = R_{p-q+1}, \tag{A44}$$

respectively. On the one hand, if $\pi_0(\widetilde{V}) = \mathbb{Z},\mathbb{Z}_2$, then the generator e_{p+q} from the corresponding Clifford algebra is unique in that no additional generator exists that anticommutes with e_{p+q} (see Appendix A 3), i.e., no additional generator e_{p+q+1} that plays the role of a normalized Dirac mass represented by a Hermitian matrix of rank $\widetilde{r}_{\rm min}$ is allowed. On the other hand, if $\pi_0(\widetilde{V}) = 0$, then the generator e_{p+q} from the corresponding Clifford algebra is not unique in that there exist additional independent generators that anticommute with e_{p+q} (see Appendix A 3), i.e., a generator e_{p+q+1} that plays the role of a normalized Dirac mass represented by a Hermitian matrix of rank $\widetilde{r}_{\rm min}$ is allowed.

For comparison, the answer to question 1 was given in Table I by the extension problems (the values of p and q are taken from Table I)

$$Cl_q = \{e_1,\ldots,e_q\} \to \{e_1,\ldots,e_q,e_{q+1}\} = Cl_{q+1} \tag{A45a}$$

for the complex symmetry classes A and AIII;

$$\begin{aligned} Cl_{p,q} &= \{e_1,\ldots,e_p;e_{p+1},\ldots,e_{p+q}\} \\ &\to \{e_1,\ldots,e_p;e_{p+1},\ldots,e_{p+q},e_{p+q+1}\} = Cl_{p,q+1} \end{aligned} \tag{A45b}$$

for the real symmetry classes BDI, D, DIII, CII, C and CI; and

$$\begin{aligned} Cl_{p,q} &= \{e_1,\ldots,e_p;e_{p+1},\ldots,e_{p+q}\} \\ &\to \{e_1,\ldots,e_p,e_{p+1};e_{p+2},\ldots,e_{p+q+1}\} = Cl_{p+1,q} \end{aligned} \tag{A45c}$$

for the real symmetry classes AI and AII. The solutions to Eqs. (A45) are the classifying spaces (the values of p and q are taken from Table I)

$$V = C_q, \quad V = R_{q-p}, \quad V = R_{p-q+2}, \tag{A46}$$

respectively. Thus the classifying space associated with question 2 in d dimensions coincides with the classifying space associated with question 1 in $d+1$ dimensions. The existence of nontrivial topological insulators in $d+1$ dimensions and the gapless Dirac Hamiltonian with no allowed Dirac mass in d dimensions are equivalent.

The final answer to the question **2** is, (1) no Dirac mass matrix of rank $\widetilde{r}_{\rm min}$ is permissible when $\pi_0(\widetilde{V}) = \mathbb{Z}$. If N

channels are added by generalizing the Dirac matrices $\widetilde{\alpha}$ to $\widetilde{\boldsymbol{\alpha}} \otimes \mathbb{1}_N$, then no Dirac mass of rank $\widetilde{r}_{\min} N$ is permissible when $\pi_0(\widetilde{V}) = \mathbb{Z}$. (2) No Dirac mass matrix of rank $\widetilde{r}_{\min}$ is permissible when $\pi_0(\widetilde{V}) = \mathbb{Z}_2$. If N channels are added by generalizing the Dirac matrices $\widetilde{\alpha}$ to $\widetilde{\boldsymbol{\alpha}} \otimes \mathbb{1}_N$, then no Dirac mass of rank $\widetilde{r}_{\min} N$ is permissible for odd N, while a Dirac mass of rank $\widetilde{r}_{\min} N$ is permissible for even N, when $\pi_0(\widetilde{V}) = \mathbb{Z}_2$. (3) A Dirac mass matrix of rank $\widetilde{r}_{\min}$ is permissible when $\pi_0(\widetilde{V}) = 0$. If N channels are added by generalizing the Dirac matrices $\widetilde{\alpha}$ to $\widetilde{\boldsymbol{\alpha}} \otimes \mathbb{1}_N$, then a Dirac mass matrix of rank $\widetilde{r}_{\min} N$ is permissible when $\pi_0(\widetilde{V}) = 0$. Table VI from Sec. VII follows.

APPENDIX B: ONE-LOOP RENORMALIZATION GROUP ANALYSIS IN 2D SPACE

We summarize the one-loop RG flows associated with the relevant 2D random Dirac Hamiltonians from Refs. [15,134] that we have used to deduce the global phase diagrams presented in Sec. V.

For simplicity, we present RG flows for vanishing mean values of all random potentials. A mean value for any random mass is a strongly relevant perturbation. This is the control parameter for the 2D phase diagrams along the horizontal axis. Although we do not present the contributions to the RG flows from nonvanishing mean values of the random masses, their contributions are essential to cross phase boundaries. They are thus implicitly assumed to be present.

1. Replica limit

Define the path integral

$$Z := \int \mathcal{D}[\bar{\psi}]\mathcal{D}[\psi]\, \exp(-S), \tag{B1a}$$

$$S := \mathrm{i} \int \mathrm{d}^2\boldsymbol{r} \left(\bar{\psi}\, \mathcal{H}_0\, \psi + \sum_\iota V_\iota\, \phi_\iota(\bar{\psi},\psi) \right), \tag{B1b}$$

$$\mathcal{H}_0 := \sigma_x(-\mathrm{i}\partial_x) + \sigma_y(-\mathrm{i}\partial_y). \tag{B1c}$$

Here, $\phi_\iota(\bar{\psi},\psi)$ is a local quadratic form for the pair $\bar{\psi}$ and ψ of independent Grassmann-valued spinors. For any pair ι,ι', the real-valued functions V_ι and $V_{\iota'}$ are random with vanishing means and with

$$\overline{V_\iota(\boldsymbol{r})\, V_{\iota'}(\boldsymbol{r}')} = \delta_{\iota,\iota'}\, g_\iota\, \delta(\boldsymbol{r}-\boldsymbol{r}') \tag{B1d}$$

as the only nonvanishing moments.

In order to compute the disorder-average over the correlations functions for the Grassmann-valued spinors, it is convenient to take the replica limit

$$\ln Z = \lim_{n\to 0} \frac{Z^n - 1}{n}. \tag{B2}$$

If we reserve the index $a,b = 1,\ldots,n$, we may write

$$\overline{Z^n} = \int \mathcal{D}[\bar{\psi}]\mathcal{D}[\psi] \exp\left(-\int \mathrm{d}^2\boldsymbol{r}\, (L_0 + L_{\mathrm{int}}) \right), \tag{B3a}$$

$$L_0 := \mathrm{i} \sum_{a=1}^{n} \bar{\psi}^a [\sigma_x\, (-\mathrm{i}\partial_x) + \sigma_y\, (-\mathrm{i}\partial_y)] \psi^a, \tag{B3b}$$

$$L_{\mathrm{int}} := \sum_\iota \frac{g_\iota}{2} \sum_{a,b=1}^{n} \phi_\iota^a\, \phi_\iota^b, \tag{B3c}$$

for the disorder average over the nth power of the partition function. The effective action

$$S_{\mathrm{eff}} := \int \mathrm{d}^2\boldsymbol{r}\, (L_0 + L_{\mathrm{int}}) \tag{B3d}$$

describes an interacting and nonunitary quantum field theory [134]. Disorder averaged correlation functions for the Grassmann fields are computed by first using the effective partition function (B3) and then by taking the replica limit (B2).

2. One-loop renormalization group β functions from the operator product expansion

Assume that space is the d-dimensional Euclidean space. Define the path integral

$$Z := \int \mathcal{D}[\bar{\psi}]\mathcal{D}[\psi]\, \exp(-S_0 - S_{\mathrm{int}}), \tag{B4a}$$

$$S_0 := \mathrm{i} \int \mathrm{d}^d\boldsymbol{r}\, \bar{\psi}\, \boldsymbol{\alpha} \cdot \frac{\partial}{\partial \boldsymbol{x}} \psi, \tag{B4b}$$

$$S_{\mathrm{int}} := \sum_a \lambda_a \int \frac{\mathrm{d}^d\boldsymbol{r}}{2\pi\, \mathfrak{a}^{d-2}}\, \Phi_a(\bar{\psi},\psi), \tag{B4c}$$

where $\boldsymbol{\alpha}$ are Dirac matrices that anticommute pairwise and square to the identity matrix, $\mathfrak{a}$ is the short-distance cutoff, $\Phi_a(\bar{\psi},\psi)$ is a local monomial of the Grassmann spinors, and λ_a is the corresponding dimensionless coupling. Assume the operator product expansion (OPE)

$$\Phi_a(\boldsymbol{r})\, \Phi_b(\boldsymbol{r}') = \frac{c_{abc}}{|\boldsymbol{r}-\boldsymbol{r}'|^{x_a+x_b-x_c}}\, \Phi_c(\boldsymbol{r}') + \cdots, \tag{B4d}$$

where the summation convention over repeated indices is implied, the tensor c_{abc} is real valued, the scaling exponent x_a of $\Phi_a(\boldsymbol{r})$ is real valued, and "..." contains all functions of $|\boldsymbol{r}-\boldsymbol{r}'|$ that are subleading relative to $|\boldsymbol{r}-\boldsymbol{r}'|^{x_a+x_b-x_c}$ in the limit $\boldsymbol{r}' \to \boldsymbol{r}$. The one-loop RG flows for the coupling constants is then

$$\frac{\mathrm{d}\lambda_a}{\mathrm{d}\ell} = (d - x_a)\, \lambda_a + \frac{1}{2} c_{abc}\, \lambda_b\, \lambda_c, \tag{B4e}$$

under the rescaling $\mathfrak{a} \to \mathfrak{a}(1 + \mathrm{d}\ell)$ of the short distance cutoff. When $d = 2$, Φ_a is quartic in the Grassmann spinors, and, after performing the rescaling

$$\lambda_a =: \pi\, g_a, \tag{B4f}$$

we find the one-loop β functions

$$\beta_a \equiv \frac{\mathrm{d}g_a}{\mathrm{d}\ell} = \frac{\pi}{2}\, c_{abc}\, g_b\, g_c. \tag{B4g}$$

3. Renormalization group flows for the AZ symmetry classes

One-loop RG flows for random masses and random gauge potentials of 2D Dirac Hamiltonians [15,134] are used in this paper to decide whether a metallic phase or a critical boundary separates topologically distinct insulating phases in the phase diagrams of Fig. 4. For the symmetry classes in which metallic conductivities acquire antiweak localization corrections, a metallic phase is stable for large bare values of g. Whether a metallic phase persists from large to infinitesimally small bare values of g along the boundary between topologically distinct insulating phases is determined by the RG flows in the

vicinity of $\mathsf{g} = 0$. If the characteristic disorder strength g is marginally relevant, then it is a metallic phase that separates two topologically distinct insulating phases for any $\mathsf{g} > 0$. (Evidently, we are assuming no intermediary fixed points between the ones at $\mathsf{g} = \infty$ and $\mathsf{g} = 0$.) On the other hand, if the disorder strength g is marginally irrelevant, then it is a critical boundary that separates two topologically distinct insulating phases. (In this case, there has to be a critical point where the phase boundary is terminated by a metallic phase.)

For these reasons, we revisit one-loop RG flows of random masses and random gauge potentials for those symmetry classes that are characterized by antiweak localization corrections, i.e., the symmetry classes D, DIII, and AII [4]. The RG equations are obtained from OPEs of operators associated with all random masses and random gauge potentials allowed in each symmetry class. The OPEs are calculated by taking contractions in a product of two fermion quartic terms in Eqs. (B3c) and (B4c) using the two-point correlation function of free Dirac fields,

$$\langle \psi^a(\boldsymbol{r})\, \bar{\psi}^b(\boldsymbol{0})\rangle = \frac{\boldsymbol{r}\cdot\boldsymbol{\sigma}}{2\pi\,|r|^2}\,\delta_{ab}. \tag{B5}$$

To begin with, we first consider symmetry classes A and C and then move on to symmetry classes D, DIII, and AII.

a. Symmetry class A

Following Ref. [15], we consider the 2D random Dirac Hamiltonian

$$\mathcal{H} := \sigma_x(-\mathrm{i}\partial_x + A_x) + \sigma_y(-\mathrm{i}\partial_y + A_y) + m\,\sigma_z + V \tag{B6}$$

of rank $r = 2$ in the symmetry class A.

We seek the one-loop RG equations obeyed by the coupling constants

$$g_M = \overline{m^2}, \tag{B7a}$$

$$g_V = \overline{V^2}, \tag{B7b}$$

$$g_A = \overline{A_x^2} + \overline{A_y^2}. \tag{B7c}$$

These couplings are the coefficients of the fermion quartic terms

$$\Phi_M = -\sum_{a,b=1}^{n} :\bar{\psi}^a\,\sigma_z\psi^a\,\bar{\psi}^b\,\sigma_z\psi^b:, \tag{B8a}$$

$$\Phi_V = -\sum_{a,b=1}^{n} :\bar{\psi}^a\,\psi^a\,\bar{\psi}^b\,\psi^b:, \tag{B8b}$$

$$\Phi_A = -\sum_{a,b=1}^{n} \frac{1}{2}(:\bar{\psi}^a\sigma_x\psi^a\bar{\psi}^b\sigma_x\psi^b: + :\bar{\psi}^a\sigma_y\psi^a\bar{\psi}^b\sigma_y\psi^b:), \tag{B8c}$$

where the interactions Φ_V, Φ_A, and Φ_M are generated by taking the disorder average over the random scalar potential, the random vector potentials, and the random mass, respectively. Their nonvanishing OPEs are [106,134]

$$\Phi_M(\boldsymbol{r})\,\Phi_M(\boldsymbol{0}) = \frac{-2}{\pi^2 r^2}\,\Phi_M(\boldsymbol{0}), \tag{B9a}$$

$$\Phi_V(\boldsymbol{r})\,\Phi_V(\boldsymbol{0}) = \frac{2}{\pi^2 r^2}\,\Phi_V(\boldsymbol{0}), \tag{B9b}$$

$$\Phi_V(\boldsymbol{r})\,\Phi_M(\boldsymbol{0}) = \frac{1}{\pi^2 r^2}\,[\Phi_V(\boldsymbol{0}) + 2\Phi_A(\boldsymbol{0}) - \Phi_M(\boldsymbol{0})], \tag{B9c}$$

$$\Phi_M(\boldsymbol{r})\,\Phi_A(\boldsymbol{0}) = \frac{1}{\pi^2 r^2}\,[\Phi_M(\boldsymbol{0}) + \Phi_V(\boldsymbol{0})], \tag{B9d}$$

$$\Phi_V(\boldsymbol{r})\,\Phi_A(\boldsymbol{0}) = \frac{1}{\pi^2 r^2}\,[\Phi_V(\boldsymbol{0}) + \Phi_M(\boldsymbol{0})], \tag{B9e}$$

where we have only kept singular parts proportional to $r^{-2} \equiv \boldsymbol{r}^{-2}$ on the right-hand sides. Then, the RG equations for symmetry class A read

$$\frac{\mathrm{d}g_M}{\mathrm{d}\ell} = \frac{1}{\pi}\big(-g_M^2 - g_V\,g_M + g_V\,g_A + g_A\,g_M\big), \tag{B10a}$$

$$\frac{\mathrm{d}g_V}{\mathrm{d}\ell} = \frac{1}{\pi}\big(g_V^2 + g_V\,g_M + g_V\,g_A + g_A\,g_M\big), \tag{B10b}$$

$$\frac{\mathrm{d}g_A}{\mathrm{d}\ell} = \frac{2}{\pi}\,g_V\,g_M. \tag{B10c}$$

As is well known [15], there is an unstable line of critical points $g_V = g_M = 0$ and $g_A > 0$. However, for the generic case $g_V > 0$ and $g_M > 0$, the coupling constants always flow to the strong-coupling regime. If so, the one-loop RG equations are no longer applicable. The (marginally relevant) coupling constants are represented by the characteristic coupling g in the phase diagram of 2D class A in Fig. 4(a). Since a stable metallic phase cannot exist in 2D systems of class A, topologically distinct insulating phases are separated by a phase boundary line on which wave functions are critical.

b. Symmetry class C

Next, we consider the 2D random Dirac Hamiltonian

$$\mathcal{H} := -\mathrm{i}\sigma_x\otimes\tau_0\,\partial_x - \mathrm{i}\sigma_y\otimes\tau_0\,\partial_y + m\,\sigma_z\otimes\tau_0 + \sum_{i=x,y}\sum_{j=x,y,z} A_{i,j}\,\sigma_i\otimes\tau_j + \sum_{i=x,y,z} V_i\,\sigma_0\otimes\tau_i \tag{B11a}$$

of rank $r = 4$ in the symmetry class C with the operation for charge conjugation represented by

$$\mathcal{C} := \sigma_x\otimes\tau_y\,\mathsf{K}, \tag{B11b}$$

where K denotes complex conjugation.

There are ten random functions allowed by the symmetry constraints that multiply the matrices

$$\begin{aligned}
&\sigma_z\otimes\tau_0 && && && \text{(mass)},\\
&\sigma_x\otimes\tau_x, && \sigma_x\otimes\tau_y, && \sigma_x\otimes\tau_z && \text{(vector potentials)},\\
&\sigma_y\otimes\tau_x, && \sigma_y\otimes\tau_y, && \sigma_y\otimes\tau_z && \text{(vector potentials)},\\
&\sigma_0\otimes\tau_x, && \sigma_0\otimes\tau_x, && \sigma_0\otimes\tau_x && \text{(scalar potentials)},
\end{aligned} \tag{B12}$$

respectively. Taking disorder average in the replicated action yields quartic interaction terms similar to those in Eq. (B8). The one-loop RG equations for the quartic terms can be found in Refs. [135,136]. Here, we discuss only a minimal set of the RG equations that allow us to deduce the phase diagram in Fig. 4(a). Taking $\sigma_x\otimes\tau_x$ and $\sigma_y\otimes\tau_x$ from the vector potentials and $\sigma_0\otimes\tau_x$ from the scalar potential along with the mass $\sigma_z\otimes\tau_0$ among the above ten terms, we find that the one-loop RG equations for the coupling constants g_V, g_A, and g_M take the same form as those in the symmetry class

A in Eq. (B10). Thus the representative coupling constant g of disorder is marginally relevant as in the symmetry class A. This indicates that the phase diagram for the symmetry class C is qualitatively the same as that for the symmetry class A, as shown in Figs. 4(a) and 4(b).

c. Symmetry class D

We consider the 2D random Dirac Hamiltonian

$$\mathcal{H} := -\mathrm{i}\sigma_x\,\partial_x - \mathrm{i}\sigma_y\,\partial_y + m\,\sigma_z \tag{B13a}$$

of rank $r = 2$ in the symmetry class D with the operation for charge conjugation represented by

$$\mathcal{C} := \sigma_x\,\mathsf{K}, \tag{B13b}$$

where K denotes complex conjugation. Disorder only enters through the mass matrix $m\,\sigma_z$ owing to the symmetry constraint imposed by the PHS for the symmetry class D.

The OPE of the fermion quartic term

$$\Phi_M := -\sum_{a,b=1}^{n} :\bar\psi^a\,\sigma_z\,\psi^a\,\bar\psi^b\,\sigma_z\,\psi^b: \tag{B14}$$

with itself delivers the RG equation [89,92]

$$\frac{\mathrm{d}g_M}{\mathrm{d}\ell} = -\frac{1}{\pi}\,g_M^2. \tag{B15}$$

Hence the variance g_m of the random mass term is a marginally irrelevant coupling and the clean critical point $g_M = \mathsf{m} = 0$ is stable as long as the mean $\mathsf{m} = 0$.

The random Dirac Hamiltonian of rank $r = 4$ in the symmetry class D with the PHS symmetry generated by conjugation with $C = \sigma_x \otimes \tau_0\,\mathsf{K}$ depends on six random functions that multiply the matrices

$$\begin{aligned} &\sigma_z\otimes\tau_0,\quad \sigma_z\otimes\tau_x,\quad \sigma_z\otimes\tau_z && \text{(masses)},\\ &\sigma_x\otimes\tau_y,\quad \sigma_y\otimes\tau_y && \text{(vector potentials)},\\ &\sigma_0\otimes\tau_y && \text{(scalar potential)}, \end{aligned} \tag{B16}$$

respectively.

Our aim is to explain why, unlike for the case of $r = 2$ in Eq. (B13), the massless clean critical point described by

$$\mathcal{H}_\star := (-\mathrm{i}\sigma_x\,\partial_x - \mathrm{i}\sigma_y\,\partial_y)\otimes\tau_0 \tag{B17}$$

is (i) unstable to disorder, (ii) this instability depends sensitively on the choice of the probability distribution for the disorder, and (iii) we are led to the choice (3.10) for the probability distribution and to Fig. 4(d) to describe qualitatively the generic phase diagram in the 2D symmetry class D with $N = 2$.

We first choose the probability distribution for the six random functions such that they are independent and Gaussian distributed with the means and variances $\mathsf{m}\in\mathbb{R}$ and $\mathsf{g}_0 \geqslant 0$ for the mass matrix $\sigma_z\otimes\tau_0 \equiv \beta_0$; $\mathsf{m}_x\in\mathbb{R}$ and $\mathsf{g}_x \geqslant 0$ for the mass matrix $\sigma_z\otimes\tau_x$; $\mathsf{m}_z\in\mathbb{R}$ and $\mathsf{g}_z \geqslant 0$ for the mass matrix $\sigma_z\otimes\tau_z$; 0 and $g_A \geqslant 0$ for the vector potentials; and 0 and $g_V \geqslant 0$ for the scalar potential, respectively. With this convention, the parameter space for the phase diagram is no less than eight dimensional with the point

$$0 = \mathsf{m} = \mathsf{g}_0 = \mathsf{m}_x = \mathsf{g}_x = \mathsf{m}_z = \mathsf{g}_z = g_A = g_V \tag{B18}$$

corresponding to the massless clean Dirac Hamiltonian $\mathcal{H}_\star$ of rank $r = 4$ in the 2D symmetry class D.

It is natural to start with the clean limit

$$0 = \mathsf{g}_0 = \mathsf{g}_x = \mathsf{g}_z = g_A = g_V. \tag{B19a}$$

In this limit, we may write [compare with Eq. (3.10)]

$$\mathcal{H} = (-\mathrm{i}\sigma_x\,\partial_x - \mathrm{i}\sigma_y\,\partial_y)\otimes\tau_0 + \mathcal{V}, \tag{B19b}$$

where the Dirac mass V is decomposed into

$$\mathcal{V} = \mathsf{m}\,\beta_0 + \mathcal{V}_0 \tag{B19c}$$

with

$$\beta_0 := \sigma_z\otimes\tau_0,\quad \mathcal{V}_0 := \sigma_z\otimes M_0,\quad M_0 := \mathsf{m}_x\,\tau_x + \mathsf{m}_z\,\tau_z. \tag{B19d}$$

The Hermitian 2×2 matrix M_0 has the $N = 2$ nondegenerate eigenvalues

$$\mathsf{m}_\pm := \pm\sqrt{\mathsf{m}_x^2 + \mathsf{m}_z^2} \tag{B20}$$

provided $\mathsf{m}_x^2 + \mathsf{m}_z^2 > 0$. The four eigenvalues of $\mathcal{V}$ are $\mathsf{m}_\pm + \mathsf{m}$ and $\mathsf{m}_\pm - \mathsf{m}$. The relevant parameter space needed to identify the distinct topological phases is two-dimensional. It is spanned by the parameters m and $\mathsf{m}_\pm$. There are three topologically distinct insulating phases that are defined by

$$\nu = \begin{cases} +1, & \mathsf{m} > \mathsf{m}_+,\\ 0, & |\mathsf{m}| < |\mathsf{m}_\pm|,\\ -1, & \mathsf{m} < \mathsf{m}_-, \end{cases} \tag{B21a}$$

where the index ν is given by [recall Eq. (3.8)]

$$\nu = \tfrac{1}{2}\,\mathrm{sgn}(\mathsf{m} + |\mathsf{m}_+|) + \tfrac{1}{2}\,\mathrm{sgn}(\mathsf{m} - |\mathsf{m}_+|). \tag{B21b}$$

The first term on the right-hand side is the dimensionless (thermal) Hall conductivity of a 2×2 massive Dirac Hamiltonian with the mass $\mathsf{m} + |\mathsf{m}_+|$. The second term on the right-hand side is the dimensionless (thermal) Hall conductivity of a 2×2 massive Dirac Hamiltonian with the mass $\mathsf{m} - |\mathsf{m}_+|$. A phase transition between the $|\nu| = 1$ and $\nu = 0$ insulating phases occurs whenever

$$|\mathsf{m}| = |\mathsf{m}_+|. \tag{B21c}$$

The phase boundaries (B21c) in the two-dimensional parameter space,

$$\{(\mathsf{m},\mathsf{m}_+)\in\mathbb{R}^2 | \mathsf{m}_+ \geqslant 0\}, \tag{B22}$$

meet at the massless Dirac point $\mathsf{m} = \mathsf{m}_+ = 0$. The massless Dirac point $\mathsf{m} = \mathsf{m}_+ = 0$ is unstable to any nonvanishing m or m_+. The line parallel to the horizontal axis in Fig. 6(a) intersects the phase boundaries (B21c) at the two critical points $\mathsf{m} = \pm\mathsf{m}_+$ at which the gap of one and only one of the two massive Dirac cones in the spectrum closes.

The origin of parameter space (B22) is a multicritical point, contrary to the two critical points at fixed value of m_+ depicted

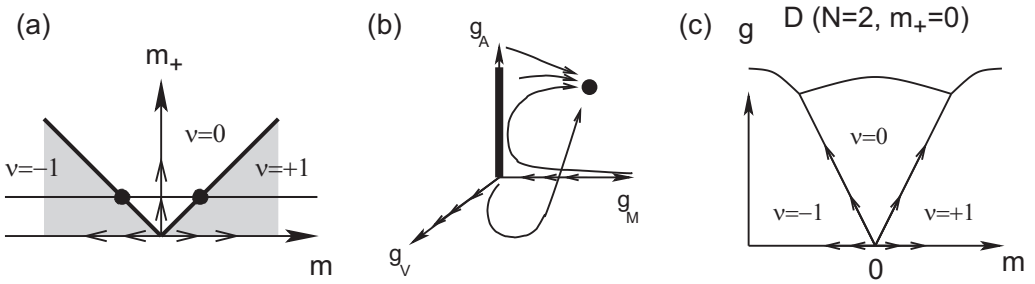

FIG. 6. (a) Phase diagram in the parameter space (B22). There are three gapped phases all meeting at the origin, the clean massless Dirac Hamiltonian of rank $r = 4$ in two-dimensional space. The origin of parameter space is a critical point that is unstable to both m or m_+ as is indicated by the arrows. The gray region with the mass $\mathsf{m} > \mathsf{m}_\pm > 0$ supports the dimensionless quantized thermal Hall conductivity $\nu = +1$. The gray region with the mass $\mathsf{m} < -\mathsf{m}_+ < 0$ supports the dimensionless quantized thermal Hall conductivity $\nu = -1$. The white region with $\mathsf{m}_+ > |\mathsf{m}| > 0$ support the dimensionless quantized thermal Hall conductivity $\nu = 0$. The critical lines $\mathsf{m} = \pm\mathsf{m}_+$ separates two insulating phases whose Chern numbers differ by the number 1 in magnitude. The line parallel to the horizontal axis at fixed value of m_+ intersects the phase boundaries at two critical points depicted by two filled circles. (b) Phase diagram in the parameter space $g_M, g_V, g_A \geqslant 0$ spanned by the variances of a random mass, a random scalar potential, and a random vector potential (all of vanishing means) in the 2D symmetry class A for a random Dirac Hamiltonian of rank $r = 2$ [15]. The bullet represents the stable flows to the critical point that describes the plateau transition in the integer quantum Hall effect. The unstable flow away from this critical point corresponds to a nonvanishing mean value of the random mass and is thus not present in this three-dimensional parameter space. (c) Projected phase diagram with the vanishing mean masses $\mathsf{m}_+ = 0$ onto a two-dimensional cut with the same horizontal axis as in (a) but with a vertical axis encoding multiples sources of disorder including the variance g associated with the random mass of mean m. The direction g can be thought of as a cross section of all the directions associated with the variances of the disorder coming out of the plane in (a).

by bullets in Fig. 6(a). This difference manifests itself in the stability of these three points to disorder. Our next task is to assess the effects of disorder on the multicritical point at the origin of parameter space (B22).

If we choose the probability distribution with

$$0 = \mathsf{m} = \mathsf{m}_x = \mathsf{g}_x = \mathsf{m}_z = \mathsf{g}_z = 0, \quad \mathsf{g}, g_{\mathrm{V}}, g_{\mathrm{A}} \geqslant 0, \tag{B23}$$

then the random Dirac Hamiltonian is reducible, as a rotation of τ_y about τ_x into τ_z brings it to the representation

$$\begin{aligned}\mathcal{H}_{\star\star} = \mathcal{H}_\star &+ (A_x\,\sigma_x + A_y\,\sigma_y) \otimes \tau_z \\ &+ M\,\sigma_z \otimes \tau_0 + V\,\sigma_0 \otimes \tau_z.\end{aligned} \tag{B24}$$

The random Dirac Hamiltonian $\mathcal{H}_{\star\star}$ of rank $r = 4$ is evidently block diagonal with irreducible blocks of rank $r = 2$ that belong to the symmetry class A. Hence the variances g_0, g_V, and g_A obey the same one-loop RG flows as in Eq. (B10) that we depict in Fig. 6(b). In particular, the variance g_0 of the random mass that commutes with all other masses flows to the strong coupling as soon as either g_V or g_A is nonvanishing.

The reducibility of the rank $r = 4$ Dirac Hamiltonian in the 2D symmetry class D is nongeneric. It is broken as soon as any one of the two variances g_x or g_z for the anticommuting pair of Dirac mass matrices is nonvanishing. In the parameter space

$$0 = \mathsf{m}_x = \mathsf{m}_z, \quad |\mathsf{m}|, \mathsf{g}_0, \mathsf{g}_x, \mathsf{g}_z, g_A, g_V > 0, \tag{B25}$$

the variance g is then expected to inherit the marginal relevance of the multicritical point (B18) in the neighborhood (B23). If the multidimensional parameter space is projected onto a two-dimensional plane parameterized by the probability distribution (3.9a), we conjecture by analogy to Figs. 3(a) and 4(b) the phase diagram shown in Fig. 6(c). This phase diagram is not the only one dictated by logic. It has the merit of simplicity, however. For example, its RG flows are more economical than conjecturing that the metallic phase precludes any direct phase boundary between two topologically distinct localized phase for any nonvanishing variance of the randomness.

The stability analysis of the two critical points intersecting the phase boundary at a nonvanishing fixed value of m_+ in Fig. 6(a) in the presence of a generic disorder from the symmetry class D is quite different from that of the multicritical point. We assume that the fluctuations are much smaller than the means at the two critical points defined by $|\mathsf{m}| = \mathsf{m}_+$ with $\mathsf{m}_+ > 0$ given in Fig. 6(a). This assumption justifies projecting the Dirac Hamiltonian of rank $r = 4$ onto the eigenspace of $\overline{m_x}\,\tau_x + \overline{m_z}\,\tau_z$ with the eigenvalue m_+ [15]. The resulting projected Dirac Hamiltonian is of rank $r = 2$ and has the same form as the rank $r = 2$ Hamiltonian defined in Eq. (B13). We can then apply the RG analysis for the Hamiltonian of rank $r = 2$ in Eq. (B13) to find that the effective coupling playing the role of g_M in Eq. (B13) is irrelevant along the phase boundary defined by the gap closing condition $\mathsf{m} = \mathsf{m}_+$. This reasoning explains why a nonvanishing mean value $\mathsf{m}_+ > 0$ is required in Eq. (3.10) in order for one of the N clean critical points at $\mathsf{g} = 0$ to be the end point of a phase boundary that separates a pair among $N + 1$ topologically distinct localized phases. This end point is the critical point that governs criticality at the phase boundary between two topologically distinct localized phases. No metallic phase prevents a direct transition between this pair of topologically distinct localized phases for not too strong disorder. The phase diagrams when $N = 1$ and $N = 2$ are depicted in Figs. 4(c) and 4(d), respectively. A phase diagram similar to that of Fig. 4(c) has been obtained from numerical simulations of network models in Refs. [91,92].

We close the discussion of the 2D symmetry class D with a generic $r = 4$ random Dirac Hamiltonian by observing that the Dirac mass

$$\begin{aligned}\mathcal{V}_0(\boldsymbol{r}) &:= m_x(\boldsymbol{r})\,\sigma_z \otimes \tau_x + m_z(\boldsymbol{r})\,\sigma_z \otimes \tau_z \\ &= m_+(\boldsymbol{r})\,[\cos\theta(\boldsymbol{r})\,\sigma_z \otimes \tau_x + \sin\theta(\boldsymbol{r})\,\sigma_z \otimes \tau_z],\end{aligned} \tag{B26a}$$

where

$$m_+(\boldsymbol{r}) := \sqrt{m_x^2(\boldsymbol{r}) + m_z^2(\boldsymbol{r})}, \quad \theta(\boldsymbol{r}) := \frac{m_z(\boldsymbol{r})}{m_x(\boldsymbol{r})}, \tag{B26b}$$

is generated by two anticommuting mass matrices, i.e.,

$$\mathcal{V}_0^2(\boldsymbol{r}) = m_+^2(\boldsymbol{r})\,\sigma_0 \otimes \tau_0. \tag{B26c}$$

The Dirac mass (B26) supports point defects defined by the two conditions that (i) $\lim_{\boldsymbol{r}\to\infty} m_+(\boldsymbol{r}) = \mathsf{m}_+$ and (ii) the phase $\theta(\boldsymbol{r})$ winds by an integer multiple of 2π along any closed path $\Gamma_{\boldsymbol{r}_{\rm vtx}}$ belonging to any open disk centered about the point $\boldsymbol{r}_{\rm vtx}$ that is not too large. The point $\boldsymbol{r}_{\rm vtx}$ thus represents a pointlike singularity of the vortex type. Jackiw and Rossi have shown in Ref. [114] that Dirac Hamiltonians of the form

$$\mathcal{H}_{\rm vtx} := \mathcal{H}_\star + \mathcal{V}_{\rm vtx}(\boldsymbol{r}) \tag{B27}$$

support n normalized zero modes if $\mathcal{V}_{\rm vtx}(\boldsymbol{r})$ is given by Eq. (B26) with the phase $\theta(\boldsymbol{r})$ winding by $2\pi\,n$ along all circles of sufficiently large radii. These zero modes are not robust to all remaining random channels compatible with the 2D symmetry class D. However, if n is an odd integer, at least one zero mode survives any perturbation arising from the scalar gauge, vector gauge, and the last massive channel, provided this massive channel associated to the Dirac mass matrix that commutes with $\mathcal{V}_{\rm vtx}(\boldsymbol{r})$ is everywhere smaller in magnitude than the asymptotic gap m_+. This is an illustration of the fact that the fundamental homotopy group for the normalized Dirac mass matrices in the 2D symmetry class D can be $\mathbb{Z}_2$. Correspondingly, the localized phase $\nu = 0$ in the phase diagram 4(d) is conjectured to support $\mathbb{Z}_2$ quasizero modes that will contribute to the density of states.

d. Symmetry class DIII

We consider the 2D random Dirac Hamiltonian

$$\mathcal{H} := -\mathrm{i}\sigma_x \otimes \tau_0\,\partial_x - \mathrm{i}\sigma_y \otimes \tau_0\,\partial_y + m\,\sigma_z \otimes \tau_y + V\,\sigma_0 \otimes \tau_x \tag{B28a}$$

of rank $r = 4$ in the symmetry class DIII with the operations for reversal of time and charge conjugation represented by

$$\mathcal{T} := \mathrm{i}\sigma_y \otimes \tau_0\,\mathsf{K}, \quad \mathcal{C} := \sigma_x \otimes \tau_z\,\mathsf{K}, \tag{B28b}$$

respectively.

There are two random functions allowed by the symmetry constraints that multiply the matrices

$$\begin{aligned}&\sigma_z \otimes \tau_y \qquad \text{(random mass)}, \\ &\sigma_0 \otimes \tau_x \qquad \text{(random scalar potential)}.\end{aligned} \tag{B29}$$

These couplings are the coefficients of the fermion quartic terms

$$\Phi_V = -\sum_{a,b=1}^{n} :\bar\psi^a\,\sigma_0 \otimes \tau_x\,\psi^a\,\bar\psi^b\,\sigma_0 \otimes \tau_x\,\psi^b:, \tag{B30a}$$

$$\Phi_M = -\sum_{a,b=1}^{n} :\bar\psi^a\,\sigma_z \otimes \tau_y\,\psi^a\,\bar\psi^b\,\sigma_z \otimes \tau_y\,\psi^b:, \tag{B30b}$$

respectively. Their OPEs are

$$\Phi_M(\boldsymbol{r})\,\Phi_M(\boldsymbol{0}) = \frac{-2}{\pi^2\,r^2}\,\Phi_M(\boldsymbol{0}), \tag{B31a}$$

$$\Phi_V(\boldsymbol{r})\,\Phi_V(\boldsymbol{0}) = \frac{2}{\pi^2\,r^2}\,\Phi_V(\boldsymbol{0}), \tag{B31b}$$

$$\Phi_V(\boldsymbol{r})\,\Phi_M(\boldsymbol{0}) = \frac{-1}{\pi^2\,r^2}\,[\Phi_V(\boldsymbol{0}) - \Phi_M(\boldsymbol{0})]. \tag{B31c}$$

We note that (i) the OPEs (B31a) and (B9a) are identical, (ii) the OPEs (B31b) and (B9b) are identical, while (iii) the OPE (B31c) differs by an overall sign from the OPE (B9c) if one ignores Φ_A in the latter OPE. The following one-loop RG equations follow from this observation,

$$\beta_M = \frac{1}{\pi}\,g_M\,(g_V - g_M), \tag{B32a}$$

$$\beta_V = \frac{1}{\pi}\,g_V\,(g_V - g_M). \tag{B32b}$$

Addition and subtraction gives

$$\frac{\mathrm{d}(g_V + g_M)}{\mathrm{d}\ell} = \frac{1}{\pi}\left(g_V^2 - g_M^2\right), \tag{B33a}$$

$$\frac{\mathrm{d}(g_V - g_M)}{\mathrm{d}\ell} = \frac{1}{\pi}\,(g_V - g_M)^2. \tag{B33b}$$

We have found the marginally relevant linear combination (B33b) of the couplings associated to the disorder. We deduce that a metallic phase must separate the only two topologically distinct localized phases in class DIII to explain the multicritical nature of the clean critical point $\mathsf{g} = \mathsf{m} = 0$ as depicted in Fig. 4(e), in agreement with numerical simulations of a network model [93].

e. Symmetry class AII

The one-loop RG analysis of a Dirac Hamiltonian of rank $r = 4$ in the symmetry class AII can be found, e.g., in Ref. [103]. Here we give a brief summary of the relevant results. The $r = 4$ Dirac Hamiltonian with the operation of reversal of time represented by $\mathcal{T} := \mathrm{i}\sigma_y \otimes \tau_0\,\mathsf{K}$ has symmetry-allowed random perturbations that include those allowed in the symmetry class DIII [Eq. (B28a)]. Therefore the set of one-loop RG equations for the symmetry class AII, which is given in Ref. [103], contains the one for the symmetry class DIII as a subset. Thus we have the same linear combination of coupling constants as in the symmetry class DIII that is marginally relevant [Eq. (B33)]. This indicates that a metallic phase always intervenes between two topologically distinct localized phases in class AII, as is shown in Fig. 4(g) [101–105,128].

[1] P. W. Anderson, Phys. Rev. **109**, 1492 (1958).
[2] A local random potential is a statistical distribution of potentials such that all nth order cumulants of the random potential at n distinct points in space decay exponentially fast with the pairwise separation of any two points.
[3] P. A. Lee and T. V. Ramakrishnan, Rev. Mod. Phys. **57**, 287 (1985).
[4] F. Evers and A. D. Mirlin, Rev. Mod. Phys. **80**, 1355 (2008).
[5] K. v. Klitzing, G. Dorda, and M. Pepper, Phys. Rev. Lett. **45**, 494 (1980).
[6] R. B. Laughlin, Phys. Rev. B **23**, 5632 (1981).
[7] B. I. Halperin, Phys. Rev. B **25**, 2185 (1982).
[8] D. J. Thouless, M. Kohmoto, M. P. Nightingale, and M. den Nijs, Phys. Rev. Lett. **49**, 405 (1982).
[9] D. Thouless, Phys. Rep. **110**, 279 (1984).
[10] Q. Niu, D. J. Thouless, and Y.-S. Wu, Phys. Rev. B **31**, 3372 (1985).
[11] D. E. Khmelnitskii, JETP Lett. **38**, 552 (1983).
[12] H. Levine, S. B. Libby, and A. M. M. Pruisken, Phys. Rev. Lett. **51**, 1915 (1983).
[13] A. M. M. Pruisken, Nucl. Phys. B **235**, 277 (1984).
[14] J. T. Chalker and P. D. Coddington, J. Phys. C **21**, 2665 (1988).
[15] A. W. W. Ludwig, M. P. A. Fisher, R. Shankar, and G. Grinstein, Phys. Rev. B **50**, 7526 (1994).
[16] B. Huckestein, Rev. Mod. Phys. **67**, 357 (1995).
[17] M. Z. Hasan and C. L. Kane, Rev. Mod. Phys. **82**, 3045 (2010).
[18] X.-L. Qi and S.-C. Zhang, Rev. Mod. Phys. **83**, 1057 (2011).
[19] T. H. Hsieh, H. Lin, J. Liu, W. Duan, A. Bansil, and L. Fu, Nat. Commun. **3**, 982 (2012).
[20] P. Dziawa, B. J. Kowalski, K. Dybko, R. Buczko, A. Szczerbakow, M. Szot, E. Łusakowska, T. Balasubramanian, B. M. Wojek, M. H. Berntsen, O. Tjernberg, and T. Story, Nat. Mater. **11**, 1023 (2012).
[21] S.-Y. Xu, C. Liu, N. Alidoust, M. Neupane, D. Qian, I. Belopolski, J. D. Denlinger, Y. J. Wang, H. Lin, L. A. Wray, G. Landolt, B. Slomski, J. H. Dil, A. Marcinkova, E. Morosan, Q. Gibson, R. Sankar, F. C. Chou, R. J. Cava, A. Bansil, and M. Z. Hasan, Nat. Commun. **3**, 1192 (2012).
[22] Y. Tanaka, Z. Ren, T. Sato, K. Nakayama, S. Souma, T. Takahashi, K. Segawa, and Y. Ando, Nat. Phys. **8**, 800 (2012).
[23] S. Murakami, New J. Phys. **9**, 356 (2007).
[24] X. Wan, A. M. Turner, A. Vishwanath, and S. Y. Savrasov, Phys. Rev. B **83**, 205101 (2011).
[25] A. A. Burkov and L. Balents, Phys. Rev. Lett. **107**, 127205 (2011).
[26] S. M. Young, S. Zaheer, J. C. Y. Teo, C. L. Kane, E. J. Mele, and A. M. Rappe, Phys. Rev. Lett. **108**, 140405 (2012).
[27] Strictly speaking, the energy spectrum is gapless in the presence of disorder. By bulk gap, we refer to the energy window that would not support energy eigenstates in the clean limit. For weak disorder the density of states in the bulk gap is exponentially small.
[28] A. P. Schnyder, S. Ryu, A. Furusaki, and A. W. W. Ludwig, Phys. Rev. B **78**, 195125 (2008).
[29] A. P. Schnyder, S. Ryu, A. Furusaki, and A. W. W. Ludwig, AIP Conf. Proc. **1134**, 10 (2009).
[30] S. Ryu, A. P. Schnyder, A. Furusaki, and A. W. W. Ludwig, New J. Phys. **12**, 065010 (2010).
[31] M. R. Zirnbauer, J. Math. Phys. **37**, 4986 (1996).
[32] A. Altland and M. R. Zirnbauer, Phys. Rev. Lett. **76**, 3420 (1996).
[33] A. Altland and M. R. Zirnbauer, Phys. Rev. B **55**, 1142 (1997).
[34] A. Kitaev, AIP Conf. Proc. **1134**, 22 (2009).
[35] T. Morimoto and A. Furusaki, Phys. Rev. B **88**, 125129 (2013).
[36] P. W. Brouwer, C. Mudry, B. D. Simons, and A. Altland, Phys. Rev. Lett. **81**, 862 (1998).
[37] C. Mudry, P. W. Brouwer, and A. Furusaki, Phys. Rev. B **59**, 13221 (1999).
[38] P. W. Brouwer, C. Mudry, and A. Furusaki, Phys. Rev. Lett. **84**, 2913 (2000).
[39] P. W. Brouwer, C. Mudry, and A. Furusaki, Nucl. Phys. B **565**, 653 (2000).
[40] R. Gade and F. Wegner, Nucl. Phys. B **360**, 213 (1991).
[41] R. Gade, Nucl. Phys. B **398**, 499 (1993).
[42] S. Guruswamy, A. LeClair, and A. W. W. Ludwig, Nucl. Phys. B **583**, 475 (2000).
[43] C. Mudry, S. Ryu, and A. Furusaki, Phys. Rev. B **67**, 064202 (2003).
[44] O. Motrunich, K. Damle, and D. A. Huse, Phys. Rev. B **65**, 064206 (2002).
[45] M. Karoubi, *K theory: An introduction* (Springer-Verlag, Berlin and New York, 1978).
[46] R. Jackiw and C. Rebbi, Phys. Rev. D **13**, 3398 (1976).
[47] J. C. Y. Teo and C. L. Kane, Phys. Rev. B **82**, 115120 (2010).
[48] C. Mudry, P. W. Brouwer, and A. Furusaki, Phys. Rev. B **62**, 8249 (2000).
[49] O. N. Dorokhov, JETP Lett. **36**, 318 (1982).
[50] P. A. Mello, P. Pereyra, and N. Kumar, Ann. Phys. (NY) **181**, 290 (1988).
[51] P. W. Brouwer, A. Furusaki, I. A. Gruzberg, and C. Mudry, Phys. Rev. Lett. **85**, 1064 (2000).
[52] M. Titov, P. W. Brouwer, A. Furusaki, and C. Mudry, Phys. Rev. B **63**, 235318 (2001).
[53] P. W. Brouwer, A. Furusaki, and C. Mudry, Phys. Rev. B **67**, 014530 (2003).
[54] P. W. Brouwer, A. Furusaki, C. Mudry, and S. Ryu, BUTSURI **60**, 935 (2005) (in Japanese), English version: arXiv:cond-mat/0511622.
[55] I. A. Gruzberg, N. Read, and S. Vishveshwara, Phys. Rev. B **71**, 245124 (2005).
[56] K. B. Efetov, Adv. Phys. **32**, 53 (1983).
[57] A. Huffmann, J. Phys. A: Math. Gen. **23**, 5733 (1990).
[58] M. Caselle, arXiv:cond-mat/9610017.
[59] M. Caselle and U. Magnea, Phys. Rep. **394**, 41 (2004).
[60] Y. Takane, J. Phys. Soc. Jpn. **73**, 9 (2004).
[61] M. R. Zirnbauer, Phys. Rev. Lett. **69**, 1584 (1992).
[62] A. Altland and R. Merkt, Nucl. Phys. B **607**, 511 (2001).
[63] A. Lamacraft, B. D. Simons, and M. R. Zirnbauer, Phys. Rev. B **70**, 075412 (2004).
[64] A. Altland, D. Bagrets, L. Fritz, A. Kamenev, and H. Schmiedt, Phys. Rev. Lett. **112**, 206602 (2014).
[65] F. J. Dyson, Phys. Rev. **92**, 1331 (1953).
[66] T. P. Eggarter and R. Riedinger, Phys. Rev. B **18**, 569 (1978).
[67] A. Altland, D. Bagrets, and A. Kamenev, Phys. Rev. B **91**, 085429 (2015).
[68] I. Mondragon-Shem, T. L. Hughes, J. Song, and E. Prodan, Phys. Rev. Lett. **113**, 046802 (2014).
[69] E. Prodan and H. Schulz-Baldes, arXiv:1402.5002.
[70] E. Prodan, Topol. Quant. Matter **1**, 1 (2014).

[71] J. Song and E. Prodan, Phys. Rev. B **89**, 224203 (2014).
[72] I. Mondragon-Shem and T. L. Hughes, Phys. Rev. B **90**, 104204 (2014).
[73] D. S. Fisher, Phys. Rev. B **51**, 6411 (1995).
[74] D. G. Shelton and A. M. Tsvelik, Phys. Rev. B **57**, 14242 (1998).
[75] L. Balents and M. P. A. Fisher, Phys. Rev. B **56**, 12970 (1997).
[76] M. B. Hastings and S. L. Sondhi, Phys. Rev. B **64**, 094204 (2001).
[77] O. Motrunich, K. Damle, and D. A. Huse, Phys. Rev. B **63**, 224204 (2001).
[78] M.-T. Rieder and P. W. Brouwer, Phys. Rev. B **90**, 205404 (2014).
[79] C. W. J. Beenakker, Rev. Mod. Phys. **69**, 731 (1997).
[80] D. H. Friedan, Ann. Phys. **163**, 318 (1985).
[81] E. Abrahams, P. W. Anderson, D. C. Licciardello, and T. V. Ramakrishnan, Phys. Rev. Lett. **42**, 673 (1979).
[82] K. B. Efetov, A. I. Larkin, and D. E. Kheml'nitskii, JETP **52**, 568 (1980).
[83] S. Hikami, Prog. Theor. Phys. **64**, 1466 (1980).
[84] R. B. Laughlin, Phys. Rev. Lett. **52**, 2304 (1984).
[85] D. E. Khmelnitskii, Phys. Lett. A **106**, 182 (1984).
[86] T. Senthil, M. P. A. Fisher, L. Balents, and C. Nayak, Phys. Rev. Lett. **81**, 4704 (1998).
[87] T. Senthil and M. P. A. Fisher, Phys. Rev. B **60**, 6893 (1999).
[88] T. Senthil and M. P. A. Fisher, Phys. Rev. B **61**, 9690 (2000).
[89] M. Bocquet, D. Serban, and M. R. Zirnbauer, Nucl. Phys. B **578**, 628 (2000).
[90] N. Read and D. Green, Phys. Rev. B **61**, 10267 (2000).
[91] J. T. Chalker, N. Read, V. Kagalovsky, B. Horovitz, Y. Avishai, and A. W. W. Ludwig, Phys. Rev. B **65**, 012506 (2001).
[92] A. Mildenberger, F. Evers, A. D. Mirlin, and J. T. Chalker, Phys. Rev. B **75**, 245321 (2007).
[93] I. C. Fulga, A. R. Akhmerov, J. Tworzydło, B. Béri, and C. W. J. Beenakker, Phys. Rev. B **86**, 054505 (2012).
[94] Not all topologically nontrivial phases in the symmetry class D can be brought to the form of the Dirac Hamiltonian studied here. For example, a spinless chiral p-wave superconducting ground state supports two topological phases that may be labeled by the index ± 1, each of which support $\mathbb{Z}_2$ vortices that bind Majorana zero modes [90]. These $\mathbb{Z}_2$ vortices are induced by a magnetic flux not by a $\mathbb{Z}_2$ vortex in a Dirac mass.
[95] C.-M. Ho and J. T. Chalker, Phys. Rev. B **54**, 8708 (1996).
[96] D. K. K. Lee and J. T. Chalker, Phys. Rev. Lett. **72**, 1510 (1994).
[97] I. A. Gruzberg, A. W. W. Ludwig, and N. Read, Phys. Rev. Lett. **82**, 4524 (1999).
[98] V. Kagalovsky, B. Horovitz, Y. Avishai, and J. T. Chalker, Phys. Rev. Lett. **82**, 3516 (1999).
[99] E. J. Beamond, J. Cardy, and J. T. Chalker, Phys. Rev. B **65**, 214301 (2002).
[100] M. Ortuño, A. M. Somoza, and J. T. Chalker, Phys. Rev. Lett. **102**, 070603 (2009).
[101] Y. E. Kraus and A. Stern, New J. Phys. **13**, 105006 (2011).
[102] Z. Ringel, Y. E. Kraus, and A. Stern, Phys. Rev. B **86**, 045102 (2012).
[103] R. S. K. Mong, J. H. Bardarson, and J. E. Moore, Phys. Rev. Lett. **108**, 076804 (2012).
[104] T. Morimoto and A. Furusaki, Phys. Rev. B **89**, 035117 (2014).
[105] H. Obuse, S. Ryu, A. Furusaki, and C. Mudry, Phys. Rev. B **89**, 155315 (2014).
[106] S. Ryu, C. Mudry, A. W. W. Ludwig, and A. Furusaki, Phys. Rev. B **85**, 235115 (2012).
[107] C.-Y. Hou, C. Chamon, and C. Mudry, Phys. Rev. Lett. **98**, 186809 (2007).
[108] R. Jackiw and S.-Y. Pi, Phys. Rev. Lett. **98**, 266402 (2007).
[109] C. Chamon, C.-Y. Hou, R. Jackiw, C. Mudry, S.-Y. Pi, and A. P. Schnyder, Phys. Rev. Lett. **100**, 110405 (2008).
[110] C. Chamon, C.-Y. Hou, R. Jackiw, C. Mudry, S.-Y. Pi, and G. Semenoff, Phys. Rev. B **77**, 235431 (2008).
[111] S. Ryu, C. Mudry, C.-Y. Hou, and C. Chamon, Phys. Rev. B **80**, 205319 (2009).
[112] L. Santos, S. Ryu, C. Chamon, and C. Mudry, Phys. Rev. B **82**, 165101 (2010).
[113] L. Santos, Y. Nishida, C. Chamon, and C. Mudry, Phys. Rev. B **83**, 104522 (2011).
[114] R. Jackiw and P. Rossi, Nucl. Phys. B **190**, 681 (1981).
[115] K. Slevin and T. Ohtsuki, Phys. Rev. Lett. **78**, 4083 (1997).
[116] K. Slevin and T. Ohtsuki, Phys. Rev. Lett. **82**, 382 (1999).
[117] K. Kobayashi, T. Ohtsuki, K.-I. Imura, and I. F. Herbut, Phys. Rev. Lett. **112**, 016402 (2014).
[118] R. Roy, Phys. Rev. B **79**, 195322 (2009).
[119] J. E. Moore and L. Balents, Phys. Rev. B **75**, 121306 (2007).
[120] L. Fu, C. L. Kane, and E. J. Mele, Phys. Rev. Lett. **98**, 106803 (2007).
[121] R. Shindou and S. Murakami, Phys. Rev. B **79**, 045321 (2009).
[122] L. Fu, Phys. Rev. Lett. **106**, 106802 (2011).
[123] C.-K. Chiu, H. Yao, and S. Ryu, Phys. Rev. B **88**, 075142 (2013).
[124] Observe that the classifying space is the set of two points $\{\pm\beta\}$ for the minimal rank $r = r_{\min}$.
[125] For one mirror plane, the mirror Chern number is 2. It protects the Dirac cones at two L points out of the four inequivalent L points. Here, the four inequivalent L points can be arranged into two pairs related by a $\pi/2$ rotation of the mirror plane.
[126] M. Diez, D. I. Pikulin, I. C. Fulga, and J. Tworzydło, New J. Phys. **17**, 043014 (2015).
[127] I. C. Fulga, B. van Heck, J. M. Edge, and A. R. Akhmerov, Phys. Rev. B **89**, 155424 (2014).
[128] L. Fu and C. L. Kane, Phys. Rev. Lett. **109**, 246605 (2012).
[129] E. J. König, P. M. Ostrovsky, I. V. Protopopov, and A. D. Mirlin, Phys. Rev. B **85**, 195130 (2012).
[130] P. M. Ostrovsky, I. V. Protopopov, E. J. König, I. V. Gornyi, A. D. Mirlin, and M. A. Skvortsov, Phys. Rev. Lett. **113**, 186803 (2014).
[131] J. E. Moore, Y. Ran, and X.-G. Wen, Phys. Rev. Lett. **101**, 186805 (2008).
[132] R. Kennedy and M. R. Zirnbauer, arXiv:1409.2537 [math-ph].
[133] H. B. Nielsen and M. Ninomiya, Nucl. Phys. B **185**, 20 (1981).
[134] D. Bernard, arXiv:hep-th/9509137 [hep-th].
[135] A. Nersesyan, A. Tsvelik, and F. Wenger, Nucl. Phys. B **438**, 561 (1995).
[136] C. Mudry, C. Chamon, and X.-G. Wen, Nucl. Phys. B **466**, 383 (1996).